MODIFICATION OF THE SURFACE CHARACTERISTICS OF FABRICS BY PLASMA PROCESS

Mr. Kanchit Kamlangkla

A Dissertation Submitted in Partial Fulfillment of the Requirements
for the Degree of Doctor of Philosophy Program in Nanoscience and Technology
(Interdisciplinary Program)
Graduate school
Chulalongkorn University
Academic Year 2010

Thesis Title	MODIFICATION OF THE SURFACE CHARACTERISTICS OF FABRICS BY PLASMA PROCESS
By	Mr. Kanchit Kamlangkla
Field of Study	Nanoscience and Technology
Thesis Advisor	Assistant Professor Satreerat K. Hodak, Ph.D.
Thesis Co-Advisor	Assistant Professor Boonchoat Paosawatyanyong, Ph.D.
Thesis Co-Advisor	Assistant Professor Varong Pavarajarn, Ph.D.

Accepted by the Graduate School, Chulalongkorn University in Partial Fulfillment of the Requirements for the Doctoral Degree

..... Dean of the Graduate school
(Associate Professor Pornpote Piumsomboon, Ph.D.)

THESIS COMMITTEE

..... Chairman
(Associate Professor Vudhichai Parasuk, Ph.D.)

..... Thesis Advisor
(Assistant Professor Satreerat K. Hodak, Ph.D.)

..... Thesis Co-Advisor
(Assistant Professor Boonchoat Paosawatyanyong, Ph.D.)

..... Thesis Co-Advisor
(Assistant Professor Varong Pavarajarn, Ph.D.)

..... Thesis Co-Advisor
(Professor Joëlle Levalois-Grützmacher, Ph.D.)

..... Examiner
(Assistant Professor Sukkaneste Tungasmita, Ph.D.)

..... Examiner
(Rutthapol Rangkupan, Ph.D.)

..... External Examiner
(Assistant Professor Jose H. Hodak, Ph.D.)

THAI ABSTRACT PAGE

4989715820 : MAJOR NANOSCIENE AND TECHNOLOGY
KEYWORDS : PLASMA / HYDROPHOBICITY / HYDROPHILICITY / FLAME RETARDANTCY

KANCHIT KAMLANGKLA : MODIFICATION OF THE SURFACE CHARACTERISTICS OF FABRICS BY PLASMA PROCESS. THESIS ADVISOR : ASST. PROF. SATREERAT K. HODAK, Ph.D., THESIS CO-ADVISOR : BOONCHOAT PAOSAWATYANYONG, Ph.D., VARONG PAVARAJARN, Ph.D., 206 pp.

This thesis focuses on the improvement of hydrophobicity of cotton fabric by radio frequency inductively coupled SF_6 plasma under the different of RF power pressure and exposure time conditions. The absorption time of treated cotton fabrics reaches the maximum of 210 min and the contact angle reaches the maximum of 149^o. The water absorption time of the fabric follows the same increasing trend as the fluorine/carbon ratio at the fabric surface. We studied on the hydrophilicity improvement of polyethylene terephtalate (PET) fabrics by capillary rise method after treating with O_2, N_2 and Ar plasmas under different plasma conditions. The treated fabrics of all gases provide the mean pore radius and the diffusion coefficient values increased with exposure time, pressure and RF power. The treated PET fabric with O_2 plasma results in the largest pore radius values. The increasing of weight loss is related to the etching rate and tensile strength. The enhancement of O/C after treatment on PET fabrics is also related to the obtained higher K/S values. For the improvement of flame retardantcy on silk fabric by argon plasma induced graft polymerization process, phosphate and phosphoramidate monomers were grafted on silk fabric. The grafted silk fabrics show a good flame retardantcy and durable after laundering.

Field of Study : . Nanosciene and Technology . Student's Signature .....

Academic Year : ..... 2010 ..... Advisor's Signature .....

Co-Advisor's Signature .....

Co-Advisor's Signature .....

Acknowledgements

I would first like to express my sincere appreciation and gratitude to my advisor, Assistant Professor Dr. Satreerat K. Hodak for her invaluable guidance, encouragement, patience and support. Knowing her has improved me as a good researcher throughout my Ph.D study. I would like to thank my co-advisors, Assistant Professor Dr. Boonchoat Paosawatyanyong and Assistant Professor Dr. Varong Pavarajarn and Assistant Professor Dr. Jose H. Hodak for kindly being as examiner committee. I also would like to thank my chairman and committee members, Associate Professor Dr. Vudhichai Parasuk, Assistant Professor Dr. Sukkaneste Tungasmita and Dr. Ratthapol Rankupan for providing valuable suggestions during my study and for serving as committee. Many thanks are owed to the Commission on Higher Education which provides the scholarship to do research in Switzerland for one year. Support from graduate school and The 90^{th} Anniversary of Chulalongkorn University Fund (Ratchadaphisaksomphot Endowment Fund) and Nanoscience and Technology program allowed me to attend many outstanding conferences and I have benefited personally from these experiences.

I would like to express my sincere appreciation to Prof. Dr. Hansjörg Grützmacher and Prof. Dr. Joëlle Levalois-Grützmacher for their support, guidance and encouragement throughout my research work during the time in Eidgenössische Technische Hochschule (ETH), Zürich, Switzerland. I also thank Mr. Sirawat Seaning for assistance with AFM measurement and Mr. Thanakorn Tepamat for the help of SEM measurement. I would like to thank Mr. Opas Chowananon, Textile Engineering at Rajamangala University of Technology Krungthep (RMUTK), for allowing me in using tensile strength machine. Thanks to all colleagues in plasma research group at Chulalongkorn university and all colleagues in group of Grützmacher research Group at ETH Zürich in Switzerland for their helps and giving me a nice time.

Finally, I would like to thank my father, my mother and my sisters who have supported me unconditionally throughout the years.

Contents

Chapter **Page**

Chapter **Page**

Chapter **Page**

Chapter **Page**

List of Tables

Table **Page**

Table **Page**

List of Figures

Figure **Page**

Figure **Page**

Figure **Page**

Figure **Page**

Figure **Page**

Figure **Page**

Figure **Page**

Figure **Page**

CHAPTER I

Introduction

1.1 Thesis motivation

Nowadays, textile industry plays a very important role in the Thai economic development. The textile products are commonly used in the production of garments, fabrics, and yarn to cite few examples. The textile markets have continuously grown in order to respond to the customer needs and to reach higher profits. The textile industry has tried to improve the quality of their products. The finishing process is an important step to improve the quality of the textiles. Both chemical and physical methods which are used as the surface modifications have been employed to achieve the desired characteristics.

The conventional chemical treatment is done by soaking in solutions of chemicals, followed by drying and curing. These treatments use a large amount of chemicals and reagents that could affect on environment and human's quality of life [1]. Recently, the coating with nanopaticles has been developed for textile modification to enhance or to provide special properties of textiles. For example, cotton can be coated with nano-silica particles, forming nano-whiskers, in order to improve the hydrophobic property [2]. Titanium dioxide was coated on cotton for the application of UV-protection [3]. Nano-silver inhibits cell growth and metabolism, leading to enhanced of anti-bacterial properties [4]. Also, the wrinkle resistance of silk was improved with nano-silica particles and maleic anhydride as a catalyst [5]. However, the nanoparticle coating still uses chemicals in the preparation, and some of them are toxic. Also these treatments make the fabric

less durable or less comfortable to wear. Widespread use of nanoparticles has not yet been tested for carcinogenic potential. Alternative techniques have been investigated over the past two decades to reduce amount of chemicals on fabric surface. Plasma treatment is a technique which can be used to modify fabric surface in the nanometer scale without affecting bulk properties [6]. Besides, plasma treatment is known as a dry process using low amounts of chemicals, but it can change the functional groups on the material surface in a similar way to chemical treatments. Therefore, plasma techniques in textile industry have become more interesting as a novel finishing technology that significantly reduces toxic-chemical pollution and receive enormous attention as a solution for environmental problems in textile industry. Plasma treatments have seen a rapid development and commercialization over the past decade.

Plasma consists of a low pressure mixture of free electrons, radicals and ions [7]. The plasma processes such as etching, grafting, implantation and cross-linking can take place simultaneously [8]. Reactive species in the plasma collide with the molecules on the fabric surface, leading to chemical interaction and generating new functional groups and radicals. Radicals could induce the cross-linking on the upper few mono-layers of textile. Photon emission arises from the excited states of molecules, ions and free radicals that are formed in the plasma. The energy of the emission is sufficient to break chemical bonds and can also be useful for treating textiles [9]. Recently, low gradient temperature plasma systems, sometimes called the cold plasma, are widely used for generating plasma. This plasma can be produced under vacuum conditions by using direct current (DC), radio frequency (RF) or microwave (MW) generators which can applied to surface modification of textile. In this thesis work, I propose to apply the plasmas for the improvement of desirable properties including hydrophobicity, hydrophilicity and flame retardancy of fabrics. I am interested in the correlation between these properties and physical, chemical and thermal change on the fabric surface. Furthermore, our goal also focuses on multifunctional surface modification of hydrophobicity on flame retardancy of silk fabric to approach the commercialization.

1.2 Literature review

Plasma technologies can be used for modifying any material surface, espectially for fabric and textiles. Many reseach groups have focused on various surface modifications of fabrics and textiles such as hydrophobicity [10], [11], [12], hydrophilicity [13], [14], [15], flame retardantcy [16], [17], [18], UV-protection [3], shink resistance [19], anti-bacterial [4], adhesion and dyeability [20]. It is clearly seen that plasma plays an important role in the success of their applications. In this thesis, I am interested to apply the plasma method for the improvement of desirable properties including hydrophobicity, hydrophilicity and flame retardancy of fabrics by cold plasma treatment.

1.2.1 Previous research work on hydrophobic surface for textile finishing

Hydrophobicity which is sometimes called water repellency is one desirable property for textiles. Considerable researches on hydrophobicity have been conducted for many years. This property is generally achieved by the plasma based on fluorine containing gases such as tetrafluoromethane (CF_4), hexafluoropropylene (C_3F_6), tetrafluoroethylene (C_2F_4) and perfluorohexane (C_6F_{14}). McCord et al. [10] studied the hydrophobicity of the cotton fabric with CF_4 and C_3F_6 plasma. They found that C_3F_6 plasma can increased the hydrophobicity better than CF_4 plasma. This is due to C_3F_6 plasma can generate polymers on the fabric through both plasma polymerization and plasma-induced polymerization process, while CF_4 plasma can generate only plasma polymerization process. Li and Jinjin [11] studied the hydrophobicity of silk and cotton with (C_3F_6) plasma. The contact angle and water absorption time of treated silk and cottton fabrics were measured before and after washing to analyze the hydrophobic property. For both fabrics after plasma treatments, the contact angle can reach 120^o while water absotption time can be as high as 60 min. It is due to the incorporation of fluorine up to

50% or more on to the surface. They also found that washing can remove more fluorine compounds from cotton fabric while silk fabric is slightly more efficient for removal from surface. This is due to the nature of the fabrics and the different products have been generated during the surface reactions. Iriyama et al. [12] studied the hydrophobicity of nylon treated with fluorocarbon plasmas of CF_4, C_2F_6, C_2F_4 and C_3F_6 plasmas. After treatment by the fluorocarbon plasmas, the surface became very hydrophobic and water drops remained on the surface. The values of contact angle are very high, as high as over 130^o, which represents a high degree of hydrophobicity. After the washing test, surfaces treated with CF_4 and C_2F_6 plasma had better durability than those treated by C_2F_4 and C_3F_6 plasmas. It is due to fluorocarbon of CF_4 and C_2F_6 plasma introduce longer chains leading to better durability than C_2F_4 and C_3F_6 plasma, which have not much interaction between the plasma polymer and the surface. However, the implantation forms chemical bonds between the substrate and the hydrophobic segments, which are expected to have good durability.

1.2.2 Previous research work on hydrophilic surface for textile finishing

Hydrophilicity or wettability is a contrary characteristic to hydrophobicity. The surface wettability of fabrics is tightly related to many fields, such as in printing, spraying, adhesion, and dyeing. The hydrophilic surfaces can be obtained by incorporation of oxygen-containing functional groups. Good wettability and high surface energy of fabric surfaces were demonstrated by the implantation of some polar groups such as hydroxyl (-OH), carbonyl (-CO), or carboxyl (-COOH). An increase in the wettability manifested by the water absorbency is due to the formation of the hydrogen bonds between water and surface groups. Lai et al. [13] studied the improving of the hydrophilicity of polycarbonate (PC), polypropylene (PP), polyethylene terephthalate (PET) surfaces by microwave-induced argon plasma treatment. They found that C=O bond is the key factor to

the improvement of hydrophilicity of three polymer surfaces. In addition, the reduction of surface roughness in micron scale can also improve hydrophilicity. Wong et al. [14] showed that the hydrophilic property of linen fabrics can be achieved by using oxygen and argon plasmas. They found that low temperature plasma with short treatment times on linen is effective for surface modifications such as substantial increases in polar groups and water uptake. Pandiyaraj and Selvarajan [15] investigated the hydrophilic improvement of cotton fabric by DC glow discharge air plasma. The fabrics were treated for different exposure times, discharge potentials and pressure levels. After the plasma treatment, the wettability of the fabric was characteried by contact angle and dynamic wicking rate measurements. It was found that the surface hydrophilicity and surface energy were increased. It was explained by the increase in the porosity and the enhancement of polar groups on the fabric surface. Mokbul et al. [21] investigated the plasma activation of polyester (PES) fabric structures to improve their wettability. The hydrophilic modification was carried out by low pressure plasma treatments using the mixtures of gas O_2 with Ar and O_2 with He. Both Ar/O_2 and He/O_2 plasma were found to yeild good hydrophilization of textile. Because the addition of small amounts of oxygen to Ar or He in the feed gas generates more excited species in the plasma zone such as long-living He^* and Ar^* metastables, and long-living O atoms, which are able to penetrate into textile structures. The penetration of plasma species into the textile led to the losser structured fabrics and the reactive gas particles easily moved into inter-yarn and inter-fiber spaces in fabrics resulting in improved wettability or capillarity.

1.2.3 Previous research work on flame retardant surface for textile finishing

Flame retardant materials are defined as any materials used to impart resistance to burning. The meaning of burning is the ability to increase the ignition temperature in oxygenated atmospheres. A fiber is considered flame-retardant when it self-extinguishes upon removal of the flame source. Most flame retardant textile products are mainly designed to reduce the ignition and the rates of flame propagation. Heat resistant textiles are not only expected to reduce ignition and flame propagation, but also form a barrier to heat and flame penetration to the underlying textile surfaces. The fire resistance property can be obtained by using cold plasma fed with the monomers. However, there are many types of flame retardant monomers incorporate either chlorine or bromine, phosphorous, antimony, and boron related compounds [22]. Most of compounds act as flame retarding agents in condensed phase by increasing the amount of carbonaceous residues or by increased char formation [23]. Recently, phosphorous and nitrogen compounds are the most commonly used as flame retardant monomers. Akovali et al. [16] studied three different types of flame-retardant monomers (hexamethyldisiloxane, ethyldichlorophosphate and tris (butoxyethyl) phosphate on polyacrylonitrile (PAN) fiber. The graft polymerization can overcome the negative effect of cross-linking and chain scission. With an increase in grafting, the ignition time and the oxygen index were increased. Guan and Chen [17] studied flame retardance of a silk fabric treated with a vinyl phosphate dimethyl 2-(methacryloyloxyethyl) phosphate (DMMEP) onto silk fabric by a graft copolymerization technique. Treated silk fabric was self-extinguished when ignited with a candle-like fire with LOI range of 28-32%. Microscale combustion calorimetry (MCC) test showed that the heat release rate of DMMEP treated silk fabric decreased to a large extent and the total heat release still decreased compared with the control silk fabric. Thermal analysis showed that the initial decomposition temperature and thermal decomposition activation energy of DMMEP treated silk fabric decreased, and more char formed

of DMMEP treated silk fabric. All the results of thermal analysis showed good flame-retardant effectsof DMMEP monomer. Grützmacher's group [18] produced a multifunctional surface which was water repellent and fire retardant on cotton by using cold plasma. This method uses Ar plasma induced graft polymerization (PIGP) of flame retardant monomers (acrylate phosphate and phosphonate derivatives)combined with a water repellent treatment by CF_4 and 1,1,2,2, tetrahydroperfluorodecylacrylate (AC8). They found that the increase of hydrophobicity was much greater for the samples treated with AC8 than for those treated in CF_4 plasma. The reason is that AC8 compound, a fluorinated polymer is grafted onto the surface while the treatment in CF_4 gas plasma result in surface fluorination.

Several research groups have demonstrated the ability of various plasma methods on fabrics to improve their specific property. Therefore, the knowledge obtained from these studies can be applied to the development of other properties of fabric and new applications of plasma method in finishing process for textile industry in the future.

1.3 Objectives of thesis

The purpose of this thesis is to modify surface characteristics of fabrics such as hydrophobicity, hydrophilicity and flame retardancy by cold plasma treatment. The scope of this research focuses on the influence of plasma treatment with different types of gas and plasma-induced graft polymerization (PIGP) procedure on the modifications of fabric surface by means of physical, chemical changes and thermal properties.

In the beginning, I have chosen cotton fabrics to investigate the improvement hydrophobic properties due to its high absorbency as a result of the abundant hydroxyl groups. Method goal to produce hydrophobicity on cotton fabrics becomed a desirable. The SF_6 gas, which is nontoxic fluorine-based gas as plasma media, was used to improve hydrophobic properties on cotton fabric by using radio

frequency (RF) plasmas under different plasma operating conditions such as gas power, gas pressure and exposure time. Normally, the SF_6 gas is used as both etching process and depositing process on surface. Therefore, it is used to explain the main reason for improvement hydrophobicity that it is due to the increase in surface roughness or the formation of fluorinated groups on treated fabric affect more on the improvement on the hydrophobicity. The surface morphology, etching and chemical change were obtained by scanning electron microscopy (SEM), atomic force microscopy (AFM) and X-ray photoelectron spectroscopy (XPS), respectively. The tensile strength and the percentage weight loss which are relate to mechanical property of fabrics were evaluated. The durability of the treatment on cotton fabrics to washing was also tested.

For the next main topic, we used the different gases as plasma gas such as O_2, Ar and N_2 gases for improvement the hydrophilic properties of poly (ethylene terephthalate) (PET) fabrics by treatment with radio frequency (RF) plasmas under different operating conditions. Because the molecular structure of PET lacks of polar groups, such as -COOH and -OH groups causing low surface-free energy and poor wettability, the hydrophilicity improvement is suitable for PET fabric. Chemical functionalizations may occur consequent to the incorporation of polar groups such as hydroxyl, carbonyl and carboxyl onto the surface after plasma treatment. The influences different types of plasmas, pressure, and power and exposure time were investigated and compared. The pore radius and the diffusion of water on fabrics, which is related on wettability in capillary rise method, were determined by using Lucas-Washburn equation. The improvement of dyeability for fabrics is evaluated. In addition, physical and chemical changes were also analyzed by SEM, AFM and XPS.

Finally, we study the effectiveness of the plasma-induced graft polymerization (PIGP) procedure to produce flame retardancy on silk fabric in which argon microwave (MW) plasma is used to induce. The plasma-induced polymerization of monomers containing phosphorus and nitrogen compound is used to reduce flammability of silk fabric. Although, silk exhibits a low natural flammability due

to its high nitrogen content (15-18%), it still produces fuel for fire. Therefore, it is worth investigating new fire retardant finishes for silk fabric in order to render it more difficult to ignite or provide better self-extinguishing properties when removed from a flame. The flame retardant properties of untreated and treated fabrics are evaluated by the LOI method. This work also investigates the color fastness, tensile strength and surface morphology. The chemical properties were characterized by using FTIR and XPS. The thermal properties were investigated by thermal gravimatric analysis (TGA), differential thermal gravimetric (DTG) and pyrolysis combustion flow calorimetry (PCFC) of untreated and treated fabrics are presented and discussed. Furthermore, I also study a two step protocol in order to produce multifunctional silk fabrics.

1.4 Outline of thesis

In plasma treatment of fibers and polymers, low temperature plasma or cold plasma has recently emerged as a novel technique for textile applications. In addition, cold plasma treatments result in the changing of surface chemistry and surface morphology leading to the increasing of specific surface area without affecting the bulk properties of fibers. Chapter 2 reviews the definition and characterization of plasma, classification of cold plasma generation use in textile which consists of direct current glow discharge, radio frequency discharge and microwave discharge. Several factors of the plasma treatment and fundamental reactions in cold plasma and textile surface or mechanism of plasma treatments are also described. The contact angle measurements are the main technique which fundamentally identifies the ability to repel water or hydrophobicity of the fabric. The hydrophilic properties are explored by the capillary rise method for determination pore radius of textile by modified Washburn equation. For flame retardant properties on textile, I introduced the basic of mechanism of flame retardancy, the type of flame retardant monomers and the characteristics for burning behavior of different textile fibers. The plasma reactor, materials, monomers and characteri-

zation methods of the physical, chemical and thermal property changes on fabrics discussed in this thesis are given in Chapter 3. The physical properties are characterized by several techniques consist of SEM, AFM, tensile strength, weight loss contact angle, absorption time, color fastness and washing test. The characteristic of wettability is explained with capillary rise and dyeability technique. The chemical changes on fabrics were anlyzed by FT-IR and XPS. The method of evaluation flame retardantcy on fabrics was obtained by LOI and thermal properties were also introduced by TGA, DTG and PCFC technique. Chapter 4 presents the results and discussions of the improvement of hydrophobic propeties on cotton fabric surface with SF_6 gas and hydrophilic properties on PET fabrics surface with O_2, Ar and N_2 under radio frequency inductively plasma (RF-ICP plasma). The results of flame retardant and multifunctional fabrics combining multiple properties of hydrophobicity with flame retardancy on silk fabric by the plasma-induced graft polymerization (PIGP) procedure under Microwave plasma (MW) system is also reported effectiveness. Chapter 5 presents the conclusions of this work and offer recommendations for future work in this area.

CHAPTER II

THEORETICAL BACKGROUND

2.1 Definition and characterization of plasmas

2.1.1 Definition of plasma

A gas is a material in which the molecules have high enough to overcome intermolecular attraction forces and all the molecules are free and individual but there is not enough energy to ionize any of the molecules [24]. However, when the temperature of a gas is raised its molecules gain energy until the electrons in the gas leave the nucleus of the atom. The gas then exists in the form of charged ions, electrons and neutral particles. Normally, gas is an electric insulator. When it is applied to sufficient large voltage, it will breakdown and conduct electricity. The electrically neutral atoms or molecules of gas have been ionized into positive and negative charge ions which show a collective response induced by electric and magnetic fields. This occurs is often called a discharge or plasma. Therefore, plasma is defined as a partially ionized gas consisting of electrons, positive ions, negative ions, metastables atoms, free radicals and photons as shown in Fig.2.1. Also, the interactions of the electrically charged particles with each other and with contact surface create the unique physical and chemical properties of the plasma environment which is distinct from solids, liquids and gas. For this reason, plasma is sometimes called the fourth state of matter.

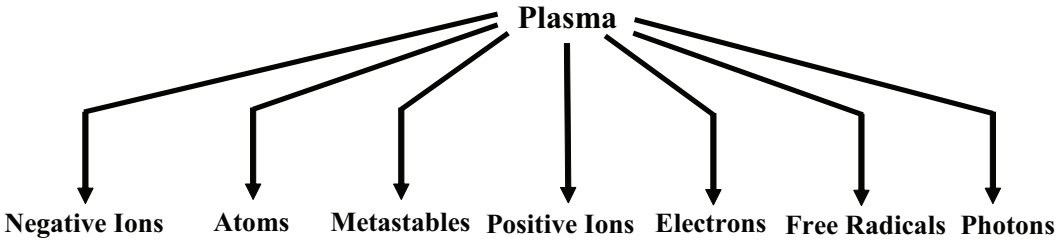

Figure 2.1: Scheme of constituents of plasma.

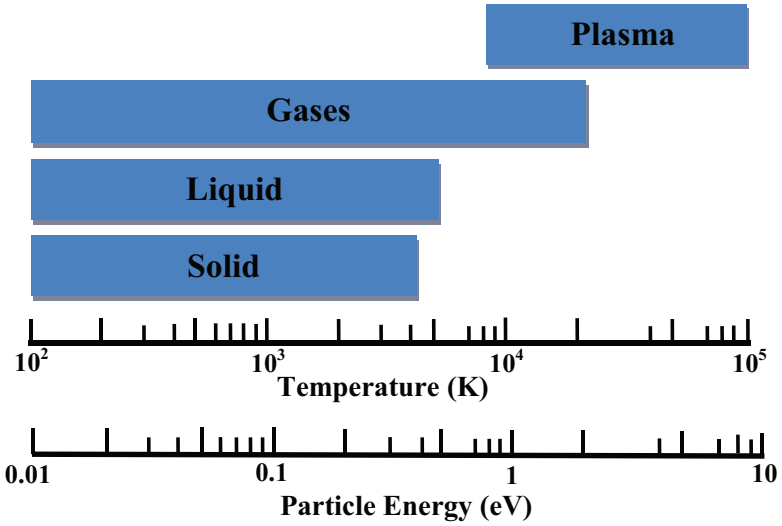

Figure 2.2: State of matter versus temperature and particle energy [23].

Figure 2.2 presents schematically the ranges of temperature and particle energy in which each of the four forms of matter occur in nature [25]. As we know, a solid substance in thermal equilibrium generally passes into a liquid state as the temperature is increased at fixed pressure. The liquid state was changed when the temperature is further increased. At a significantly high temperature or its molecule gain energy, the molecules in gas decompose to form a gas of atoms that move freely in random directions. If the temperature or particle energy is further increased, the atoms decompose into freely moving charged particles (electrons and positive ions) and the substance enters the plasma state.

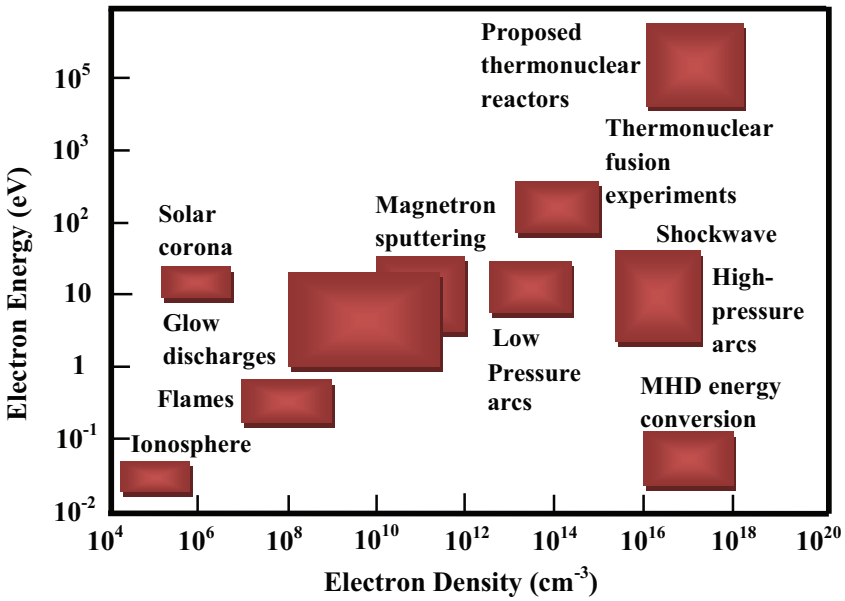

Figure 2.3: Typical regions of average electron density and electron energy that are found in various sources [24].

2.1.2 Classification of plasma

The plasmas can be found in nature cover a very large range of electron densities and electron energies. Mostly, the electron density plasma is found in the range between 10^4 and 10^{20} cm^{-3} while the electron energy can vary between 10^2 and 10^5 eV [26]. These two parameters distinguish plasmas into different categories are shown in Fig. 2.3.

Plasmas are presented in many regions of the universe and it makes up most of the universe as it can be seen such as example in the creating of thermonuclear fusion, it is necessary to create plasmas with electron energy above 10 keV and with ion densities between 1x10^{14} - 2x10^{14} cm^{-3} at atmospheric pressure. However, the various plasma applications depend on the characteristic of plasma. Plasmas are generally classified as equilibrium and non-equilibrium plasmas which correspond to its temperature and pressure as shown in Fig. 2.4.

In case of equilibrium (hot) plasmas known as thermal plasmas, when the pressure of gases in the system increases to atmospheric pressure causing increase

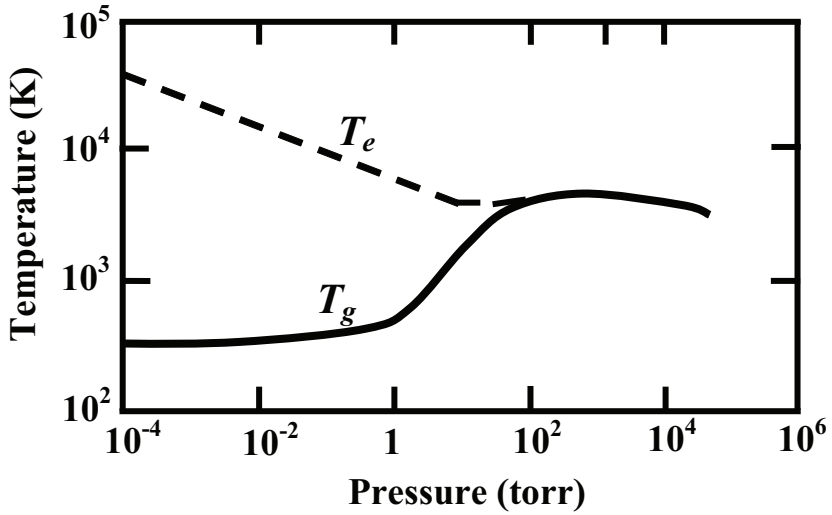

Figure 2.4: Schematic of the electron and gas temperature as a function of pressure in a plasma discharge at constant current[25]. [27].

the number of collision or a short collision mean free path between electrons, ions, and neutral species. It leads to the efficient energy exchange between them. The result is all the approximate of species reach the same temperature in the plasma and their temperature is about several thousand degrees (^{o}C) when the reaction is maintained. A well known example in nature is the solar corona which has temperature about 10^7 K. It is clearly seen that this thermal plasma is not suitable for treatment on textile surface. However, these types of plasmas are mainly used for applications where heat is required such as for spraying, cutting, waste destruction and welding applications [28].

In contrary, non-equilibrium plasmas known as non-thermal plasmas or cold plasmas are produced the electrons reach a very high temperature of 10^4-10^5 K (1-10 eV) while ions and neutrals remain at room temperature or a little above room temperature (Fig. 2.4). Non-thermal plasma electrons have a much higher temperature than gas temperature ($T_e >> T_g$) because of the very low density and very low heat capacity of the electrons [27]. And also the low pressure of system and the mean free path of gases are so large. The collisions of electrons

with other species are quite rare so it cannot transfer energy between particles which lead to the different temperatures of the plasma species. It is often referred to as cold plasma. However, Figure 2.4 is found that when the pressure in the cold plasma increases, the energy transfer from electron to neutrals increases, causing an increase in the pressure of the gas and decrease of the electron temperature until the two temperatures are about equal (T_e=T_g), the distribution of all species becomes thermal equilibrium [29]. Non-thermal plasma or cold plasma is particularly suited to apply to textile processing which without excessive heat causing substrate degradation. In recently, the applications of cold plasmas are used widespread in textile and use in a variety of fields.

2.2 Generation of cold plasma for using in textile applications

In addition to low and high temperature plasmas, they are distinguished by the ways of plasma generation. The cold plasma is obtained at low pressure or low temperature. It is widely considered for surface modifications while the thermal plasma is produced under atmospheric pressure at high temperature. A comparison of difference in the two processes appears in Table 2.1.

Although two ways of plasma generation can be used in material processing, the only ones applicable to treatment textiles at this time are the cold plasma. Because textiles require lower plasma densities and energies in order to heating will not alter the fabric or fabric treatment. Hence, this thesis will focus on only non-thermal or cold plasma or low pressure plasma for modification of textile surfaces. Fortunately, plasma exists in various forms and a lot of it can be applied to study and control the parameters that make it possibly achieve desired outcomes on textiles surface. In recent years plasmas have continually development and creation of plasmas for application on textiles surface. Different manufacturers of equipment for plasma treatment can be classified according to the nature of energy

Table 2.1: Comparison of different in two process of thermal plasma and cold plasma.

	Thermal Plasma	Cold Plasma
Pressure	Atmosphere	Low (> 1 Torr)
Appearance	Inhomogeneous	Homogeneous
Plasma State	Equilibrium	Non-equilibrium
Types	Plasma jet, DC corona torch Arc discharges	Glow discharges, RF, Microwaves
Uses	Ultra-fine particle spraying, Sputtering	Deposition Surface treatment

input and the gas pressure. The most widely used method for plasma generation utilizes the electrical breakdown of a neutral gas in the presence of an external electric field. Two different forms of electrical discharge in gases depend on the gas pressure [30].

(1) Corona discharge is generated at gas pressures equal to or near to the atmospheric pressure with an electromagnetic field at high voltage (>15 kV) and low frequency in the 20-40 kHz range for most practical applications.

(2) Glow discharge is generated at gas pressures in the low pressure range (0.1-10 MPa) with an electromagnetic field in a lower voltage range (0.4-8.0 kV) and a very broad frequency range (0-2.45 GHz).

Cold plasma or low pressure plasma, also known as glow discharge plasma, is one of the earliest applications on plasma treatment of textiles. A vacuum chamber is necessary for low pressure plasma generation. To better understand of cold plasma system, Figure 2.5 shows a scheme of the different parts that usually compose a cold plasma reactor including six modules or functions: pumping system, power supply, matching network, reactor chamber, controller (gauge and mass flow) and substrate holder.

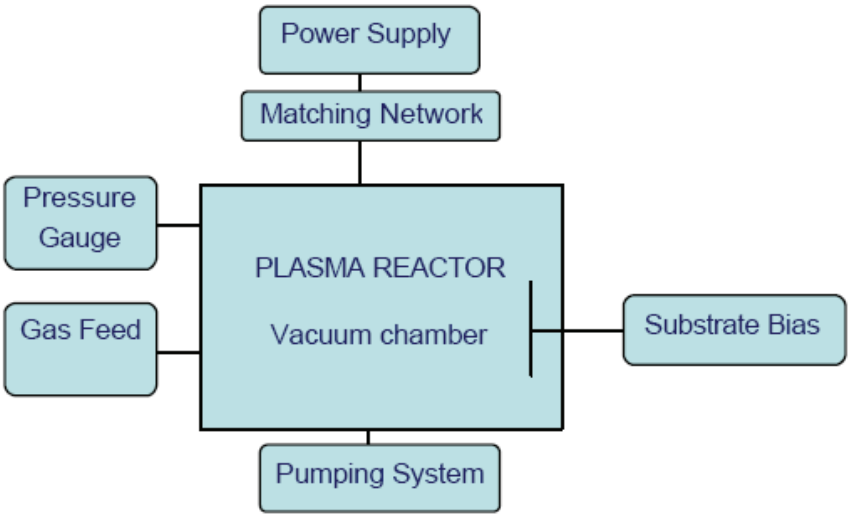

Figure 2.5: Scheme of components of a cold plasma reactor

Cold plasma systems have become a very important tool for nanotechnology processing for the production of textiles and the modification of materials. It is confirmed methods for surface modification because of the stability of the discharge. It is generally operated at pressure range from 0.1 - 3.5 Torr and the plasma excitation power is in the range from 50 W to 5000 W which depend on the size of reactor [31]. Plasmas can be generated in the wide range of plasma sources depending on the application. Recently, plasma rectors have been built utilizing a wide range of several frequencies from direct current (DC) to microwave (MW) discharge.

DC plasma is not advantage due to the need for current limiting resistor to stabilize the plasma. Most plasma reactors are used in AC electrical power supplies by operating at audio, radio or microwave frequency. The power supply of plasma generation is usually operated at low frequency (LF, 50-450 kHz), radio frequency (RF, 13.56 or 27.12 MHz) and microwave (MW, 915 MHz or 2.45 GHz) [31]. The excitation frequency is important because it influences the behavior of the electrons and the ions of the plasma.

Low frequency (LF) plasmas (50-450 kHz) are sometimes used because the generator is less expensive than other frequencies and they do not require precise impedance matching. However, it is found that the reaction rates tend to be slower than with RF and MW frequencies and there is more of a tendency to arc at LF.

Radio Frequency (RF) plasma (13.56 - 27.12 MHz) is easily generated with equipment that is stable and reliable. It is necessary to use a matching network to match the impedance of the plasma with the generator output which can be accomplished either manually or with automatically. At frequencies of 13.56 MHz or higher, the plasma is very stable and reactive because the quenching time of the plasma species is longer than the half cycle period of the applied field [32].

Microwave (MW) plasma (2.45 GHz) is often more reactive than RF and the MW generator may be less expensive. In recent years, there has been a continuous shift from RF to MW plasma generations. However, the development of plasma sources operating with cold plasma was strongly linked with the requirements for industrial treatment of textiles.

2.2.1 Direct current (DC) discharges

Cold plasmas in DC discharges are generally created in closed discharge vessels using interior electrodes. Different types of discharges and plasmas can be obtained depending on the applied voltage and the discharge current as shown in Fig.2.6 [33]. It shows the variation in the existence of plasma as the current is increased. The townsend discharge is a self-sustained discharge characterized by a low discharge current. The transition to a sub-normal glow discharge and to a normal glow discharge is marked by a decrease in the voltage and an increase in the current. In an abnormal glow discharge develops as the current is increased even further. Finally, at very high currents, the discharge undergoes a transition down into an arc. For arc discharges, due to heavy bombardment of the cathode at high currents reach temperatures which are too high for safe surface modification techniques. Therefore, the corona and glow discharge regions are normally

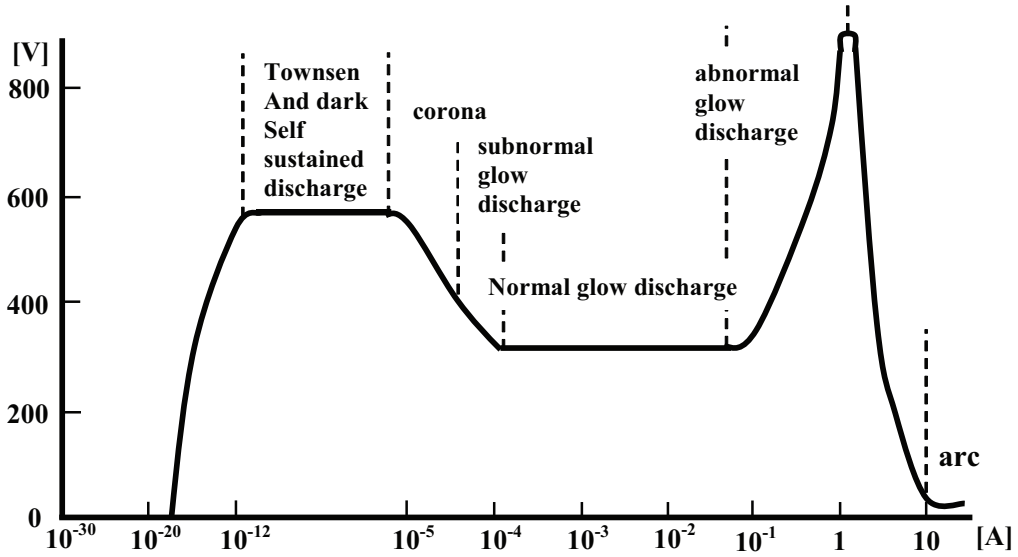

Figure 2.6: Diagram of voltage-current characteristics of various kinds of DC discharge [31].

suitable for surface modification. The corona region of dark discharge is used in atmospheric plasmas while cold plasmas usually lie in the normal glow discharge region [34].

In direct current (DC) discharge is produced by applying a DC voltage between two conductive electrodes inserted into a gas at low pressure as shown in Fig. 2.7. DC glow discharge consists of the cathode which is the electron emitter and the anode receives the electrons. A DC glow discharge at high-impedance power supply is used to provide the electrical field. It is the mechanism to sustain the plasma which involves the bombardment of the cathode with positive ions, resulting in the generation of secondary electrons. The secondary electrons in turn are accelerated away from the cathode until they have gained enough energy to ionize a molecule lead to the glow discharge self-sustaining plasma. The discharge in a long cylindrical tube with dielectric walls shows different characteristic regions as show in Fig. 2.8 [34].

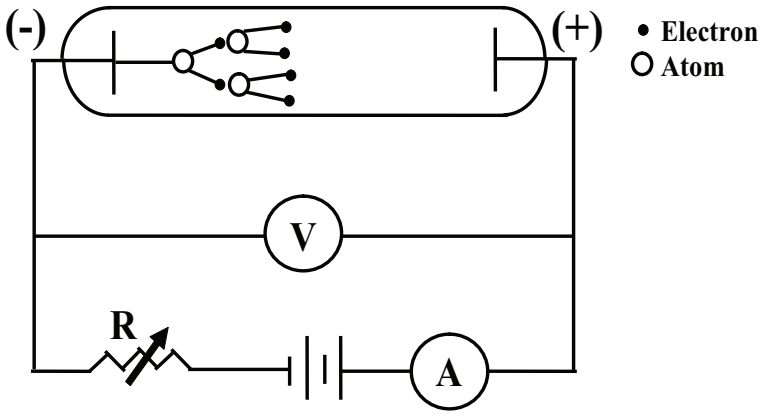

Figure 2.7: DC glow-discharge set-up [28].

Figure 2.8 shows the variation of the different visible regions in normal glow discharge which is used explaining in DC glow discharge system. The process in the normal glow discharge occurs when a voltage difference is applied between two electrodes. Most of the applied voltage appears across the space between the cathode and the negative glow. When ions formed in the dark space and negative glow regions are accelerated into the cathode surface by the inelastic collisions, leading to excitation and ionization and causing secondary electron emission. The emitted electrons are then moved back across the dark space and cause ionization directly or by transferring their energy to electrons in the plasma. Here electrons equilibrate with the electric field and create the positive column [34]. This process creates a steady state discharge by keeping an equal ion-electron pair generation rate, and makes the glow discharge a self-sustaining plasma [35]. Therefore, the cathode regions of the discharge play a crucial role in sustaining the glow discharge. To avoid the redeposition of the sputtered on cathode, the magnetic field is added in perpendicular direction to the electric field lead to increasing the path length of the electrons. A high ionization rate and high plasma density are obtained. Recently, the magnetron discharge mainly applied in sputter devices by the application of an external magnetic field approximately parallel to the cathode surface as shown in Fig. 2.9. For sufficient low pressures (10^{-1} Pa), the electrons

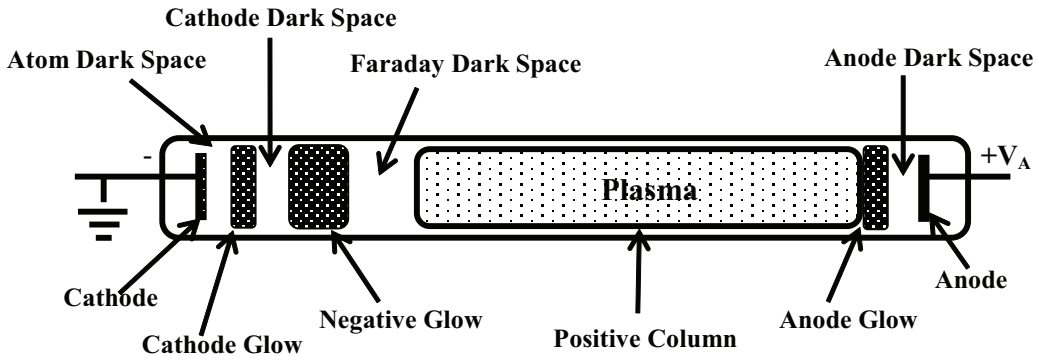

Figure 2.8: Variation of the different visible regions in normal glow discharge [32].

are trapped by rotation movement. This prolonged mean free path length enables a satisfactory ionization rate at very low gas pressures. The ions are not trapped and collide with energy for sputtering at the surface [36].

However, DC glow discharge is limited as narrow ranges of pressure, eliminating the contact between the electrodes causing substrate contamination and inhibit current conduction when it use with insulating materials [28]. For these reasons, the alternatives are the radio frequency (RF) (13.56 or 27.13 MHz) or microwave (2.45 GHz) discharges. DC glow discharges are mainly used as sputtering/deposition source, modifying thus the deposition rate, the physical proprieties of the deposited films [37]. In addition, it is used for sputtering gold on non-metallic surface for the purpose of scanning electron microscopy (SEM) to eliminate static charges and glaring under SEM.

2.2.2 Radio frequency (RF) discharges

Radio frequency discharges or RF discharges incorporate many of the same outstanding characteristic of the DC glow discharge, including sheath formation, which creates a strong electric field resulting in the acceleration of ions and electrons. In addition, at low frequencies, both DC and RF discharges behave similarly

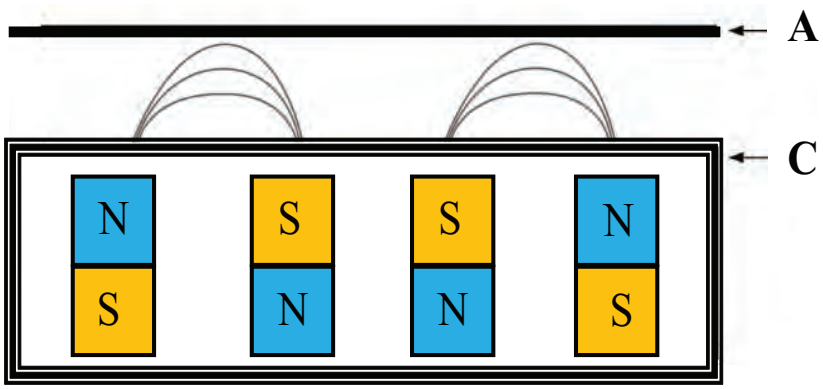

Figure 2.9: DC magnetron discharge. Magnetic field lines are sketched near the cathode. NS: permanent magnets with N and S pole, C: cathode and A: anode [33].

that are the ions collide with the electrode surface and generate secondary electrons while at the higher frequencies, the ions and the electrons cannot reach the electrode surface during the acceleration phase of the external electric field. The charge carriers are produced by electron impact ionization of heavy particles in the volume [34]. In the plasma technology, radio frequency power is mostly used in alternating current (AC) discharge. It is usually operated in the frequency range of 1-100 MHz, the wavelengths in rang of 3-300 meter and plasma density generated from RF is broadly range from 10^6 - 10^{10} cm^{-3}. However, the power supply must be connected with the reactor by via an impedance matching network which provides the power transfer is maximized and the reflected RF power is minimized [38].

In practice, radio frequency glow discharge processes operate at 13.56 MHz which is generally frequency in the standard industrial. It is applied with the system becomes high much enough frequency. It takes electrons and ions to traverse the sheath between the plasma and the electrodes. Electrons will instantaneously respond to changes in electric field as they oscillates, while ions respond to time-average changes due to their heavy mass and inertia [36]. Energetic ions striking

the electrode will cause the formation of secondary electrons, which can then be accelerated through the sheath and cause ionization. In addition, the oscillating electric fields in the plasma bulk can input energy directly into the electrons, similar to the positive column of the DC discharge. Finally, electrons in a RF discharge could thus accumulate enough energy to cause ionization even at low-electric field. As a result of this behavior, the RF discharge is more efficient than the DC discharge in promoting ionization and sustaining the discharge known as a "surf-riding" mechanism, unique to the RF discharge [34].

The major advantages of RF plasma generators are no internal electrodes and the plasma is easily sustained at a low pressure. So, it has no impurities or contamination of the process caused by material sputtered off the electrodes. Generally, there are two different principles of radio frequency discharges are used for coupling of the high frequency electromagnetic including inductively coupled plasma (ICP) and capacitively coupled plasma (CCP). The difference in the way of the RF field is induced in the discharge space.

The ICP methods are based on electromagnetic induction and require a high inductance between a coil and the plasma (large RF currents). In the CCP methods, the voltage from the RF generator is applied across the electrodes and requires a high capacitance between the electrode and the plasma (large amplitude RF voltages). In addition, in a capacitive discharge, the periodic electron current flow to the electrode causes a modulation of plasma potential. In an inductive discharge, the time varying current induces a time varying magnetic field which induces a time varying electric field that can sustain the plasma [39].

Capacitive coupled radio frequency (RF-CCP) discharges

Capacitively coupled reactors are the most widely used plasma source for materials processing. It generates the RF plasma between two electrodes with electron densities up to 10^{10} cm^{-3} and gas pressures between 10^{-1} up to 10^{3} Pa [35]. Capacitive coupled sources drive an alternate RF field across the electrodes in the

range of 1-150 MHz and RF voltage of 100 to 1000V [40]. In practice, many RF glow discharge processes operate at 13.56 MHz, because this is a frequency which can radiate a certain amount of energy without interfering with communications.

For plasma processing applications, capacitively coupled RF discharges, also called "RF-diodes", consist in the simplest case of a vacuum chamber containing two planar electrodes separated by a distance of several centimeters and an impedance matching network [41] as shown in Fig. 2.10 [36]. If moderate pressures, capacitively coupled RF discharges occur in two forms called α and γ modes [42], [43]. The α mode is characterized by lower currents and a positive V-I characteristic while the γ mode corresponds to higher currents and a partially negative V-I characteristic. The sheath regions in front of the electrodes are quite different in the two modes. Electrical conductivity and charge carrier concentration in the α sheath are very small which in contrast to the γ sheath. In addition, the α refers to the townsend ionization coefficient for charge carrier generation in the volume. In the γ mode refers to the electron generation by impacts of positive ions to the cathode surface [43].

Although capacitive sources work well for many processing applications, there are several disadvantages due to configuration of capacitively coupled reactors are limited to plasma densities of 10^{16} m^{-3}. Higher densities may be obtained by increasing the RF power which will increase the corresponding voltage across the electrodes. Electrons are then accelerated by a higher sheath voltage resulting in less efficient heating of the plasma bulk. This result leads to overall inefficiency of the device. However, the use of capacitive devices for commercial applications has continually increased.

Inductive coupled radio frequency (RF-ICP) discharges

Inductive coupled discharges by using radio frequency power supplies are widely used for plasma processing. The advantage of inductively coupled discharges is electrodeless ring discharge. The inductively coupled RF discharges

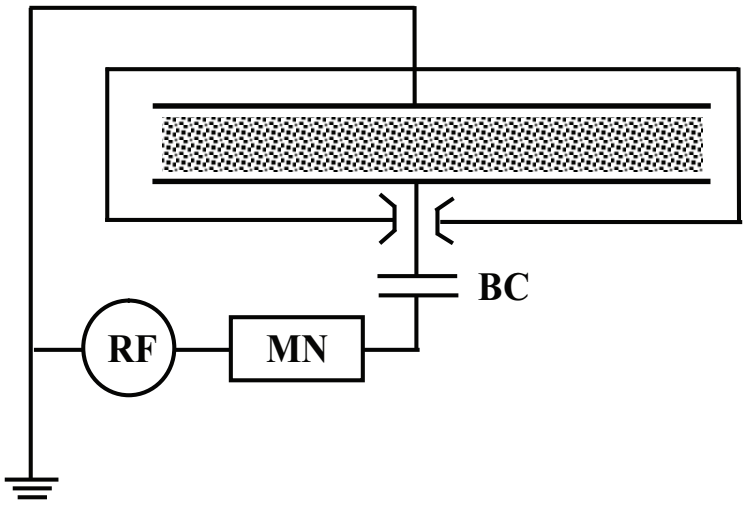

Figure 2.10: Schematic of a capacitive coupled RF discharge with parallel electrodes. RF: generator, MN: matching network, BC: coupling capacitor [34].

have two modes including the E mode and H-mode. At a low incident power, plasma ignites and sustains by a inductive coupling discharge are called E-mode while an inductive coupling discharge suddenly starts up as increasing an incident power is called H-mode [43]. Inductive coupled discharges are generally excited by two configurations which consist of a RF electric field from a helical coil surrounding the plasma volume or a RF electric field from a spiral coil in front of the plasma. These methods are shown in Fig. 2.11 [44].

In case of the inductive coupled discharges with a spiral coil configuration (Fig. 2.11(a)), the plasma generating voltage is induced by the varying magnetic field generated with the RF current in the exciting coil. The coupling between the coil and the plasma can be understood as a transformer with many primary windings of the coil and the plasma as one winding. For the inductive excited plasma typicaly high electron densities (10^{11}-10^{12} cm^{-3}) are achieved at low electric fields [45]. The inductive coupled plasma differs from the capacitively coupled plasma only by the small sheath voltage in front of the wall or of the substrate

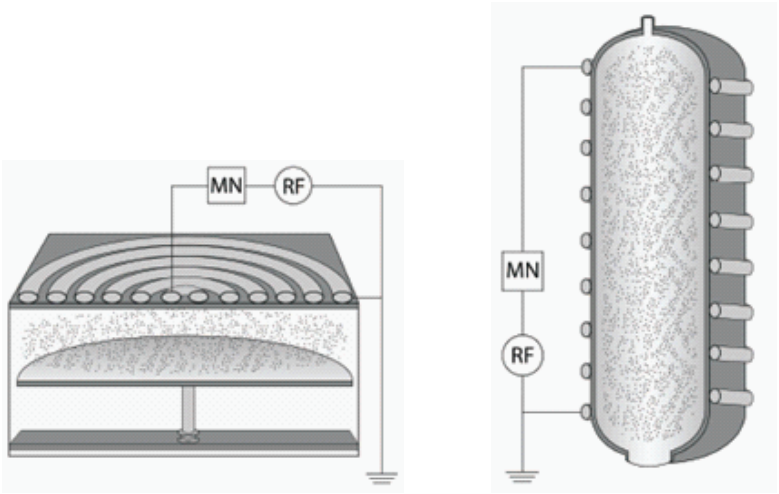

Figure 2.11: Schematic of an inductively coupled RF discharge with (a) spiral coupler and (b) helical coupler. RF: generator, MN: matching network [37].

(20-40V) such as low ion energies. The low kinetic energy of the positive ions makes plasmas suitable for material treatment with reduced surface damage of various heat sensitive materials. The application of a spiral coil in front of the plasma volume generates plasma for homogeneous treatment of a planar object.

For the inductive discharge in the helical coil configuration as shown in Fig. 2.11(b), a coil is wound around the discharge chamber. It is operated with a static longitudinal homogeneous magnetic field (0.005-0.03T) in a cylindrical vacuum vessel (10^{-2}-10 Pa). The helicon waves are generated by specially shaped antennas in the frequency range between 1-50 MHz. This type of discharge achieves electron densities of up to 10^{12}-10^{13} cm^{-3} in the 0.1 Pa pressure ranges [46]. However, this form of discharge is also maintained by electromagnetic field of the primary coil.

2.2.3 Microwave (MW) discharges

Plasma generation by microwaves is widely used in many applications. A characteristic feature of microwaves is the wavelength, which is comparable to the dimensions of the plasma apparatus (2.45 GHz,λ= 12.24 cm) and the short period of the exciting microwave field [35]. Microwave generated discharges are the cheaper and simpler method to achieve a higher degree of ionization which play an important role in surface modifications. Furthermore, it has effective power absorption in a broad pressure range 1-10^5 Pa, high electron densities ranged from 10^8 to 10^{12} cm^{-3} and low sheath potentials causing low ion energies at the wall or the target surface which can reduce the surface damage. In addition, the advantage of plasma generation by microwaves is an electrodeless discharge which eliminates the contamination of the reaction and the bombardment of the treated materials with energy ions which can extend the operating lifetime of the device in reactive gases.

Microwave excited plasma discharges are created a number of ways using microwave power supply, a circulator, the applicator, and the plasma load. The transmission lines are rectangular waveguides. In each of these applicators, the microwave generated in a source is transmitted to a vacuum region where the few free electrons are heated by the high frequency electric field. The applicator should optimize the energy transfer into the plasma and minimize the power reflection. However, the systems have a circulator to protect the power supply from reflected power. Subsequently, the energy of these primary electrons becomes high enough to insure an effective ionization kinetics and then to ignite and maintain the plasma discharge. The composition and temperatures of the obtained plasma strongly depend on the electromagnetic field which in turn is affected by the discharge. Microwave discharges can be generated in closed structures, open structures and on a plasma resonance as shown in Fig. 2.12(a), (b) and (c).

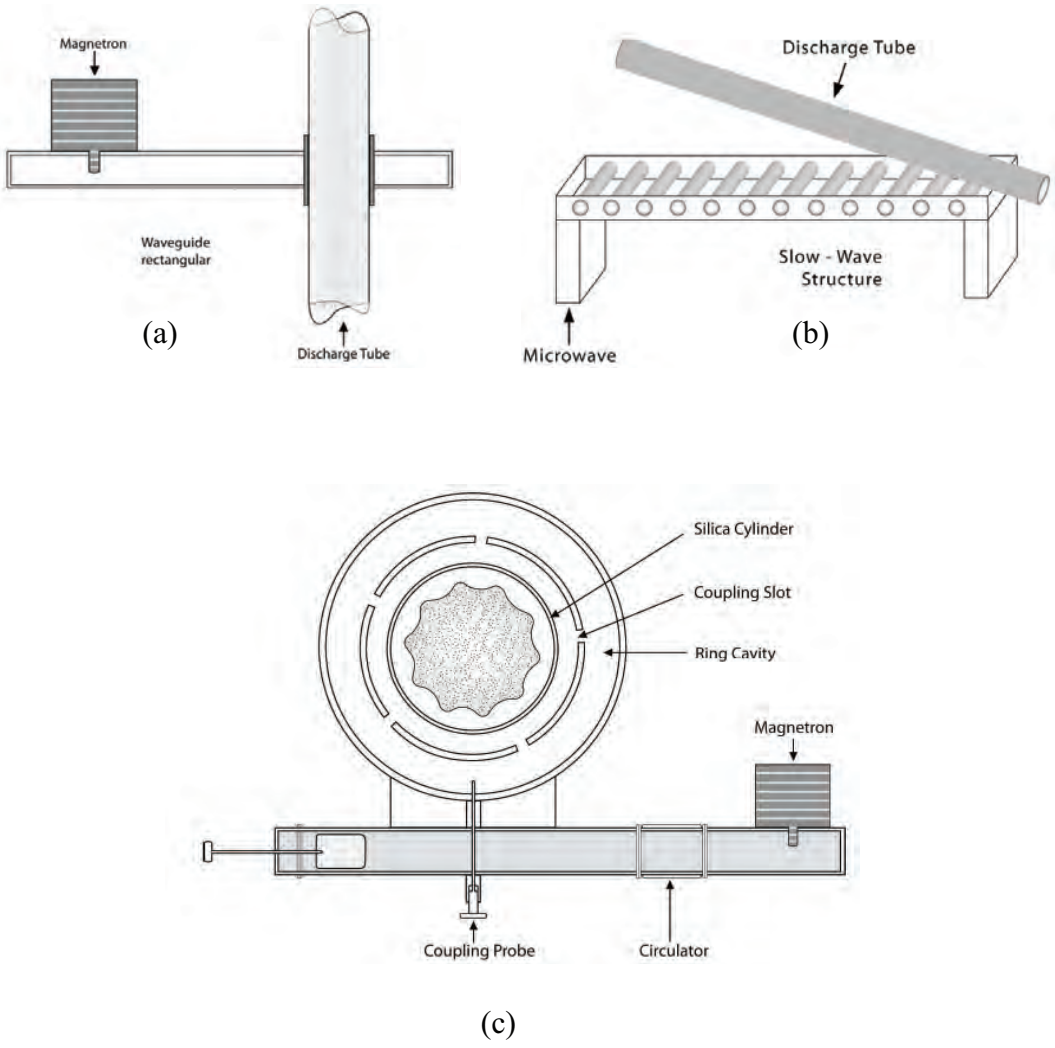

Figure 2.12: Scheme of the coupling of discharge tube and magnetron with (a) a rectangular wave guide and (b) a slow wave structure [47] and (c) the slot antenna plasma source (SLAN) [45,46].

The closed structures of plasma generation is achieved by the coupling of the discharge tube with a rectangular waveguide as shown in Fig. 2.12(a). The plasma chamber is surrounded by metallic walls. Resonant cavities of high quality with their high electric field allow an easy ignition of discharges, even at high pressure. For the example of plasma generation in open configurations is the slow wave structure as shown in Fig. 2.12(b) which the constant excitation is achieved by the varying distance between exciting antenna and plasma tube.

The microwave excitation of large volume plasma in a broad pressure range (10^{-3}-10^{5} Pa) can be generated by a plasma resonance are the slot antenna (SLAN) plasma sources as shown in Fig. 2.12(c). The microwave energy is transferred from a ring cavity through equidistantly positioned resonant coupling slot antennas into the silica cylinder. Between the generator and the plasma load have a port circulator directs the reflected power from the plasma into a water-cooled dummy load to protect the magnetron from possible damage. In order to match the impedance of the plasma, the immersion depth of the capacitive coupler into the ring resonator can be varied. Furthermore, the end position of the input waveguide is adjustable by means of a shorting plunger. These two degrees of freedom for the matching system allow for adjustment of the impedance of virtually any plasma load to the waveguide impedance. The homogeneity power distribution is achieved by the resonant ring cavity [49].

2.3 Fundamental interaction in cold plasma and textile surfaces

Solid surfaces and phenomena which occur at their surfaces are very important in various fields of science and engineering. Every material, whether textiles, metals, and ceramics has a surface at the boundary with air or has an interface where it contacts another material [50]. The chemical and physical properties at the surface are different from those of the bulk material and special functions may operate at the surface or the interface such as hydrophobicity and hydrophilicity etc. The surface modification of textiles with cold plasma is a useful way to obtain functional textiles by controlling their surface properties. However, plasma surface modification technique is restricted to a shallow depth of the material (1000 ^{o}A) undergoing surface modification and the deeper layers of bulk material should not be modified or maintains original properties.

Generally, the characteristics of plasma-treated surface might involve reactive species such as positive and negative ions, neutral species, atoms, metastables and free radicals in plasma which results mainly from inelastic collisions of species in the gaseous phase between electrons and heavy species or collisions between heavy species. Therefore, the chemical reaction in plasma a large number of involves elementary reactions. The various kinds of main reactions in the plasma include excitation, ionization and dissociation as shown in Fig. 2.13.

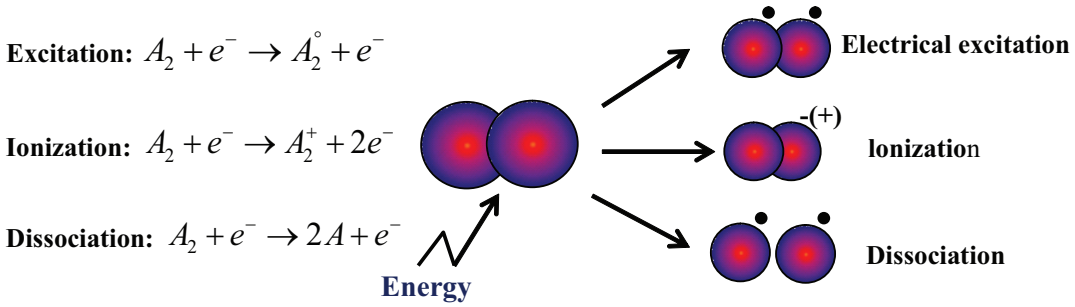

Figure 2.13: Elementary processes occur in cold plasma

For Fig. 2.13, the excitation process involves increase of translational energy and transition of internal energy to a higher state. When energy is given in excess of that required for excitation, most loosely bound electrons are removed from an atom causing ionization. The electron impact ionization is the major source of charged species in the discharge. Normally, the energy required for ionization is greater than that of dissociation. Excitation and ionization may be due to the reactions by electron collision, ion collision, neutral particle collision and radiation. In case of the dissociation occurs as a result of inelastic collision of a molecule with an electron, ion and photon. Therefore, the neutral fragments, either hot or in an excited state that which are generated by this process will impact on the substrate surface and they affect the process chemistry.

In addition, the generation of reactive species (positive and negative ions, atoms, neutrals, metastables and free radicals) causing lead to the chemical and physical interactions between the plasma and the substrate surface. The effects of plasma on material surface are discussed based on the phenomena of plasma-surface interaction in the plasma bulk. When ions and neutral species in plasma collide with the molecules on the substrate surface, and then etch away physically lead to etching effect. From this result, the long molecular chains were broken into short ones or call chain scission. Also, the reactive species lead to chemical interaction with surface molecules, generating new functional groups or functionalizations and radicals. Radicals induce cross-linking generation a few mono-layers on the upper of surface. In addition, they can result in deposition or plasma polymerization which is obtained by using monomer gas. Therefore, in plasma treatments are normally found in four major effects on surfaces as shown in Fig. 2.14 [51].

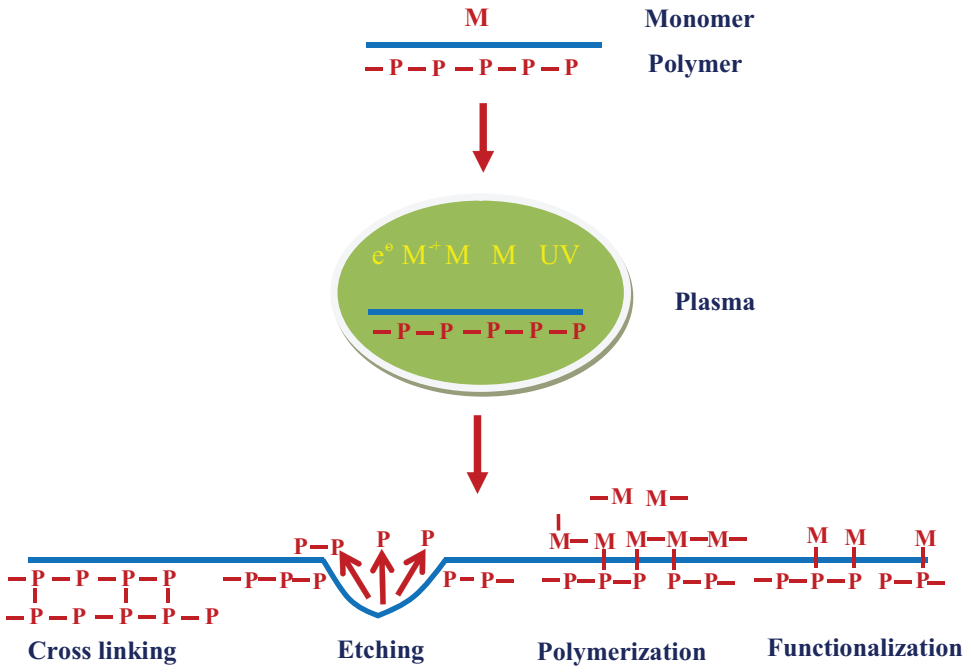

Figure 2.14: Phenomena of plasma-surface interaction in the plasma bulk occur in cold plasma [49].

2.3.1 Etching on textile surfaces

Plasma etching involves the mechanical removal of surface contaminants such as cutting oils, skin oils mold releases by energetic species and ion bombardment. For the surface contaminants of textiles, etching process breaks down weak covalent bonds (C-H bonds) in textile contaminants under the influence of ions, free radicals and electrons of plasma. Surface contaminants undergo repetitive chain scission until their molecular weight is sufficiently low for them to boil away in the vacuum that is the reactive species collide with the molecules on substrate surface, and the etching species could be re-deposited by interaction with the active particles on the substrate surface [52]. Etching affects only the outermost molecular layers of the textile. The process of etching reaction can conclude the steps as follows [33]:

1) Removal or penetration of adsorbed mono-layers by energetic ions and etching species

2) Adsorption of etching species on the surface of the layer to be etched

3) Dissociation of the molecules of the etching species

4) Formation of a reaction product on the surface

5) Desorption of the product molecule

Therefore, the deposited species would generate new polymer layers or tiny particles. The new polymer layers would be etched by the ions in plasma, and deposited again. The etching and deposition processes are repeatedly conducted. Also this reason, the etching effect obtains both surface morphology change and surface roughness change of the substrate surface. Generally, argon, helium and oxygen are often used for its high etching efficiency [53].

2.3.2 Functionalization on textile surfaces

Surface functionalization by plasma treatment occurs via the chemical interactions between gas phase species and activated radicals on the substrate surface. For this reason, functionalization is directly dependent on the type of plasma gases such as oxygen, nitrogen and ammonia react with the surface. In the case of textiles, these processes refer to the activation of surfaces of textiles by attaching different active species on the surface. The surface activation involves the radical formation and then replacement of chemical groups on textile surface from the plasma gas [54]. So, the radical formation is essential to initiate functionalization on textile surface. The collisions between active species, UV-radiation and molecules on substrate surface lead to the radical formation and formation of functional groups by chain scission of molecules and abstraction of atoms as shown in Fig. 2.15.

Radical formation by abstraction of atoms

When the active species in the plasma interact with textile surface, it can break down weak surface bonds in the textile by elimination atoms on the backbone

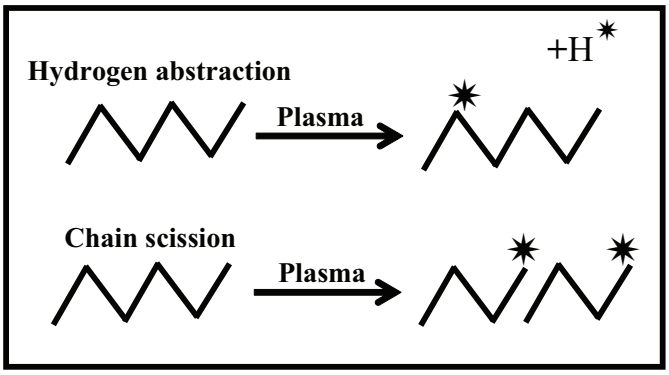

Figure 2.15: Formation of free radicals on surface by abstract hydrogen from the textiles chain and chain scission[51].

of molecules of textiles surface, causing the generation of carbon radicals on textile surface. Then, chemical combination of carbon radicals with other radicals in the plasma lead to the formation of functional groups on the textile surface as shown in Fig. 2.15.

Radical formation by chain scission

The chain scission happen when electron and ion bombardments on textile chains result is chain scission of polymer chain and formation of radicals at the end of polymer chains leading to the reduction of molecular weight on the textile surface and occurring carbon radicals. The results of chemical combination of carbon radicals with other radicals in the plasma can formation of functional groups on the polymer surface as shown in Fig. 2.15. For the applications, the characteristics of functional group on the surface such as wetting and adhesion can enhance adhesive strength and permanency lead to the improvement in the production of characteristic fabrics [53]. For example of functionalization as shown in Fig. 2.16, the surface of polyethylene which normally consists of only carbon and hydrogen, after treatment with plasma of oxygen and nitrogen can produce the functional groups on surface such as hydroxyl, carbonyl, peroxyl, carboxylic, amino and amines to obtain of hydrophilicity.

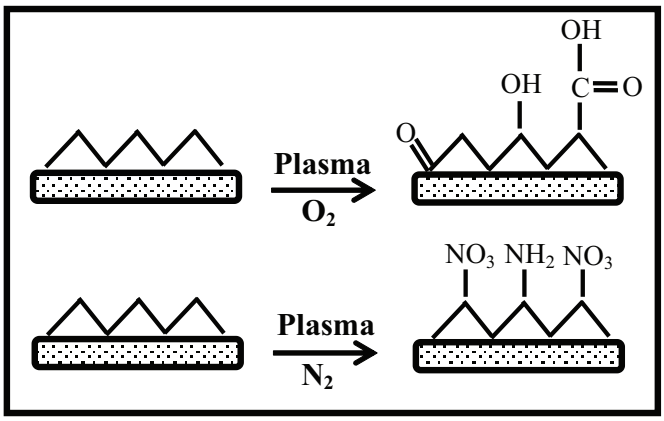

Figure 2.16: Surface activation with O_2 and N_2 plasma by substituting hydrogen in a polyethylene chain with other groups [51].

2.3.3 Crosslinking on textile surfaces

Crosslinking occurs when two polymer molecules join to form one large molecule or network. This happens when radical sites are created in the textile resulting in the setting up of chemical links between the molecular chains of textiles. Generally, plasma-induced crosslinking employs inert gases such as argon or helium to remove some atomic species from the surface, and generates reactive surface radicals. These radicals react within the surface forming chemical bonds, which results in cross-linked surface. The crosslinking process with inert gases can produce a stronger and harder substrate microsurface. In addition, crosslinking through plasma treatment can also give additional wear or chemical resistance to a material [53]. In comparison the crosslinking process with other processes, it is well known that the radical formation is related to ion bombardment and UV-radiation. Cross-linking can be obtained by recombination of molecular radicals, leading to the increase of higher molecular weight molecules, while chain scission in etching process reduces molecular weight. In addition, chain scission occurs at the surface while cross-linking is dominated in the subsurface. Ion bombardment produces the radicals introducing mainly surface functionalization, while UV photons have sufficient energy to penetrate much deeper into the textile substrate, and then create radicals [55].

2.3.4 Polymerization on textile surfaces

Besides the surface activation of textiles by a simple modification of the surface structure of the material or functionalization by using non-polymerizable gases such as O_2, N_2, H_2, NH_3,CO_2, etc. The plasma polymerization process, which can produce thin films with unique chemical and physical properties, has also found in various textile applications. In this process, gases in the plasma undergo polymerization through a free-radical initiation process. Then, propagation of the reaction is the actual formation of polymeric chain. Methane, ethylene, propylene, fluorocarbon monomers and organosilicon compounds can be polymerized by this method [56]. In recently, plasma polymerization often refers to as plasma-induced grafted-polymerization procedure which knows as a novel method for application on textile without affecting the bulk properties. This method can show in a single step for activation of surface by inert gas plasma and simultaneous grafting and polymerization of a non-volatile monomer in the plasma chamber as shown in Fig. 2.17 [57]. The plasma initiates polymerization at the surface of liquid or solid monomers which must contain polymerizable structures such as double bonds, triple bonds or cyclic structures. It differs from plasma polymerization in which the plasma gas itself is a monomer. The advantage of as plasma-induced polymerization procedure is the polymerization occurs with structure retention of the monomer. Furthermore, the desired properties are obtained by creating covalent bonds between the substrate and the growing polymer on the surface leading to a durable effect.

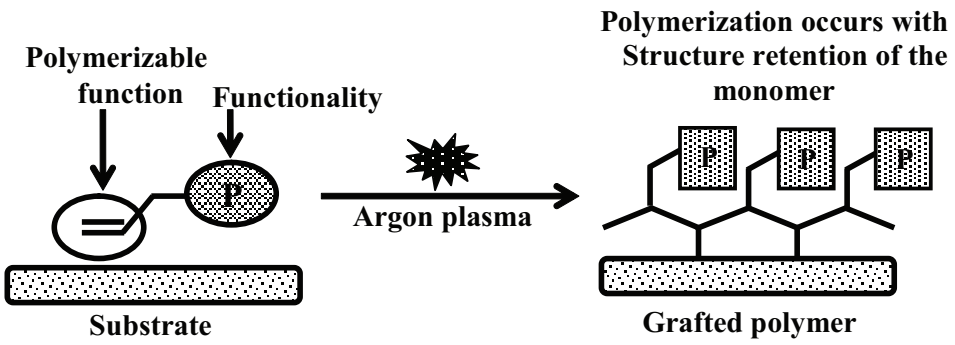

Figure 2.17: Plasma-induced grafted polymerization (PIGP) procedure [57].

2.4 Factors affecting plasma treatment on textile surface [30]

Plasma is a gases mixture consisting of electrons, charge ions, molecules and atoms. Many reactions occur simultaneously in a plasma system. Therefore, the effectiveness of plasma treatment on textile or polymer depends on several different factors. Factors which have the effect of plasma treatment consist of the nature of gas used, pressure, power, flow rate, duration of treatment and ageing of the plasma-treated surface.

2.4.1 Nature of gas

The result of plasma treatment and the characteristics of plasma depend strongly on the nature of the gas used in glow discharge. The glow discharges of non-polymerizing gases such as noble gas, nitrogen, oxygen, hydrogen and ammonia can modify polymer surfaces through processes, such as oxidation, ablation, cross-linking and grafting.

Inert gas : The inert gases such as helium, neon, and argon are commonly used in plasma technology. Mostly, inert gas plasma has been used for the pre-treatment of substrates for cleaning purposes before reactive gases are applied. Treatment of polymer surfaces by exposure to inert gas plasma has been utilized to improve the adhesive characteristics of polymers. The exposure several minutes of treatment with inert gas are sufficient to abstract hydrogen and to form free radicals at or near the surface, which then interact to form cross-links and unsaturated groups with chain scission. The gas plasma also removes low-molecular weight materials or converts them to a high-molecular weight by cross-linking reactions. This treatment has been known as cross-linking by activated species of inert gases.

Oxygen-containing gas : Oxygen and oxygen-containing plasma are most commonly employed to modify polymer surfaces. It is well known that the oxygen plasma can react with a wide range of polymers to produce a variety of oxygen functional group, including C-O, C=O, O-C-O and C-O=O at the surface. For example, oxygen plasma has two processes which occur simultaneously including etching and functionalization of the polymer surface. It can generate the reactions of atomic oxygen with the surface carbon atoms and the formation of oxygen functional groups at the polymer surface through the reactions between the active species obtained from the plasma and surface atoms.

Nitrogen-containing gas : Nitrogen-containing plasma is widely used to improve wettability, printability, bondability and biocompatibility of polymer surfaces. Mostly, it is used to improve the interfacial strength between fibers and matrix.

Fluorine-containing gas : The fluorine-containing plasma can occur simultaneously of surface reactions, etching and plasma polymerization which reactions predominate will depend on the gas feed, the operating parameters and the chemical nature of the polymer substrate and electrode. Halogen atoms, especially fluorine and chlorine atoms are the major etching species for a variety of materials. Ions and electrons can influence the plasma-substrate interaction process. Their bombardment of the surface can either alter the surface bonds of the lattice or promote the desorption of some chemisorbed species. The extent of bombardment can influence the etching rates, degree of anisotropy and polymerization. For example, tetrafluoromethane shows the highest relative etching characteristics for a material reactive with fluorine atoms.

Hydrocarbon : Hydrocarbons, such as methane (CH_4), ethane (C_2H_6), ethylene (C_2H_2), acetylene (C_2H_2)and benzene (C_6H_6), have been widely used in the generation of plasma-polymerized hydrogenated carbon films. The outstanding

physical properties of these films, such as microhardness, optical refractive index and impermeability, provide them with numerous potential applications such as anti-reflection and abrasion-resistant coatings.

Halocarbon : Plasma of fluorine-containing inorganic gases, such as fluorine (F), hydrogen fluoride (HF), nitrogen trifluoride (NF_3), bromine trifluoride BrF_3), sulphur tetrafluoride (SF_4) and sulphur hexafluoride (SF_6), is used to incorporate fluorine atoms into polymer surfaces to produce hydrophobic materials.

2.4.2 Pressure of system

The pressure system used may affect the energy of the plasma species. If the pressure is high (>1 mbar) causing of collision between plasma species will be increased which lead to the loss of energy of the species before interacting with the material. At a low pressure (<1 mbar), the collision of gas molecules with the material surface is higher than the collision of gas-gas collision [15].

2.4.3 Discharge power

The intensity of plasma is a combined factor of pressure and discharge power. Normally, the higher the discharge power applied, the more kinetic energy the plasma species will carry, resulting in strong intensity of plasma action. In general, there will be a change in the total amount of the excited particles inside the plasma and their energy level accordingly when the input power increases under a constant pressure, resulting in the increase in the charged ion concentration.

2.4.4 Flow rate

The effect of gas flow rate can be explained by the number of reactive species. When the flow rate is further increased, the number of reactive species is also increased.

2.4.5 Duration of treatment

The duration of treatment plays an important role in the plasma treatment. Generally, the longer the duration of treatment, the more severe the modification of the material surface will occur sputtering or etching. A longer duration will not only affect the material surface but also provide an opportunity for the plasma species to penetrate into the interior region of the material. This may alter the morphology of the polymeric material. However, when the treatment duration is too long, this will adversely affect the material and therefore careful control of treatment duration is required.

2.4.6 Ageing of the plasma-treated surface

The concentration of functional groups introduced to a polymer surface by the plasma treatment may change as a function of time which depend on the environment and temperature. It is due to the polymer chains have much greater mobility at the surface than in the bulk, allowing the surface to reorient in response to different environments. Surface orientation can be accomplished by the diffusion of low-molecular weight oxidized materials into the bulk and the migration of polar function groups away from the surface. Ageing of plasma-treated polymer surfaces can be minimized in a number of ways. An increase in the crystallinity and orientation of a polymer surface enhances the degree of order and thus reduces mobility of polymer chains, resulting in slower ageing. A highly cross-linked surface also restricts the mobility of polymer chains and helps to reduce the rate of ageing.

Effects of environment : Various surface studies indicate that when the treated surface is placed in a low energy medium, such as air or vacuum, the decrease in surface energy is caused by the rotation of the polar groups in the bulk or the migration of low-molecular weight fragments to the surface to reduce the interfacial energy. The ageing of plasma-treated polymer surfaces is a very

complex phenomenon that is strongly affected by the treatment parameters, nature of the polymer and storage conditions.

Effect of temperature : The important factor that affects the ageing characteristics of a plasma-treated polymer surface is temperature. A lower storage temperature reduces the rate of ageing. The rapid change in the contact angle at high temperatures supports the idea that the changes in the surface structure are caused by polymer chain motion, resulting in reorienting the polar groups into the bulk.

2.5 Characteristic and mechanical physical and chemical properties of textile

Textile fabrics are planar structures produced by interlacing or entangling yarns or fibers. Each individual fiber is made up of millions of individual long molecular chains of discrete chemical structure. Generally, the polymeric molecular chains found in fibers have a definite chemical continuity which repeats itself along the length of the molecule. The total number of units which repeat in a chain varies from a few units to several hundred and is referred to as the degree of polymerization (DP) for molecules within fiber [58]. Generally, textile fibers are classified as two principle groups which consist of natural fibers and manmade fibers as shown in Fig. 2.18.

Figure 2.18 shows a classification chart for the type of fibers in which all fibers is classed together following similar chemical structure. From the classification chart of type of fibers, all fibers can classify two main types, Firstly, they come from natural sources which consist of animals, plants and mineral which do not require fiber formation or reformation are classed as natural fibers. Natural fibers include the protein fibers such as wool and silk, the cellulose fibers such as cotton and linen, and the mineral fiber such as asbestos. Secondly, man-made

fibers consist of fibers which are made by chemical synthesis are often called synthetic fibers such as the polyamides (nylon), polyesters, acrylics, etc. while fibers that are the polymers from natural sources fibers are called regenerated fibers or natural polymer fibers such as rayon, rubber, etc [59]. The distinction for two types of man-made fibers are synthetic fibers in which man is involved in the actual fiber formation process but regenerated fibers are provided by nature in ready-made form.

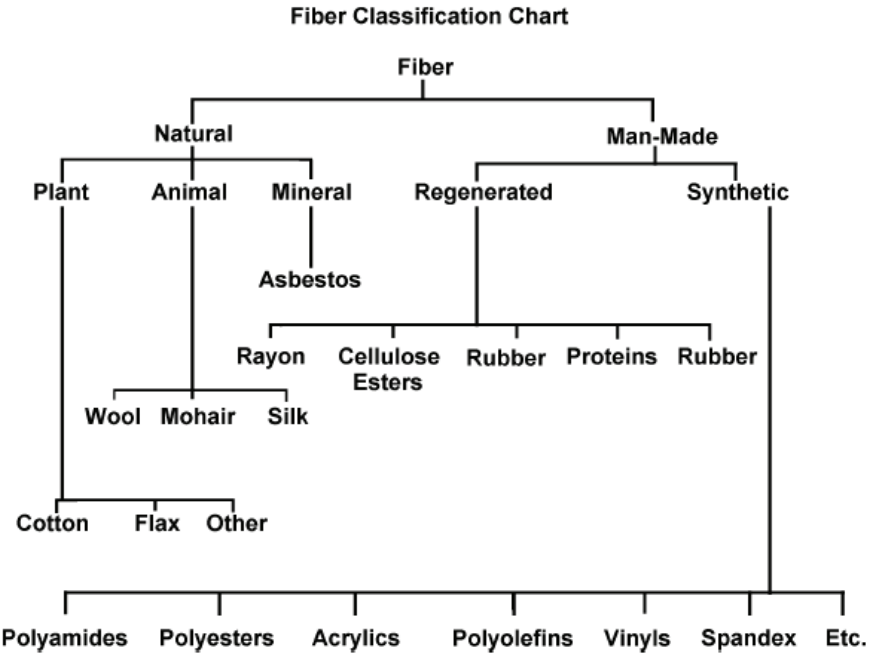

Figure 2.18: Classification chart of natural and man-made fibers [58].

2.5.1 Cotton fabrics for hydrophobic surface

Cotton is a soft fiber that grows around the seeds of the cotton plant. It is a valuable crop because only about 10% of the raw weight is lost in processing. Once traces of wax, protein, etc. are removed, the remainder is a natural polymer of pure cellulose. This cellulose is arranged in a way that gives cotton unique properties of strength, durability, and absorbency. Also, the hydrophilicity or superior absorbency of cotton in nature, coupled with its ability to desorb moisture,

makes it a very comfortable fiber to wear. Today, the main uses of cotton are in the form of garments, home furnishings, and industrial cloths. Cloth made of cotton is more comfortable, durable and suitable to resist all kinds of weather. The comfort quality of the cotton is due to its twisted or coiled shape. It traps air within the fabric structure and help for a thermal insulation process, resulting protection from heat in summer and cold in winter. Individual cotton fibers are ribbon structures which quite irregular diameter with periodic twists along the length of the fiber as shown in Fig. 2.19.

Figure 2.19: Structure of cotton with SEM (X1000)[58].

Structural properties

Cotton is composed of pure cellulose of a naturally occurring polymer. The cellulose molecule is a long linear chain of glucose units. All cellulose fibers cotton contains carbon, hydrogen and oxygen with reactive hydroxyl (OH) groups as shown in Fig. 2.20 [58].

The hydrogen bonds in cotton will hold several adjacent cellulose chains in close alignment to form crystalline areas called microfibrils. These microfibrils in turn align themselves with each other to form larger crystalline units called fibrils which are laid down in a spiral shape within the fiber.

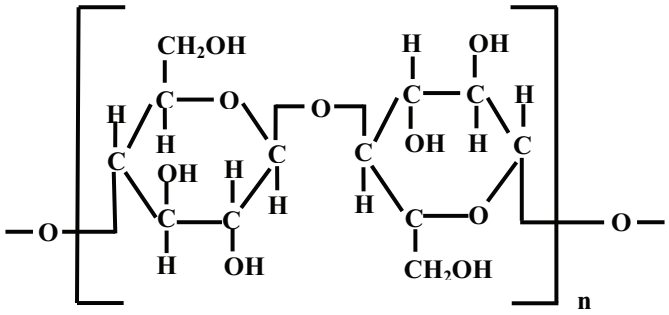

Figure 2.20: Chemical structure of cotton.

Physical properties

The high crystallinity associated with forces between chains in cotton result in a strong fiber about 2-5 gram per denier (g/d). The cotton fiber has enough strength in the dry and wet states. The tensile strength of cotton will change with changes in moisture content. It is found that wet cotton is about 20% stronger than dry cotton resulting from the increased strength of wet cotton which makes its long useful life. Cotton has low resiliency and poor recovery from deformation or it wrinkles easily in both the dry and wet states. Cotton has a density of 1.54 g/cm^3 and moisture regain of 7%-9% at standard conditions because the hydroxyl groups of cotton possess great affinity for water. The electrical resistivity of cotton is low at moderate relative humidity and it has low static electricity buildup characteristics [60].

Chemical properties

Cotton is hydrolyzed by hot dilute or cold concentrated acids to form hydrocellulose in which it is not affected by dilute acids near room temperature. Cotton has excellent resistance to alkalies and concentrated alkali solutions swell cotton, but the fiber is not damaged. Cotton is only slowly attacked by sunlight because cellulose lacks for the most part groups which absorb ultraviolet light between 300 and 400 nm. In addition, the degradation of cotton when it is heated in the air at 150 ^{o}C for long periods due to oxidation reaction and spontaneous ignition and

burning of cotton occurs at 390 ^{o}C. At low humidity in the absence of heat and light, cotton will not deteriorate over long periods of storage.

2.5.2 PET fabrics for hydrophilic surface

Polyethylene terephthalate or often referred to as PET is thermoplastic synthetic fibers in which it is part of the polyester family. It is an inexpensive fiber with a unique set of desirable properties such as highly elastic and resistant to wrinkling; possess high durability dimensional stability, resistant chemical and environmental attack. It is widely used for home furnishings and industrial applications. The suitability of polyethylene terephthalate for producing clothes is restricted because the characteristic of fiber is hydrophobic and nonabsorbent without chemical modification. In addition, polyethylene terephthalate is also difficult to dye due to its hydrophobicity and high crystallinity. Polyester fibers are usually smooth and rodlike with round as shown in Fig. 2.21.

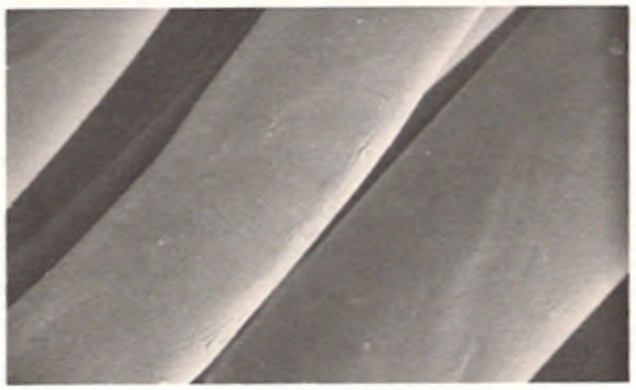

Figure 2.21: Structure of polyester with SEM (X1000)[58].

Structural properties

The structure of polyethylene terephthalate is formed through step growth polymerization of terephthalic acid with ethylene glycol as shown in Fig. 2.22. The polyester molecules within the fiber tend to pack tightly and are held together by

van der waals forces. It has highly crystalline because the polar ester groups in polyethylene terephthalate hold the polyester into strong crystals [59].

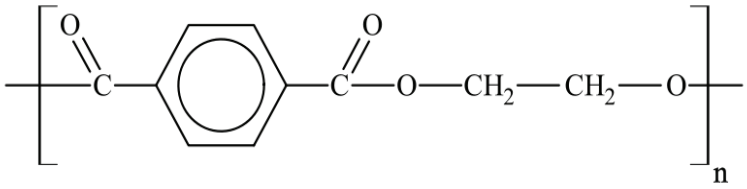

Figure 2.22: Chemical structure of polyethylene terephthalate.

Physical properties

Polyethylene terephthalate is an extremely strong fiber with a tenacity of 3-9 gram per denier (g/d). The elongation at break of the fiber varies from 15% to 50% depending on the degree of orientation and nature of crystalline structure within the fiber. The PET fiber shows moderate (80%-95%) recovery from low elongations (2%-10%). The fiber is relatively rigid and possesses excellent resiliency and recovery from bending deformation. The fibers have a density of 1.38 g/cm^3. It is quite hydrophobic with a moisture regain of 0.1%-0.4% under standard conditions. The fiber exhibits moderate heat conductivity and has high resistivity, leading to extensive static charge buildup.

Chemical properties

Polyethylene terephthalate is highly resistant to chemical attack by acid, bases, oxidizing and reducing agents. It is only attacked by hot concentrated acids and bases. On exposure to sunlight, the fiber slowly undergoes oxidative attack without color change with an accompanying slow loss in strength. On heating, the fiber softens in the 210^{o}C - 250^{o}C range with fiber shrinkage and melts at 250^{o}C - 255^{o}C. The burning of polyethylene terephthalate falls away from the unignited material and self-extinguishes lead to producing dark smoke and acid odor and exhibits a melt-drip characteristic.

2.5.3 Silk fabrics for flame retardant surface

Silk is a natural protein fiber excreted by the moth larva Bombyx mori which is known as the silkworm. Natural silk is highly appreciated for its mechanical properties and its outstanding characteristics such as luster, handing draping, resistant wrinking and comfort wearing. Therefore, silk fabric is widely used as blouses, dresses, scarves, pants and ties. It can also be made into curtains, draperies, cushion covers and sofa covers. In addition, silk is highly moisture absorbent so it is easy to dye with a wide variety of dyes and give dyed fibers with high colorfastness. Silk fibers are smoothing surface and translucent with some irregularity in diameter along the fiber as shown in Fig. 2.23.

Figure 2.23: Structure of silk with SEM (X1000) [58].

Structural properties

Silk fiber composes of two main parts called fibroin and sericin that holds the filament together. Both fibroin and sericin consist of the same 18 amino acids but different in their amounts. Sericin or silk gum is a minor component of silk fiber about 25% of silk fiber and it also has some impurities such as waxes, fats and pigments. It is a brittle and inelastic which conceals the unique luster of fibroin. Fibroin is the major component of silk fiber about 75% of silk fiber. It has highly oriented and crystalline structure. The fibroin contains repetitive amino acids

(Gly-Ser-Gly-Ala-Gly-Ala)n as shown in Fig. 2.24.

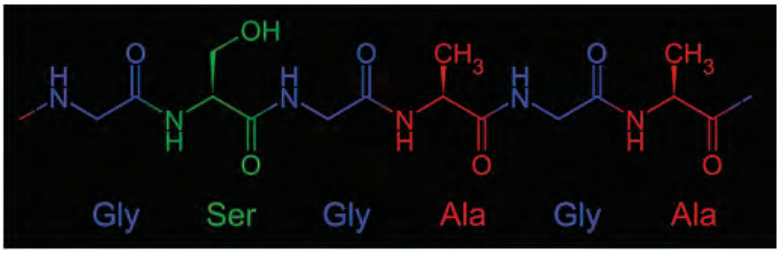

Figure 2.24: Crystalline structure of polypeptide chains in silk fibroin.

Physical properties

Silk is one of the strongest fibers which are only slightly less strong than steel wires but at the same time also one of the lightest. Silk has a dry tenacity in the range of 3 to 6 grams per denier and wet tenacity in the range of 2.5 to 5 grams per denier. At the same time it is very elastic fiber with an elongation value of 18 - 22%. It has good resiliency and recovery from deformation. Silk has a density of 1.25 - 1.30 g/cm^3 and it is very hygroscopic and absorbs moisture about 11% under standard conditions.

Chemical properties

Acids and allies cause hydrolysis of the polypeptide chains in the fiber. Acid hydrolysis tends to be more damaging to fiber than alkaline hydrolysis by acid hydrolysis occurs at nearly all the peptide linkages in the chain while alkali hydrolysis firstly attacks at the end of peptide chain. It is sensitive to chlorine bleaches and is easily damaged by sunlight. For the changing of thermal properties, silk burns slowly and self-extinguishes when removed from a flame.

2.6 Contact angle and young equation

When a liquid drop is placed on a solid surface, the angle formed by the solid surface and the tangent line to the upper surface at the end point is called the contact angle. It is know that a water droplet would try not to touch large area of the surface and the shape of the droplet would be spherical or the angle (θ) is greater than 90 degrees which are known as hydrophobicity (see in Fig. 2.25(a) on the left side). This condition is exemplified by poor wetting, poor adhesiveness and the solid surface free energy is low. For hydrophilicity surface, contact angles (θ) below 90 degrees indicate a water droplet would spread more on that surface. This condition reflects better wetting, better adhesiveness, and higher surface energy as shown on the right side in Fig. 2.25(a) on the right side [59]. Figure 2.25 (b) shows the schematic diagram of the contact angle and the surface tension forces of water droplet, due to the balance of surface tension forces at interfaces between solid/liquid (γ_{SL}), solid/vapor (γ_{SV}) and liquid/vapor (γ_{LV}) at equilibrium. The relation between contact angle and surface tension is determined by the Young equation which note that surface roughness is neglected given below [66]:

$$Cos\theta = \frac{\gamma_{SV} - \gamma_{SL}}{\gamma_{LV}} \tag{2.1}$$

2.7 Capillary theory

Capillarity is a phenomenon that allows a liquid to rise into a thin tube (capillary) as a result of differences in pressure across a curved liquid-solid interface. The most important mechanisms causing flow in permeable media are viscous forces, gravity forces, capillarity forces and diffusion [61]. For a capillary flow in fabrics, liquid rises in the fabrics structures follows the Washburn law, which gives the variation of the liquid height H as a function of time t in a capillary of radius R. Capillary rise method is used for the determination of the pore radius on the

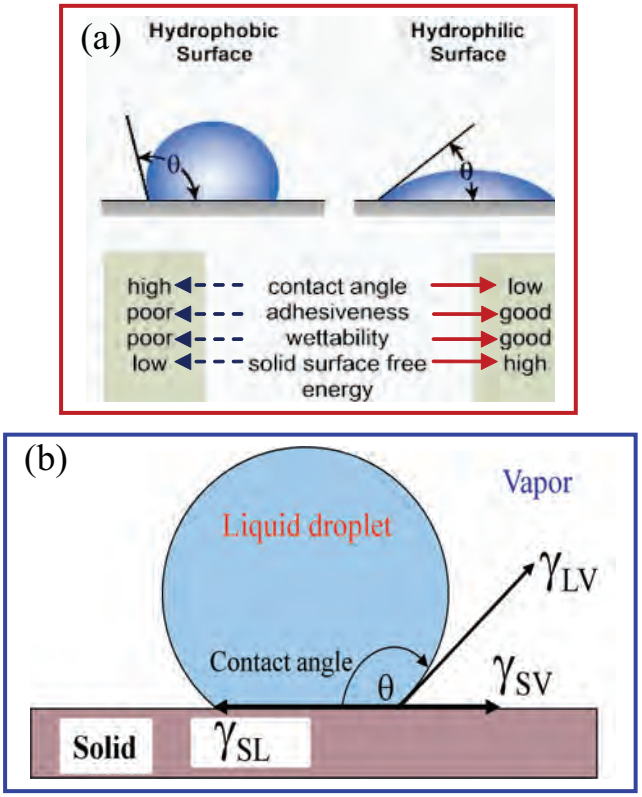

Figure 2.25: Schematic diagram of contact angle and surface absorbs water [61]

fabric surface by Lucas-Washburn equation. This technique has been quite popular in studying the porous structure of several inorganic materials and synthetic polymers [15].

2.7.1 Lucas-Washburn equation

A wetting liquid placed in contact with a textile yarn penetrates it. The yarn can be considered as assemblies of vertical capillary tubes of radius. In a capillary of radius, from a dynamic view point, the fluid progression is described by the following relation given by equation (2.2) [63].

$$\frac{d}{dt}(Mv) = F - F_\eta - P \tag{2.2}$$

where, M is the liquid mass, υ is the liquid speed, and F is the capillary force

$$F = 2\pi R\gamma \cos\theta \tag{2.3}$$

where, γ is the surface tension, θ is the contact angle, and R is the radius of the capillary. In a vertical capillary, it is given by

$$F_\eta = 8\pi\eta\upsilon H \tag{2.4}$$

where, F_η is the friction force, η is the viscosity, υ is the rise speed of the liquid, and H is the liquid front height.

$$P = \rho g\pi R^2 H \tag{2.5}$$

where, P is the column weight, g is the gravitational constant, and ρ is the liquid density. Generally, the progression of the fluid is slow and the inertia of the fluid can be neglected. Replacing every expression in Equation (2.2) by its value, the rise, in these conditions, is given by the Equation (2.6):

$$2\pi R\gamma \cos\theta = 8\pi\eta H\frac{dH}{dt} + \rho g\pi R^2 H \tag{2.6}$$

The Equation (2.6) allows writing the following one:

$$\frac{dH}{dt} = \frac{R}{8\eta H}[2\gamma \cos\theta - \rho gRH] \tag{2.7}$$

Equation (2.7) is called the "Washburn equation"

Assuming that the hydrostatic pressure can be neglected in the early stages of the process when the height at initial times is very smaller than the height at equilibrium, i.e., H << H_{eq}. The Equation (2.7) allows writing the following one:

$$\frac{dH}{dt} = \frac{R\gamma \cos\theta}{4\eta H} \tag{2.8}$$

An integration of Equation (2.8) with the initial condition (H=0 at t=0) [64] gives:

$$H^2 = \frac{R\gamma \cos\theta}{2\eta} t \tag{2.9}$$

where R represents the size of the equivalent capillary pore radius. This equation is used for investigating of the effective pore radius (R) when the liquid can penetrate in vertical plane of textile under capillary pressure. The distance traveled of liquid increases with both the surface tension in the solid-liquid interface and capillary pore radius. However, it is known that a wettability of liquid on textiles are formed a contact angle less than 90 ^{o} or approximated contact angle with liquid is zero (cosθ=1). Therefore, the expression of Equation (2.9) can be written as

$$\frac{2\eta H^2}{\gamma} = Rt \tag{2.10}$$

In equation (2.10) can separate determination of capillary pore radius R from the slope of the linear graph of the relationship between (2η H^2 /γ) and (t). In addition, from Equation (2.9) can be new written as

$$H^2 = D_C t \tag{2.11}$$

where D_C = R γ cos $\theta/2\eta$ is the diffusion coefficient of liquid which relates to the size of pore radius (R), the viscosity of the liquid (η) and surface tension (γ). This value can determine from the slope of plotting graph between H^2 and t which is linear.

2.7.2 Capillary rise in a textile

The movement of liquids in textiles is an interesting because the control of capillary penetration kinetics in textiles is an important in various applications such as dyeing, printing, coating, finishing, composite processing, liquid filtration, and thermal comfort [65], [66]. The spontaneous liquid penetration in fiber networks is due to capillary forces, which are governed by the liquid properties, liquid-media surface interaction, and geometric configurations of the pore structure in the media [67], [68]. When a capillary or a porous body is set in contact with a wetting fluid, the fluid spontaneously wets the pore walls and penetrates inside. Capillary phenomenon occurs when the free energy of the solid-vapor interface exceeds the free energy of the solid-liquid interface [69].

The study of capillary flow in fibrous materials can obtain better understanding of liquid-fiber contact and it paves the way to the characterization of textile structures, their heterogeneity, and more precisely their porosity resulting from the capillaries formed by the inter-filament spaces in which the liquid flows. The interaction of liquids with fibrous assemblies is normally described by wicking, liquid transport. Liquid-wicking into textile fabrics is further complicated by the surface roughness, the heterogeneity, the diffusion of liquid into the fiber, and the capillary action of the fiber assemblies [70], [71]. Many factors of textile structure and construction such as the type of weave pattern, density(g/m^2) of fabric, type of the fiber content, fiber fineness (ends/inch, picks/inch), and also the yarn parameters like the twist factors as well as the internal volume and the pore size distribution make the wetting phenomena of fabrics non-ideal [72]. Generally, fabrics consist of two surfaces, one which is macroscopic and visible by the naked eye, and another which is the actual inner surface comprised of the inter-fiber/filament space, the inter-yarn space and the pore size distribution. Thus, because of heterogeneous complex structure, which makes the plasma activation more complicated than for solid polymeric materials, the plasma treatments on textile fabrics are limited [73], [74].

Theoretically, the capillary rise in a textile is produced by the organization of the parallel capillaries, which is in fact a capillary system composed of individual fibers/filaments in yarns. The fabrics consist of straight yarns containing fibers/continuous filaments laid more parallel to each other yielding a higher axial liquid flow in the vertical direction (warp direction) and transverse flow in the horizontal direction (weft direction). The liquid flow is slightly interrupted in the interlacing zone only as shown in Fig. 2.26 [75]. In contrast, the flow front was either inhomogeneous, or the liquid wicking into the structured fabric did not occur spontaneously. It is due to absent of fully axial or transverse yarns resulting in a complex phenomenon of capillarity and wicking.

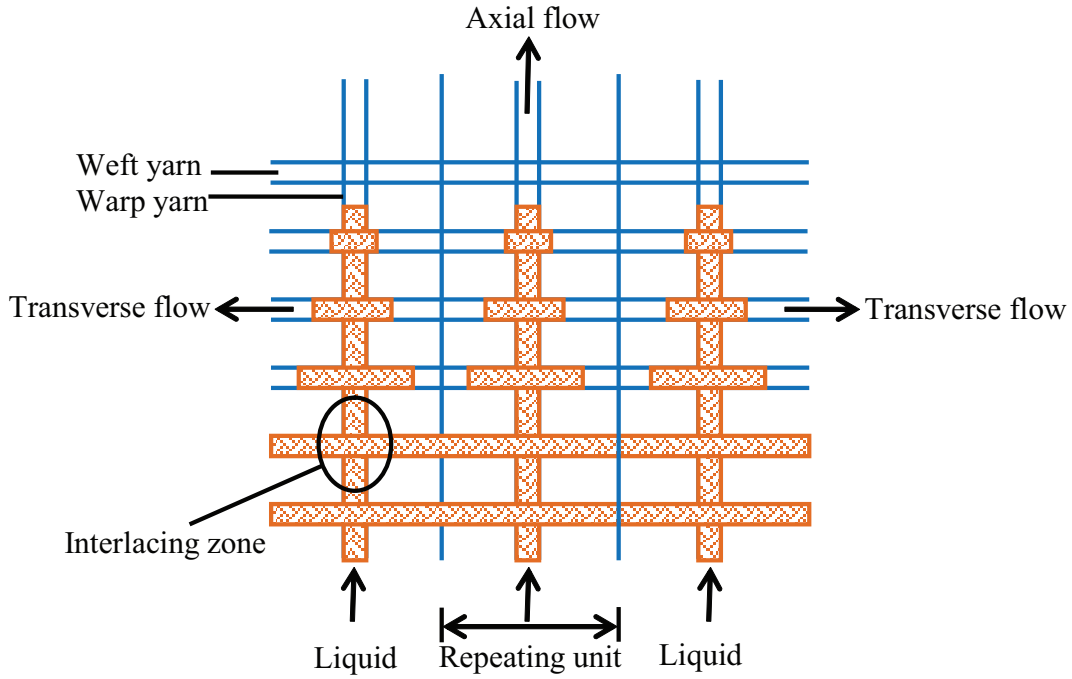

Figure 2.26: Simplified representation of the liquid flow in the plain weaved fabrics [16]

2.8 Mechanism of flame retardancy on textiles

In recently, we know that personal and property losses by fire occur mostly in residences such as furniture, electronic apparatus and clothes are frequently the fuel. One of the possibilities to make them more difficult to ignite and to significantly reduce the spread fire is the use of flame retardants. They can save lives, reduce injury, reduce economic loss, and reduce local environmental pollutants. One of all of materials which are excellent fuels of fire in residences is clothes and textiles.

2.8.1 Flammability of different textiles

All fabrics will burn but some are more combustible than others. The physical characteristic of fabric can obtain of different of ignition. The weight and weave of the fabric will affect how easily the material will ignite and burn. Heavy and tight weave fabrics will burn more slowly than loose weave and light fabrics of the same material. The surface texture of the fabric also affects flammability. Fabrics with long, loose, fluffy pile will ignite more readily than fabrics with a hard, tight surface.

Flame retardant systems for synthetic or natural fibers can act physically and/or chemically by interfering at particular stages of burning. In terms of flammability, most synthetic fabrics such as nylon, acrylic or polyester resist ignition. However, once ignited, the fabrics melt. This hot, sticky, melted substance causes localized and extremely severe burns. The natural fibers such as cotton, linen and silk burn more readily than wool, which is more difficult to ignite and burns with a low flame velocity. Acetate and triacetate are as flammable as or slightly less flammable than cotton. Nylon, polyester and acrylic tend to be slow to ignite but once ignited, severe melting and dripping occurs. Wool is comparatively flame-retardant. If ignited, it usually has a low burning rate and may self-extinguish. Glass fibers and moacrylic are almost flame-resistant. These syn-

thetic fibers are designed and manufactured to possess flame-retardant properties. The characteristic of burning of different textile fibers can conclude in Table 2.5.

There are many different fire retardant systems and they act in different ways. In order to understand how flame retardants reduce the flammability of polymer materials, it is necessary to explain the mechanism of flammability process.

2.8.2 Flammability process and flame resistant in a textile

To understand the action of a flame retardant first the process of ignition and burning is described in short. Fundamentally, four processes are involved in polymer flammability as shown in Fig. 2.27: (1) preheating, (2) decomposition, (3) ignition and (4) combustion and propagation.

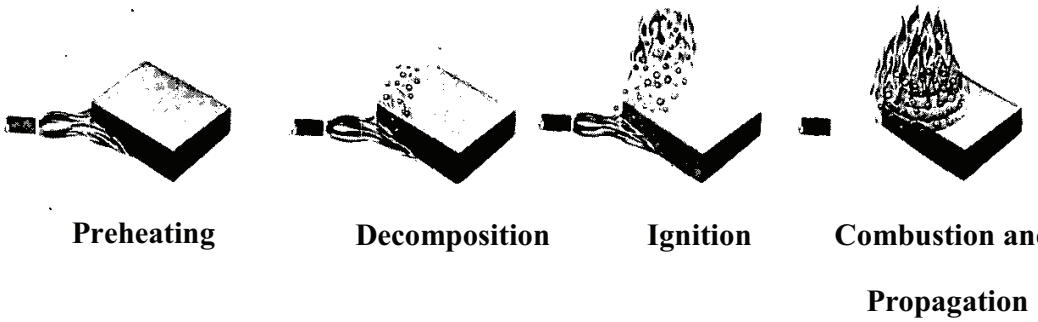

Figure 2.27: Process involved in polymer flammability [76]

Preheating involves heating of the material by means of an external source which raises the temperature of the material at a rate dependent on the thermal intensity of the ignition source, thermal conductivity of the material, and latent heat of fusion and vaporization of the material. When sufficiently heated, the material begins to degrade, for example it loses its original properties as the weakest bonds begin to break. Gaseous combustion products may be formed with the rate dependent on such factors as intensity of external heat, temperature required for decomposition and rate of decomposition. The products of this decomposition include combustible gases, non combustible gases and carbonaceous char.

Flammable gases increase until a concentration is reached that allows sustained oxidation in the presence of the ignition source, the ignition characteristics of the gas and the availability of oxygen are two important variables in any ignition process. After ignition and removal of the ignition source, combustion becomes self-propagating if sufficient heat is generated and is radiated back to the material to continue the decomposition process. The combustion process is governed by such variables as rate of heat generation, rate of heat transfer to the surface, surface area and rates of decomposition. Flame retardancy, therefore, can be achieved by eliminating any one of these processes.

2.9 Types of flame resistant for textile [77]

There are many different types of flame retardants which have working in different ways. Some flame retardants are effective on their own but sometimes are used cooperation with other flame retardants to increase the effective of flame retardant on textiles.

Halogenated compounds : The halogenated flame retardants, which contain chlorine or bromine atoms, are effective flame retardants in textile materials. These act by effectively removing the H^+ and OH^- radicals in the gas flame phase. These results can slow or prevent the burning process which lead to the reducing heat generation and so the production of further gaseous flammable material. The mechanism is as follows. When exposed to high temperatures, the flame retardant molecule releases bromine (Br) or chlorine (Cl), as free radicals (Br^- or Cl^-) which react with hydrocarbon molecules (flammable gases) to give HBr or HCl. These then react with the high energy H^+ and OH^- radicals to give water and the much lower energy Br^- or Cl^- radicals. However, the halogen-containing flame retardant mainly acts in the gas phase, resulting in the release of more toxic gases and smoke during combustion.

Organophosphorus compounds : Phosphorus containing flame retardants take action efficiently in the solid phase of burning materials. When heated, the phosphorus is transformed into phosphoric acid during the combustion or thermal degradation. This acid causes the material to char formation, forming a glassy layer, and so inhibiting the "pyrolysis" process (break down and release of flammable gases) which is necessary to feed flames.

Nitrogen based compounds : The mechanisms of nitrogen containing flame retardants have several effects when it is added to textiles. These effects consist of the formation of cross-linked molecular structures in the treated material. These are relatively stable at high temperatures, thus physically inhibiting the decomposition of materials to flammable gases. In addition, it releases nitrogen gas which dilutes the flammable gases and thus reduces flames. However, nitrogen based flame retardants are often used in cooperation with phosphorus containing flame retardants by reinforcing their function.

2.9.1 Classification according to the durability of the finish of textiles.

1. Non durable flame retardants, as for example boric acid, aluminum sulphate, ammonium salts, phosphates. These substances are not fast to laundering/washing and hence the substrates are to be treated after each wash. All earlier attempts, involving water-soluble chemicals, are applied on to fabric by immersion, padding or spraying.

2. Semi durable flame retardants, e.g. by phosphorylation of cellulosic fibers or by a combination of cyanamide plus phosphoric acid. These flame retardants are used for example for tents, carpets or curtains. The impregnation is resistant to water but not to dry cleaning or repeated (50 or more) washings. Semi-durable finishes have a level of durability to washing/laundering in between the non-durable and durable finishes.

3. Durable flame retardants. Textiles for clothes are mainly impregnated durably with e.g. organic phosphorus compounds or organic, brominated phosphorus compounds. Durable finishes are durable to multiple launderings. These are more complex and difficult to apply.

Figure 2.28: The characteristic of burning of different textile fibers [78]

.

Type textiles	The characteristic of burning of different textile fibers
Cotton and Linen	Burns with a hot, vigorous flame, light colored smoke, and leaves red glowing ember after flaming stops. Does not melt or draw away from the flames.
Rayon and Lyocell	Burns similarly to cotton and linen, except that it may shrink up and become tighter to the body.
Acetate	Burns with a rapid flame and melts when burning. May meltand pull away from small flames without igniting. Melted areamay drip off the clothing carrying flames with it. When flameshave died out, the residue is a hot, molten plastic and is difficult to remove from any surface.
Nylon, Lastol, Olefin, Polyester, and Spandex	Burns slowly and melts when burning. May melt and pull awayfrom small flames without igniting. Melted area may drip off clothing carrying flames with it but not to the extent of acetateand acrylic. Residue is molten and hot and difficult to remove. May self-extinguish.
Acrylic	Burns similarly to acetate, except that it burns with a veryheavy, dense, black smoke. It drips excessively.
Wool and Silk	Burns slowly and is difficult to ignite (especially in winter garments). May self-extinguish.

CHAPTER III

EXPERIMENTAL METHODS

3.1 Plasma Reactors

3.1.1 Radio Frequency Inductively Coupled Plasma (RF-ICP) System

The experiments for improving hydrophobic properties of cotton by SF_6 plasma and hydrophilic properties of PET by O_2, N_2 and Ar plasma were carried out at low pressures by using radio-frequency inductively coupled plasma (RF-ICP) reactors. A schematic of the radio-frequency plasma generation is shown in Fig. 3.1 and Fig. 3.2. The main components of the radio-frequency inductively coupled plasma system are the reactor chamber, the RF generator, the impedance matching network, the pressure and gas supply system. The reactor is a cylindrical chamber of stainless steel, which has several ports for feeding gas and plasma diagnostic equipments. The top stainless steel plate has a circular opening of 20 cm in diameter where a quartz window is mounted to isolate the vacuum and still let the RF field from planar coil place above the quartz plate to couple into the plasma. A flat coil (7 turns) with maximum diameter of 150 mm is mounted directly on top of the quartz window to induce the plasma at 13.56 MHz power source which operated at 50 ohms and delivered up to 1000 watts of power. The matching network is placed inside a perforated aluminium cylinder which acts as a faraday cage protecting the electronic instruments from the effect of stray RF fields. A variable capacitance-matching network connected the induction coil to

the power source and allowed the coil to be tuned to match the source resistance. A base pressure at 2x10^{-5} Torr was achieved using a turbo molecular pump backed by a rotary vane pump. After the base pressure was reached, then gas is allowed to enter the chamber via mass flow controller. The pressure, which was used in this work, is in the range of 5x10^{-3}-5x10^{-1} Torr.

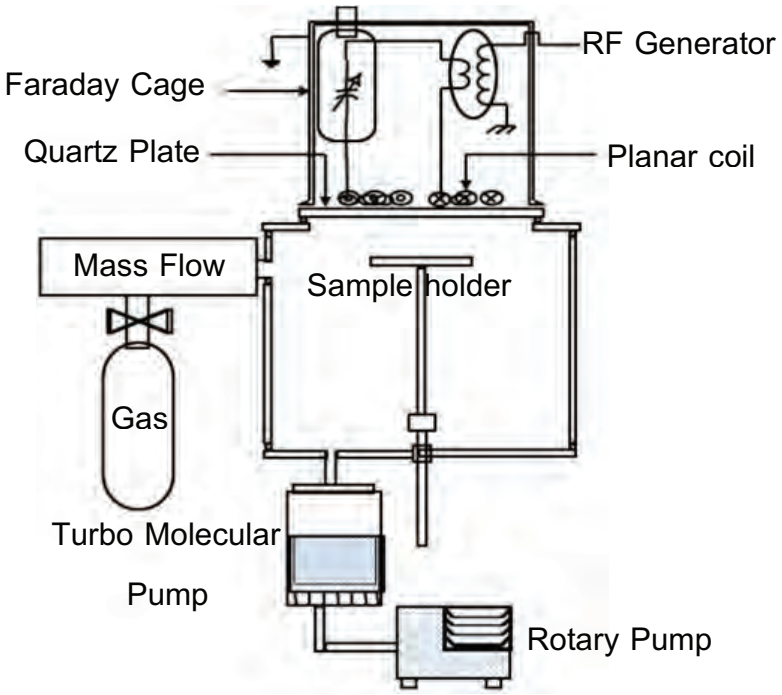

Figure 3.1: Schematic diagram of the radio-frequency inductively coupled plasma reactor.

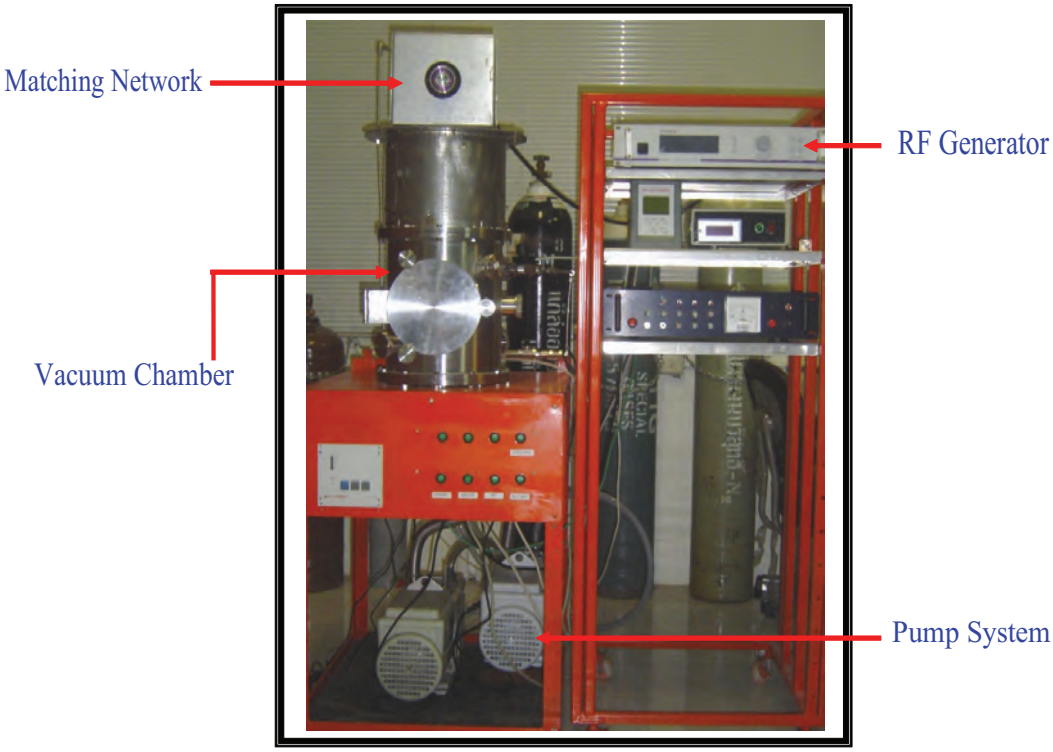

Figure 3.2: Photograph of the radio-frequency inductively coupled plasma reactor.

3.1.2 Microwave (MW) Plasma System

Ar plasma treatments of both for activation and for graft polymerization were performed in a microwave plasma reactor. Plasma was generated by a Europlasma DC 300PC system as shown in Fig. 3.3 and Fig. 3.4. In this work, the microwave plasma reactor is used to study the flame retardant of silk fabrics by plasma-induced graft-polymerization method. The microwave plasma system consists of three main parts: microwave generator, the vacuum chamber and vacuum pumping system. The microwave generator operates at 2.45 GHz with a tunable power ranging from 0 to 600 W. The vacuum system consists of the vacuum chamber, which is an aluminum based container, and the vacuum pump. In addition, there are a set of mass flow controllers and valves in order to bring in the process gases in a controlled way. However, the entire equipment can be controlled by a programmable logic controller (PLC).

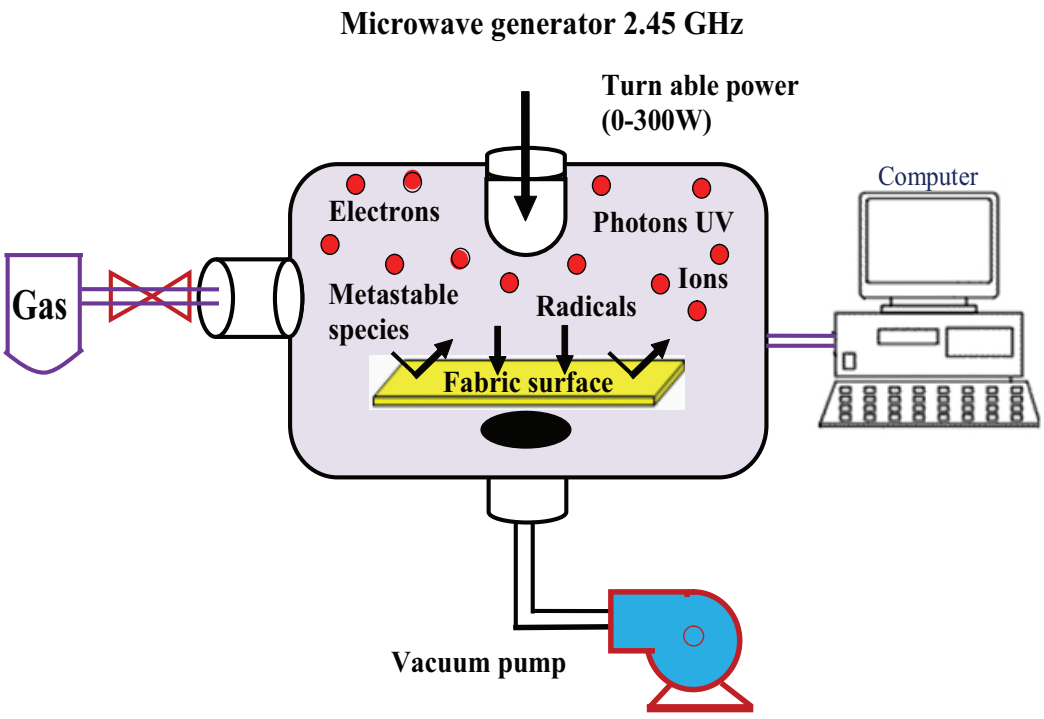

Figure 3.3: Diagram of the microwave plasma reactor.

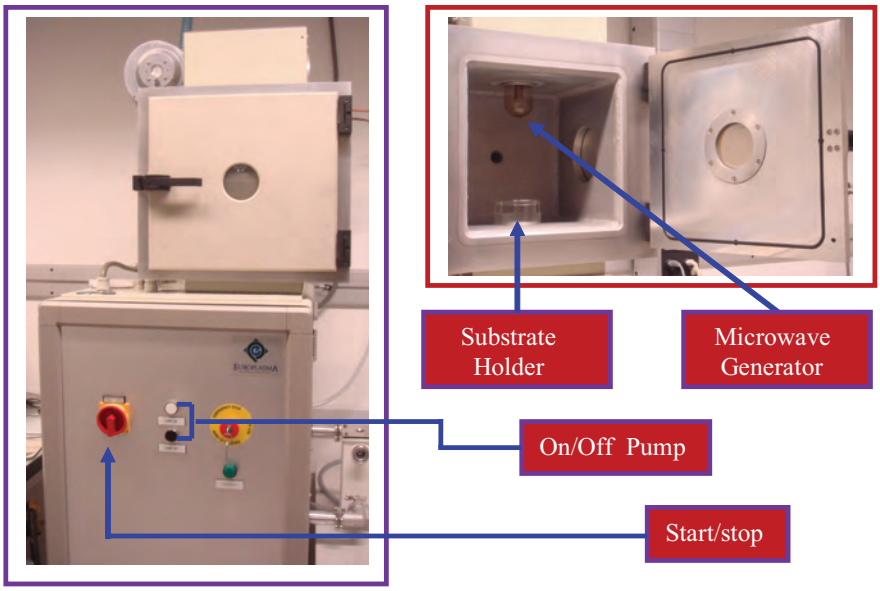

Figure 3.4: Photograph of the microwave plasma reactor.

3.2 Materials and Monomers

3.2.1 Materials

Cotton fabric for hydrophobic surface modification

The fabric used in this study was 100% cotton fabric which it has density 120 g/m^2. The density of warp and weft were 50 ends/cm and 25 picks/cm, respectively and the yarn count for warp and weft directions were 38 cm/g and 42 cm/g respectively. Fragments of cotton were cleaned with dilute detergent, repeatedly washed with distilled water and dried in air atmosphere. Then, the cotton fabrics were cut to the size of diameter about 8 cm and were placed in standard condition with relative humidity of 65% and temperature 20 ^{o}C for at least 24 hr before measurements. Samples were then dried in a oven at 80 ^{o}C for 60 min. In the experiment with cotton, we would like to observe the etching phenomena done by SF_6 plasma. Thus, vacuum treatments on fabrics were performed to eliminate

outgassing as the source of the mass loss before obtaining their initial weights prior to exposure with plasma. The sample was held horizontally stretched with the aid of a holding circle providing a treatment area of 50 cm^2 as shown in Fig. 3.5.

Figure 3.5: The photograph of circular holder for holding cotton sample fabrics.

We used the cotton sample held with the circular holder to measure the absorption time and contact angle. The reason for using such a circular holder is because it is easy to measure the position that we want to drop the water droplets on fabric in order to obtain the absorption time. The water droplet 40 μl in volume was released using micropipet at three different positions at the radial distance of 3 cm from the center of each sample (Fig. 3.12). The plasma system here used in the range of 25-75 watts RF power. It has an electron temperature during the glow discharge in the range of 2.5 to 4 eV. The sample was positioned parallel to the planar coil 2 cm away from the quartz window separating the chamber from the flat coil antenna. The total distance between the sample and the antenna is 4 cm. In our system, the sample was grounded and no bias was applied to the sample. To carry out the treatment the chamber was evacuated down to a pressure of 2x10^{-5} torr using a turbo molecular pump backed by a rotary vane pump. The sample was maintained at this pressure for 30 min to allow for out gassing of any remaining moisture. Then, the chamber was filled with the desired pressure of SF_6. The samples were exposed to plasma for various treatment times in the 15 s - 30 min range with a fixed SF_6 pressure of 0.5 torr and an RF power of 50 watts. In another series of experiments, SF_6 pressures were adjusted in the

0.005 -0.5 Torr range while a treatment time was fixed to 5 min.

PET fabric for hydrophilic surface modification

Commercially available 100% PET woven fabrics were used as the samples which it has density 75 g/m^2. Prior to plasma treatment, fabrics were washed twice in ultrasonic bath for 10 min at room temperature. The first washes were performed with a water solution containing 5% by weight of non-ionic non-residue detergent. The second washes were performed with only de-ionized water. Samples were then dried in a oven at 80 ^{o}C for 60 min. The samples were exposed to the varying plasma treating time between 0.5 - 30 min with processing pressure of 0.05 - 0.5 Torr and RF power of 25 - 75 watts. In case of hydrophilicity study, the sample size must be long enough in order to perform the capillary test. The detail of the capillary test was described in section 2.6. Thus, we use a rectangular holder with 12 x 17 cm for holding PET sample. The stretch holder is rectangular in shape and having the treatment area of 204 cm^2 as shown in Fig. 3.6.

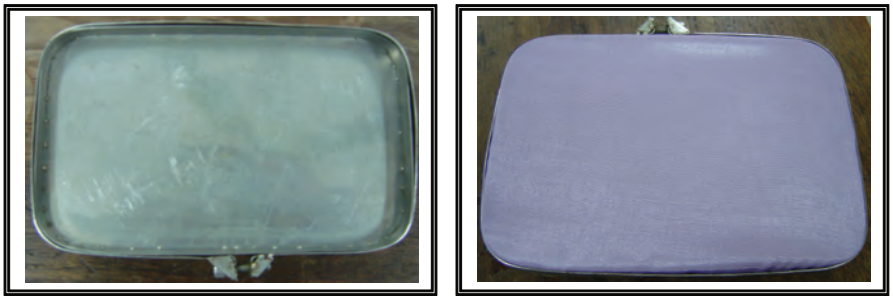

Figure 3.6: The photograph of rectangular holder for holding PET sample fabrics.

The samples were secured in a horizontal plane with a sample stretch holder and placed along the center axis of the chamber 4 cm below the quartz plate which is 3 cm below the planar coil. In the capillary test, all PET samples were cut to the dimensions of 1 cm x 15 cm and were placed in standard condition with relative humidity of 65% and temperature 20 ^{o}C for at least 24 hr before experimental. O_2, N_2 and Ar gases used in all experiment have the purity of 99.99%.

Silk fabric for flame retardant surface modification

Degummed and bleached silk fabrics (plain woven, 75.4 g/m^2) were supplied by EMPA Testmaterials Company, Zurich, Switzerland. The fabric samples were cut to the size of 5 cm x 10 cm in the warp direction and were placed in a standard condition with the relative humidity of 65 % and the temperature of 20 ^{o}C for at least 24 hr before experiments. Then, ethanol was sprayed on silk fabric to determine the pick-up ability of silk fabric. The pick-up is amount of liquor taken up by the fabric which is the difference in dry to wet weight expressed as percentage of dry. Pieces of silk were sprayed at room temperature in an ethanol containing 10%, 20% and 30% of flame retardant monomers in the presence of photoinitiator 5% of monomer and cross linking agent 10% of monomer. Silk fabric is impregnated and pressed to evacuate of solution, then it is placed on glass plate and put in the microwave plasma system to treat at condition of flow rate of 125 sccm, power 100 W, pressure 500 mTorr and exposure time 20 min. After plasma treatment, the silk fabric was washed with ethanol four times and follows with water one time in a soxhlet apparatus. This procedure or PIGP process was shown Fig. 3.7 (a). The dried silk was placed in standard condition with relative humidity of 65% and temperature 20 ^{o}C for at least 24 hr before measurements. In addition, we described a two step protocol in order to produce multifunctional silk fabrics. In the first step we applied the PIGP process of two phosphorus containing monomers the diethylacryloyloxyethylphosphate (DEAEP) and phosphoramidate (DEAEPN) onto the fabrics (Fig. 3.7 (a)). Then, the fabrics with a flame retardant finish were exposed to SF_6 plasma in a second step as shown in Fig. 3.7 (b).

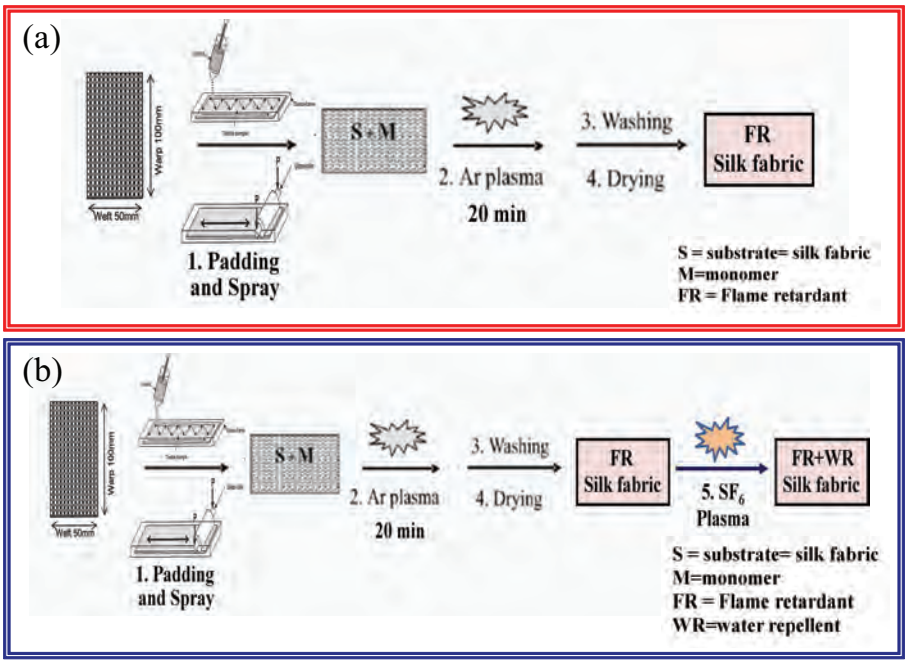

Figure 3.7: The plasma induced graft polymerization procedure (a) and two step protocol to produce multifunctional silk fabrics (b).

3.2.2 Monomers

In this thesis, we use two phosphorus containing monomers of the diethylacryloxyethyl -phosphate (DEAEP) and -phosphoramidate (DEAEPN) on to the fabrics as shown in Table 3.1. The preparation and characterization of acrylate phosphate and phosphoramidate monomers were described in appendices A

Flame retardant	Structure formula	Phosphorus content [%]	Nitrogen Content [%]	Boiling point [°C]
DEAEPN	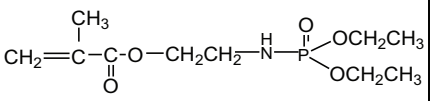	12.33	5.58	135
DEAEP	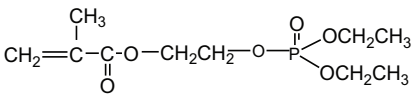	12.28	-	105

3.3 Characterization techniques

In this part, we will describe the characterization technique for determining the physical, chemical and thermal properties of studied fabrics. The common techniques for determining the physical properties of untreated and plasma-treated fabrics used in this thesis are scanning electron microscopy (SEM) and Atomic force microscopy (AFM). To test the hydrophobicity of treated cotton, the contact angle and absorption time measurements were performed. The tensile strength and absorption time measurements were obtain the etching rate in such an indirect way. To characterize the hydrophilicity of treated PET, the capillary rise method instead of the contact angle and absorption time measurements. Other extra characterization techniques for commercial applications are dyeing and washing test. Fourier transforms infrared spectroscopy (FT-IR), elemental

analysis, amino acid analysis (AA) X-ray diffractrometry (XRD) and X-ray photoelectron spectroscopy (XPS) are characterization technique for obtaining chemical properties of studied fabrics. For flame retaedantcy study of silk, thermal gravimetric analysis (TGA), pyrolysis combustion flow calorimetry (PCFC) and limiting oxygen index (LOI) were performed.

3.3.1 Physical properties on fabrics surface

Scanning Electron Microscopy (SEM)

Scanning electron microscopy (SEM) is a versatile technique used for the examination and analysis of the microstructure characteristics of sample. This technique uses an electron beam to strike a sample and cause secondary electrons, back-scattered electrons, X-rays and auger electrons to be emitted. Due to the interaction between the electron beam and the sample, several different signals are produced providing the information about the surface structure, differences of atomic number within the sample and information about the elemental contents. In this work, the morphology changes of the treated fabric surface were observed by scanning electron microscopy. A schematic diagram of Scanning electron microscope is shown in Fig. 3.8.

In Fig. 3.8, the scanning electron microscope generates a beam of electrons from the electron gun which commonly uses a tungsten-hairpin gun as the source of electrons. Generated electrons in vacuum will be focused in front of an anode to move the electrons down in the column. The electrons are focused into a small beam by a series of electromagnetic lenses in the SEM column. Scanning coils near the end of the column direct and position the focused beam onto the sample surface. The electron beam is scanned in over the surface for imaging. Various signals including secondary electrons, back scattered electrons are produced and can be detected.

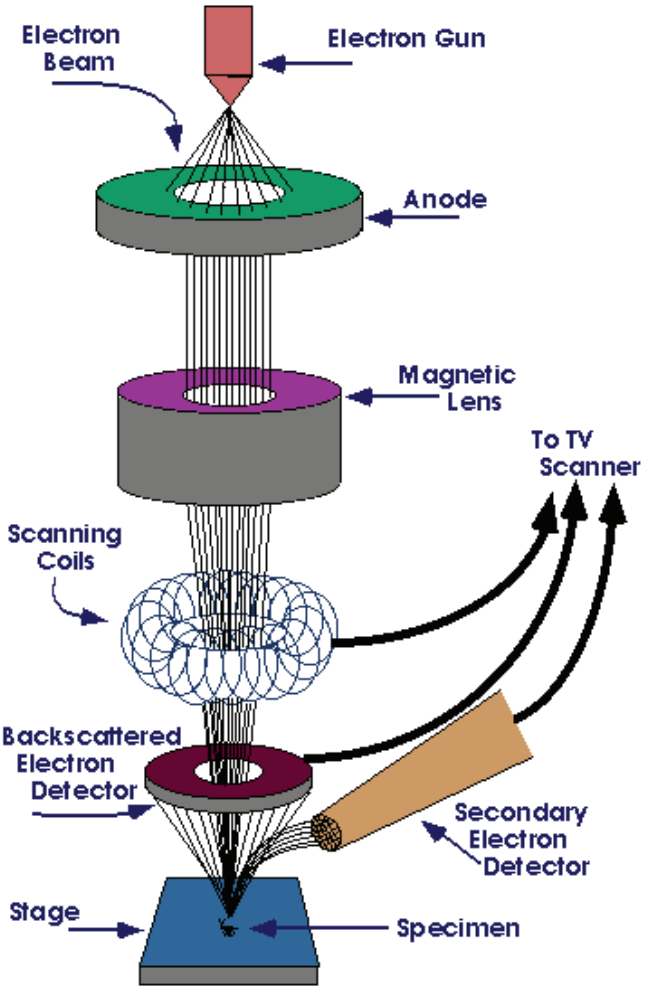

Figure 3.8: Schematic diagram of Scanning Electron Microscopy (SEM) [79]

High energy electrons that are ejected by an elastic collision of an incident electron, typically with a sample atom's nucleus, are referred to as backscattered electrons. The backscattered electron detector will detect high energy electrons that have been scattered backward and providing information about the presence of differences in atomic number of a sample. Emitted lower-energy electrons resulting from inelastic scattering are called secondary electrons. Secondary electrons can be formed by collisions with the nucleus where substantial energy loss occurs or by the ejection of loosely bound electrons from the sample atoms. The secondary electron detector will detect low energy electrons produced near the surface of the specimen providing a morphology and topography on samples. In this thesis, the thin gold layer is deposited on fabric in order to avoid electrical charging during the analysis. The SEM images were recorded by a JEOL model JSM-6400 scanning electron microscope.

Atomic Force Microscopy (AFM)

AFM is useful for quantitative information of surface morphology and roughness with a high precision. It can be used for surface characterization of any kind of materials such as polymers, biological samples, ceramics, metallic surfaces and etc. The basic principle of AFM is to measure the force experienced by a very sharp tip under the action of intermolecular interactions with atoms of the sample surface as shown in Fig. 3.9.

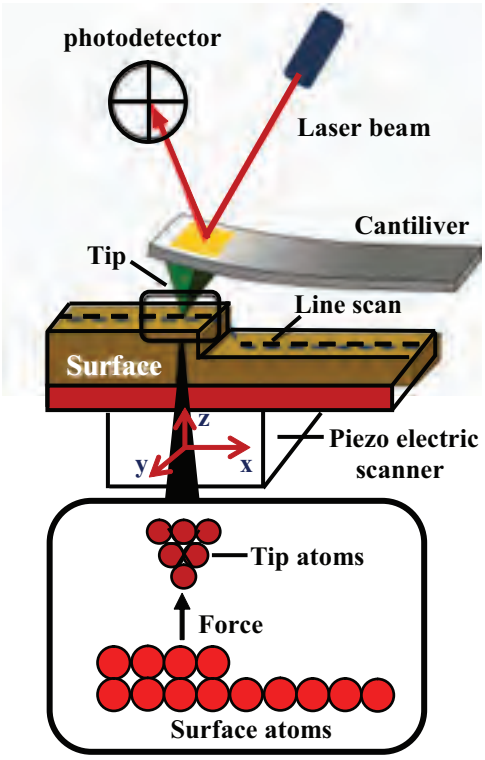

Figure 3.9: Schematic diagram of Atomic Force Microscopy (AFM) [80].

The tip is attached to the free end of a cantilever and is brought very close to the surface. Attractive or repulsive forces resulting from interactions between the tip and the surface will cause a positive or negative bending of the cantilever or every variation of the surface height changes the force acting on the tip. Therefore, the bending of the cantilever is changing while it is scanning across the sample. The bending is detected by means of a laser beam, which is reflected from the back side of the cantilever and the reflected laser is collected by a photodiode. It can be recorded line by line as an image which represents the three dimensional shape of the sample surface. In this thesis, technique (AFM model Veeco Nanoscope IV) with tapping mode is used to obtain the surface roughness on the fabrics. In the tapping mode, the cantilever is driven to oscillate near its resonance frequency typically around 50-400 kHz and Van der Waals force is in the intermittent contact range. The sample on the piezoscanner is moved up and down so that the amplitude of cantiliver osciiation is constant.

Tensile strength

Tensile strength is a mechanical property to measure the maximum force that the material can support before rupture. The mechanical and tensile property measurements can provide valuable insights into the structure of a fiber. The tensile properties of individual fibers or yarns are usually measured on a tensile testing machine. In this work, the tensile strength was measured by a testometric's M350-5 AT materials testing machine on 5x10 cm^2 specimen as shown in Fig. 3.10. However, the terms warp and weft are used in reference to textiles, specifically those which are woven. The warp is the tightly stretched lengthwise core of a fabric, while the weft is woven between the warp threads to create various patterns. In order to understand the changing of the structure of fibers, four measurements taken on both warp and weft directions and were averaged separately. The elongation to break of a fiber is a measure of the ultimate degree of extension that a fiber can withstand before breaking. In other words, the elongation to break is the strain on a sample when it breaks.

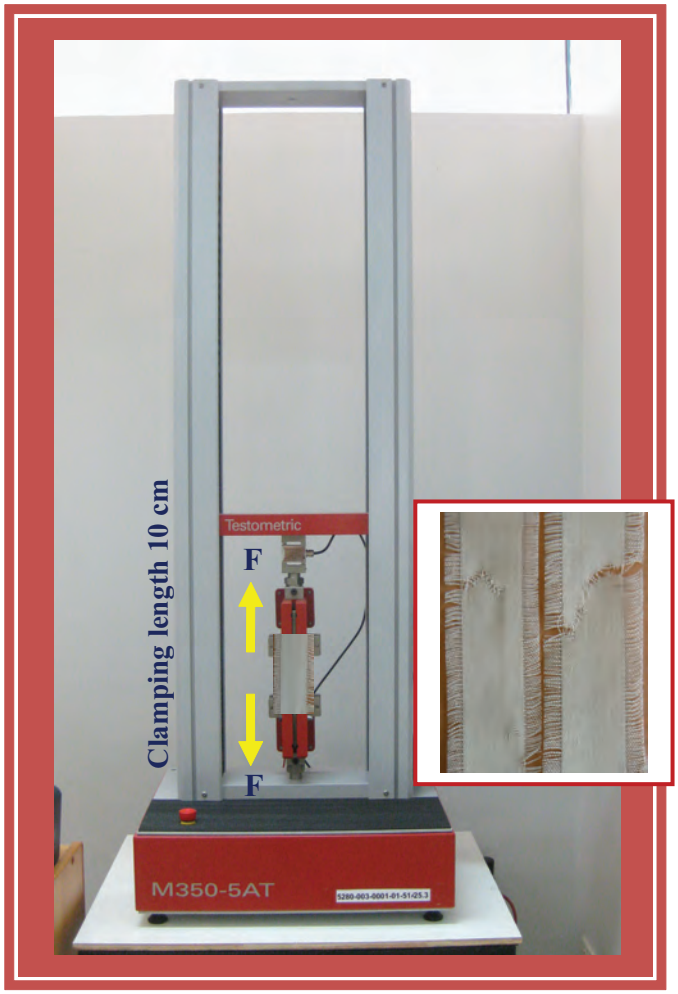

Figure 3.10: Photograph of tensile strength instrument.

Contact angle measurement

In the experimental, the water droplet contact angle of treated fabrics was measured by the Tantac CAM-PLUS contact angle meter as shown in Fig.3.11.

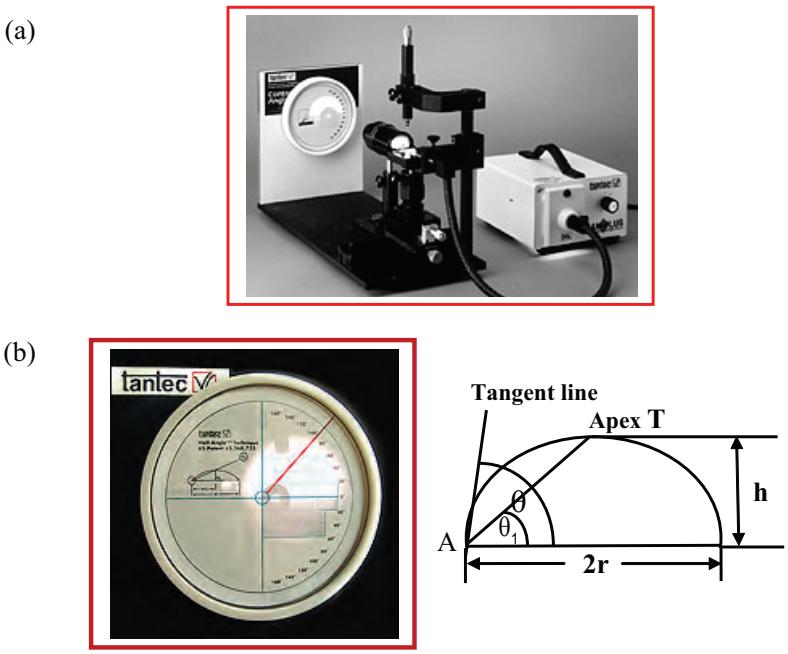

Figure 3.11: (a) photograph of the Tantac CAM-PLUS contact angle meter (b) determination of the contact angle of a droplet by Tantac CAM PLUS contact angle meter [81].

For contact angle measurement with contact angle meter, a water droplet volume 4 μl was placed on the top of surface by using microsyring. The half angle method is generally used to determine the contact angle. The image of water droplet is projected on screen and contact angle can be measured with half-angle technique, by drawing a line through the apex of the droplet from the interface point (the end point A) between the liquid and solid surfaces. The angle between the droplet base line and the line passing beyond the apex of the droplet is formed as θ_1 as shown in the Fig. 3.11. Based on the assumption that the droplet profile forms a segment of an arc, $2\theta_1{=}\theta$ is formulated by geometric theorem [62].

Absorption time measurement

The comparison of the hydrophobicity of fabrics as a function of plasma conditions by only using contact angle data is difficult. It is due to high errors of these measurements associated with roughness and irregularity of the surfaces. Another way to determine whether a surface can repel water or not is by using the absorption time. The absorption time is measured the ability of the fabric totally adsorbs water. The information of absorption time of fabric is obtain from the de-ionized water droplet volume 40 μl which was released from the micrometer pipette at three different positions on the fabric. The water droplets were laid on a circle 3 cm in radius, centered in the fabric sample as shown in Fig. 3.12.

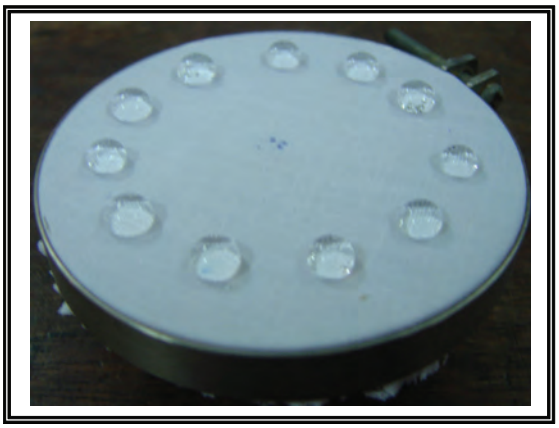

Figure 3.12: The photograph of water droplets placed on holding PET sample fabrics.

At least six measurements were averaged for each plasma treatment condition used in this work. The time required for the droplet to penetrate completely into the fabric was measured by means of a stop watch. The absorption time of fabric was measured as quickly after liquid droplets were place onto the surface. The upper limit in the absorption time was at 210 min due to the reduction of volume caused by evaporation of the water droplet. However, absorption time measurement can not use with the hydrophilic surface. It is due to high absorbtion of liquid on textiles. Also, it is difficult to measure the absorption time. The capillary rise method is replaced of this technique for studying the hydrophilicity

of plasma treated fabrics which is explained in the section of capillary rise method.

Weight loss

The more general issue of the degrading consequence occurs in the plasma-treated fabrics causing by etching process. Therefore, the weight loss of treated fabrics was evaluated in order to be correlated with etching effect of the plasma. The samples were dried in a oven at 80 ^{o}C for 60 min. Vacuum treatments on fabrics were performed to eliminate outgassing as the source of the mass loss before obtaining their initial weights prior to exposure with plasma. The weight of the sample was obtained immediately after the plasma treatment. Each sample was weighed before (W_i) and after plasma treatment (W_f), using a balance with the resolution of 0.001 g to determine weight changes or weight loss. The percent weight loss was then calculated as shown in Equation 3.1.

$$\text{Weightloss} = \frac{W_i - W_f}{W_i} \times 100 \tag{3.1}$$

X-Ray diffraction(XRD)

X-rays which diffracted from or reflected off crystalline or semicrystalline polymeric materials leading to obtain patterns related to the crystalline and amorphous areas within a fiber. The size and shape of individual crystalline and amorphous sites within the fiber are reflected in the geometry and sharpness of the x-ray diffraction pattern and provide an insight into the internal structure of the polymeric chains. In this thesis, we used X-ray diffractometer to investigate the the crystallinity of silk fiber that has changing or not after interaction with the flame retardant monomer. X-ray diffraction of patterns in the range 2θ = 2-50 degree were obtained on a Stoe Stadi P powder diffractometer equipped with a linear position sensitive detector (Cu $K_{\alpha 1}$-radiation,λ=1.54060 ^{o}, curved Ge-monochromator, 40kV, 35mA, step-width 0.010 degree in 2θ , 535.6 sec/step).

Capillary rise method

Plasma-treated PET fabrics were placed in a closed acrylic box containing 99% humidity of water vapor to allow the complete saturation leading to prevent evaporation from the wetted part of the fabric. The capillary rise method was performed inside the same acrylic box by hanging vertically a piece of PET fabric with a size of 1x15 cm^2 whereas one end of the fabric is merged 1 cm in the liquid and another end is clamped in the air as shown in Fig. 3.13. We measured the distance (H) of water traveling in the fabric and the value of H was recorded every 5 s in the first minute and every 60 s in the last seven minutes. The experiment was repeated two times and the value of H was average. The phenomenon of dynamics of capillary penetration in textiles which are related to the pore radius (R) and the diffusion coefficient (D_C) of water on fabrics were described by using Lucas-Washburn equation (2.9)

Lucas-Washburn equation is used for investigating the effective pore radius (R) when the liquid can penetrate in the vertical plane of textile under capillary pressure. The distance of traveling of liquid increases with both the surface tension in the solid-liquid interface and capillary pore radius. However, when the liquid droplets on textiles are formed contact angles are nearly zero (θ=0). Lucas-Washburn equation can be approximated as H^2=D_Ct where D_C is ($R\gamma/2\eta$). In other words, the average of pore radius (R) and the diffusion coefficient of liquid (D_C) are determined by the Lucas-Washburn of equation. A straight line was obtained from the graph of H^2 vs t whereas the slope D_C is capillary diffusion coefficient related to the size of capillary or pore radius R and to the viscosity of the liquid.

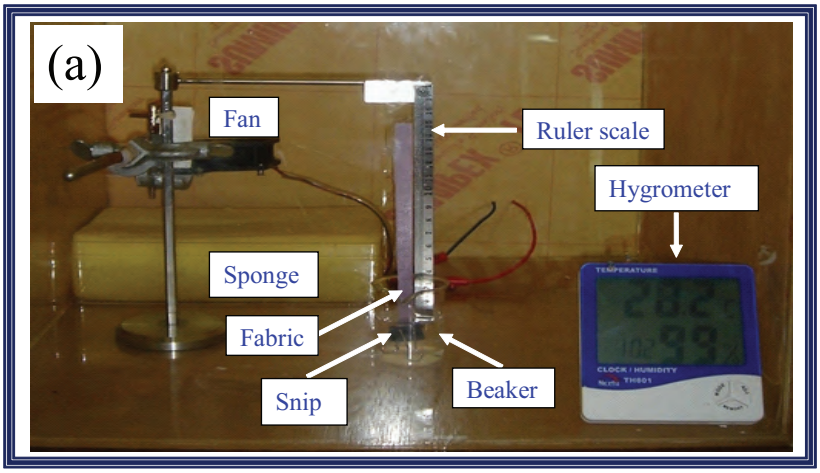

(b)

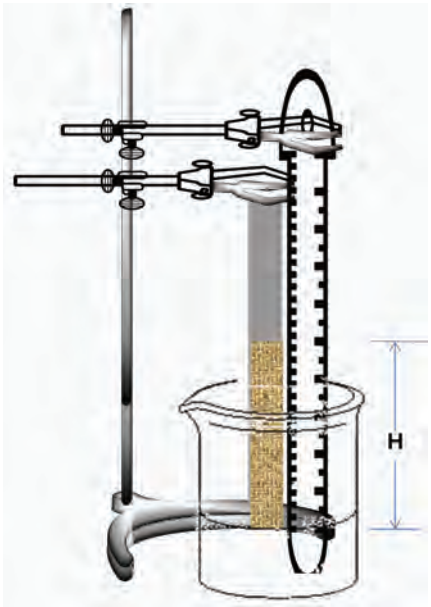

Figure 3.13: Photograph (a) and diagram (b) of capillary rise system.

Dyeing procedure

Plasma-treated PET fabrics were dyed by using 1.0 % wt. aqueous solution of disperse dyes (Foron yellow brown RD-3RSNI) and 1.0 vol.% of anionic dispersing agent (Sperse) with a liquor ratio 1:50 (1 g of fabric in 50 ml of dye solution) The solution was adjusted to pH 4 with 5 vol.% of acetic acid. An Unidye instrument was used in our experiments. The fabrics were dyed initially at 40 ^{o}C and the temperature was increased with the rate of 2 ^{o}C /min until it reached 130 ^{o}C, holding for 45 min for dyeing. Then the cooling down process was set to the final temperature of 40 ^{o}C as shown in Fig. 3.14.

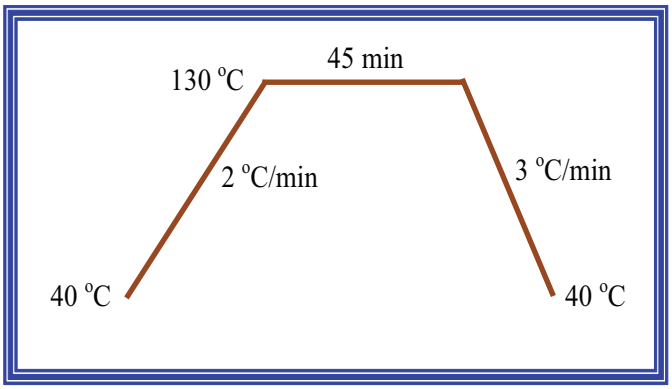

Figure 3.14: Schematic diagram of conditions used for the application of disperse dyes to the PET fabric.

The fabrics were washed in warm water and then the reduction clearing was proceeded to eliminate residual dye on fabric surface in a bath with 1 g/l of sodium dithionite ($Na_2S_2O_4$) and followed in the bath with 1 g/l sodium carbonate (Na_2CO_3) at 70 ^{o}C for 15 min. Finally, PET fabrics were rinsed with warm water and cold water and then dried at room temperature. After dyeing process, the colour of each dye PET fabrics were measured by Mcbeth ColorEye 7000 Spectrophotometry in the 400 - 700 nm wavelength range. The relative colour strength of dye fabrics was reported as a K/S value which is defined by Kubelka-Munk. Kubelka and Munk assumed that the light strikes on a surface is diffuse and considered to be scattered in only two directions, down and up. Therefore, the

reflected light intensity from the surface of the material depend on the thickness of the colorants, scattering S and absorption K coefficients of the colored materials, and the reflectance of the background, which the colorants layer lay on it. This method allows the prediction of spectral reflectance for a mixture of colorants that have been characterized by absorption K and scattering S coefficients. Therefore, the reflectance R of colorant layer is related to the ratio of the K and S coefficients thus

$$\frac{\mathrm{K}}{\mathrm{S}} = \frac{(1-R)^2}{2R} \tag{3.2}$$

In addition, the percent increase in color depth (I_{cd})was obtained from the difference between the $(\mathrm{K/S})_{tr}$ value measured for each plasma-treated sample and $(\mathrm{K/S})_0$ value of untreated PET sample dyed in the same bath as shown in equation (3.3).

$$I_{cd} = \frac{(K/S)_{tr} - (K/S)_0}{(K/S)_0} \times 100 \tag{3.3}$$

Washing Tests and Color fastness

The laundering durability and color fastness of the hydrophobicity, hydrophilicity and flame retardancy proerty on fabrics were evaluated. The durability of washing fastness tests on the treated cotton and PET fabric were washed in a washing machine (Gyrowash) according to ISO 105-C01 in an 5 g/L solution of commercial non-ionic detergent and temperature of water at 40 ^{o}C for 30 min. The samples were air dried and stored in desiccators until required. For the washing durability testing of flame retardantcy on silk fabric, it was tested according to the accelerated laundering method proposed by McSherry et al. [85] that is known to correlate very closely with 50 cycles of domestic laundering. The samples were boiled for 4 hr in a solution of 0.5% Na_3PO_4, $12H_2$ O and 0.1% triton X-100 at an approximate liquor ratio of 40:1, then dried at 80 ^{o}C.

In addition, before and after washing of the sample treated were also evaluated the color change by using gray scale according to AATCC evaluation procedure 1. The scale consists of five pairs of standard gray chips, each pair representing a different in color or contrast (shade and strength) as shown in Fig. 3.15.

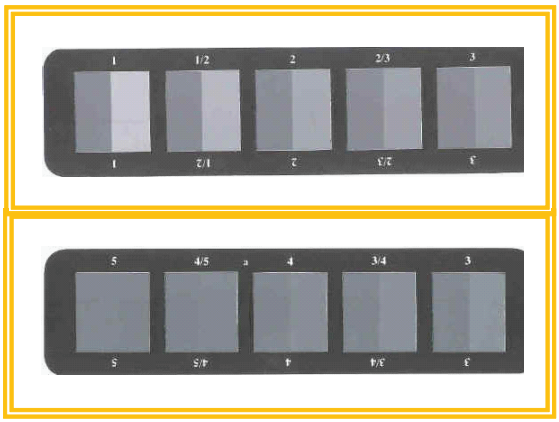

Figure 3.15: The gray change standard pairs

The result of color fastness tests are evaluated by visual observation by comparing the color on standard scale. The method is placing a part of origin textile and test specimen of it side by side in the same plane and oriented in the same direction and then place the gray scale nearby in the same plane to compare. The effect on the color of the test specimens can be de defined by reference to the gray scale for color change which classified into various as follows

Class 5 - no change as shown in gray scale step 5 (very good class)

Class 4 - a change in color equivalent to gray scale step 4 (good class)

Class 3 - a change in color equivalent to gray scale step 3 (middle class)

Class 2 - a change in color equivalent to gray scale step 2 (poor class)

Class 1 - a change in color equivalent to gray scale step 1 (very poor class)

Schmerber test

This method measures the resistance of fabric to penetration of water under hydrostatic pressure according to DIN 53886 as shown in Fig. 3.16. The textile with an area 30 mm in diameter is stretched on a frame which is connected to column of water. Water is added progressively to the column, where by the textile is exposed to an increasing pressure of water. The Schmerber value corresponds to the height of water (cm) reached when three drops of water went through the fabric. The height of the water column is directly transformed to the water pressure (1 cm of water = 0.981 mbar). This pressure Pschmerber is proportional to the cosine of the contact angle between a drop of water and the surface of the textile as show in equation:

$$P = \frac{2\gamma_L cos\theta}{R} \tag{3.4}$$

where γ_L and R are used by the nature of the textile and the liquid used, θ is the contact angle. When the values of the surface tension are used, for water at 25 ^{o}C, (γ_L =72.8)

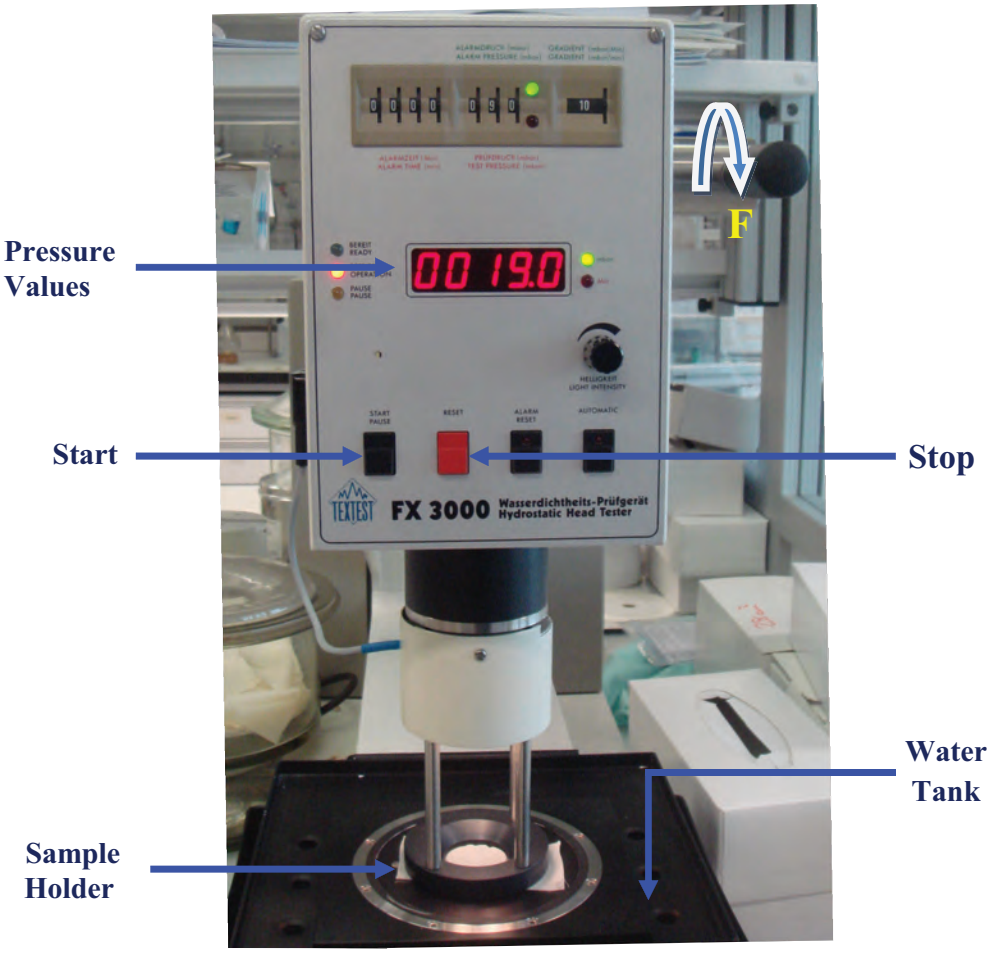

Figure 3.16: The photograph of pressure schmerber test.

3.3.2 Chemical properties on fabrics surface

Fourier transform infared spectroscopy

Fourier transform infrared spectroscopy (FTIR) is a valuable tool in determination of functional groups. Particular, functional groups in a polymer which absorb infrared energy at characteristic wavelengths leading to changes in the vibrational modes of the functional groups. As a result of the infrared absorption characteristics of the fiber, specific functional groups can be identified. The attenuated total reflection Fourier transform infrared spectroscopy (ATR-FTIR) spectra were recorded on Nicolet 6700 FT-IR spectrometry in range 4000 - 400 cm^{-1}. Functional groups of origin silk and silk-grafted with flame retardant monomer can be detected by this technique.

Elemental analysis and amino acid analysis

Elemental analysis were performed in the laboratory of organic chemistry of the ETH Zrich, the Phosphorus content of the treated fabrics were determined by the vanadomolybdophosphoric acid colorimetric method using an Uvikon 810, after perchloric acid-sulfuric acid digestion. Carbon, hydrogen and nitrogen contents were determined using a LECO CHN-900.

In addition, amino acid analysis was performed by using the UPLC Amino Acid Solution (Waters Corp., Milford, MA, USA). A small piece of approximately the same size of each sample was hydrolyzed in 6 N HCl at 110C for 24 hr under argon. The dried hydrolysate was dissolved in 70 ul derivatization buffer and 20 ul were derivatized (Accq-Tag Ultra, Waters Corp., Milford, MA, USA) according to the manufacturer's instructions. The relative amino acid content was calculated for each sample. Each experiment was performed twice and the results were averaged.

X-Ray Photoelectron Spectroscopy

X-ray photoelectron spectroscopy is a surface sensitive technique used to measure the surface atomic composition and bonding structure of materials [81]. A technique that preferentially provides more sensitivity to atoms near the surface than in the bulk away from the surface. XPS gives information limited to essentially the top 5 -10 nm of the film. This technique is commonly used in a variety of applications to identify elements and bonding structures in the outermost atomic layers, to determine depth profile, to detect contamination present at surfaces. Figure 3.17 shows a schematic of the XPS system [82]. Freshly treated fabric samples were used to perform X-ray photoelectron spectroscopy experiments using Mg K radiation (1253.6eV) (Kratos Analytical model AMICUS) in order to determine the changes in surface chemical composition of the treated fabrics.

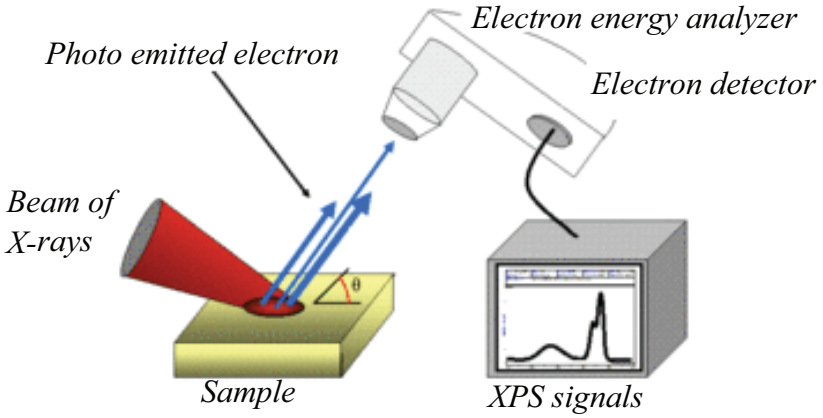

Figure 3.17: Schematic diagram of X-ray photoelectron spectroscopy [82]

The using principle of XPS is that a sample surface is bombarded with a monochromatic x-ray beam of sufficient energy in a vacuum, photons are absorbed by an atom in a sample, leading to ionization and the emission of a core (inner shell) electron. The kinetic energy distribution of the emitted photoelectrons and the number of emitted photoelectrons as a function of their kinetic energy, can be measured using an electron energy analyzer and a photoelectron spectrum can thus be recorded. The kinetic energy of emitted electrons can be measured with

an electron spectrometry and the binding energy of the electron can be obtained from the following relationship [78]:

$$B.E = h\nu - K.E - \phi \tag{3.5}$$

Where B.E. is the binding energy of the emitted electron, hν is the x-ray energy, K.E. is the kinetic energy of the ejected electron, and ϕ is the work function of material. Each element has a unique atomic structure, and thus binding energies for core electrons are distinct and readily identified using XPS. In addition, the number of detected electrons in each of characteristic peaks is directly related to the amount of element within the area irradiated.

3.3.3 Thermal properties on fabrics surface

Thermal gravimetric analysis

Thermogravimetric analysis (TGA) and derivative thermal gravimetry (DTG) are continuously measures the weight loss of a sample as a function of temperature and time and provides information about thermal stability, moisture or solvent contents, additives or filler contents, oxidation or decomposition temperatures and decomposition rate as shown in Fig. 3.18. The method starts with the placing sample in a metal pan suspended from the arm of a microbalance and situated in furnace tube. The temperature is carefully monitored by a highly accurate thermocouple. The measurement is normally carried out in air or in an inert atmosphere, such as argon, and the mass is recorded as a function of increasing temperature. In this experimental, TGA and DTG were performed on a NETZSCH STA 409C instrument by using continuous nitrogen flow of 10 ^{o}C/min and a heating flow rate of 10 ^{o}C/min at the temperature from 30 to 700 ^{o}C to study thermal properties of the flame retardantcy on silk fabric.

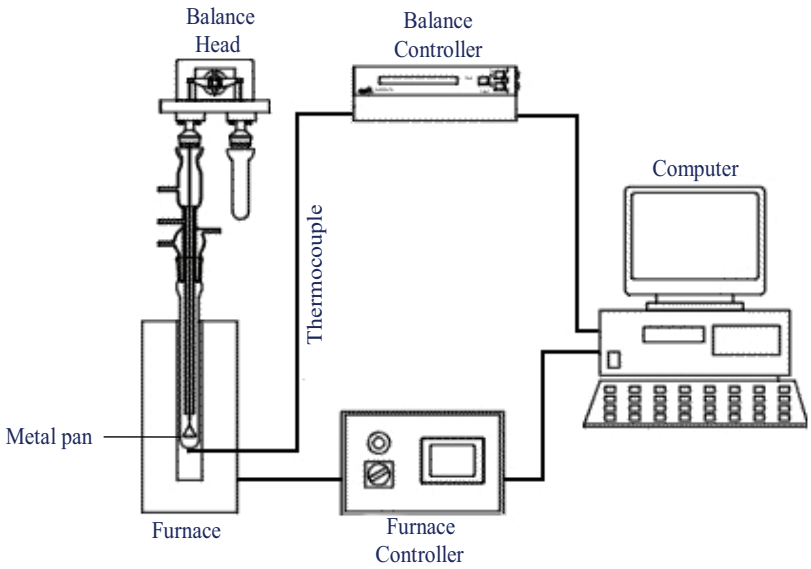

Figure 3.18: Schematic diagram of thermal gravimetric analysis (TGA) [83].

Pyrolysis combustion flow calorimetry (PCFC)

Pyrolysis combustion flow calorimetry (PCFC) is commonly used to measure the rate at which the heat of combustion of the fuel gases is released by a solid during controlled pyrolysis in an inert gas stream. The fuel gases are mixed with excess oxygen and completely oxidized at high temperature and the instantaneous heat of combustion of the flowing gas stream is measured by oxygen consumption calorimetry as shown in Fig. 3.19. In this work, the silk fabrics (∼5 mg) were heated from ambient temperature to 750 ^{o}C in nitrogen flowing at 80 cm^{3}/min at a linear heating rate of 1 ^{o}C/min. During sample heating, the volatile thermal decomposition products are swept from the pyrolysis chamber by nitrogen gas and combined with a 20 cm^{3}/min stream of oxygen prior combustion in a furnance at 900 ^{o}C during 10 s to effect complete oxidation of the decomposition products. Combustion products CO_2, H_2O and acid gases are scrubbed from the gas stream and the transient heat release rate is calculated from the measured flow rate and

oxygen concentration. Each step was performed at least twice.

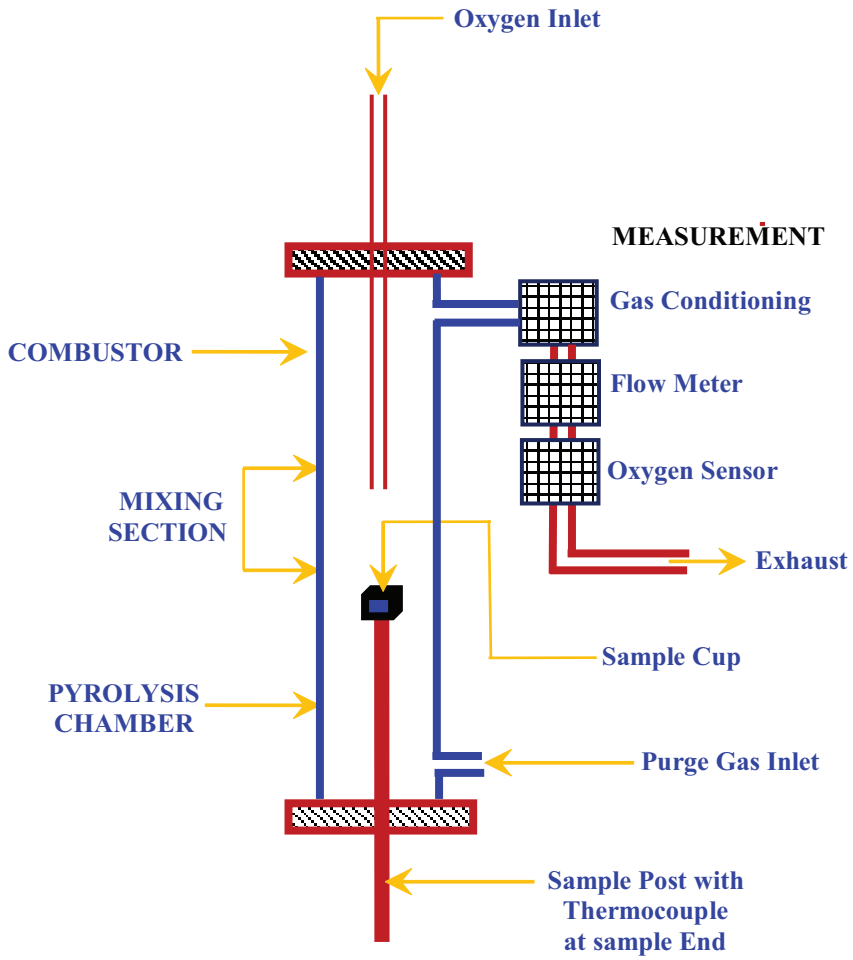

Figure 3.19: Schematic diagram of pyrolysis combustion flow calorimetry (PCFC) [84]

Limiting Oxygen Index (LOI)

The Limiting Oxygen Index (LOI) test is a widely used research and quality control tool for determining the relative flammability of textiles and other polymeric materials. A numerical index, the 'LOI' is defined as the minimum concentration of oxygen in an oxygen - nitrogen mixture, required to just support downward burning of a vertically mounted test specimen. Hence, higher oxygen concentration and LOI values represent better flame retardantcy of the specimen. The oxygen concentration is reported as volume percent. In this research, we investigated the correlation between LOI and phosphorus/nitrogen content on the silk fabric treated with that durable flame-retardant. The test method were carried out using an oxygen index test apparatus from Fire Instrumentation Research Equipment LTD with a digital readout of oxygen concentration to 0.1% as shown in Fig. 3.20. The LOI value corresponds to the minimum concentration of oxygen in an oxygen/nitrogen mixture necessary to ignite the sample during 3 min over a total length of 80 mm according to ASTM Standard Method D2863-76.

Figure 3.20: Photograph of the Limiting Oxygen Index (LOI)test

CHAPTER IV

RESULTS AND DISCUSSIONS

4.1 Hydrophobicity of cotton fabric after SF_6 plasma treatment

4.1.1 Effect of contact angle and absorption time on hydrophobic properties of cotton

The effects of the SF_6 exposure time

In this work, the cotton fabrics are treated with SF_6 plasma as a function of exposure time to improve the hydrophobic surface by RF-ICP system. The enhancement of hydrophobic properties quantified by the water droplet contact angle and absorption time of cotton with various exposure times from 15 s to 30 min at a fixed SF_6 pressure of 0.5 Torr were measured later. The results were summarized in Table 4.1.

The measured contact angle of the fresh plasma treated fabrics as the function exposure time was about 145±5 degrees while the untreated cotton absorbs water immediately leading to a contact angle of nearly zero degrees as shown in Table 4.1. We observed that the contact angle of the treated fabric, which varied in the 145-149 degrees range, was not strongly sensitive to the different plasma conditions. However, it is difficult to compare the hydrophobicity of fabrics as a function of plasma conditions by only using contact angle data due to large errors of these measurements associated with roughness and irregularity of the surfaces.

Thus, we use the water absorption times as a robust measurement of hydrophobicity. Longer exposure times cause a corresponding increase in the absorption time from 0 to beyond our limiting time 210 min.

Table 4.1: The contact angle and absorption time of cotton fabric as the function of exposure time (power 50 W, pressure 0.5 Torr).

Exposure time (min)	Absorption time (min)	Contact angle (degree)
0	0	0
0.25	60	145.0 ± 5
0.5	90	145.2 ± 5
1	> 200	145.5 ± 5
3	> 200	146.5 ± 5
5	> 200	148.0 ± 5
10	> 200	148.5 ± 5
30	> 200	149.0 ± 5

The effects of the SF_6 pressure

The results in hydrophobic characteristics of cotton after plasma treatments with various SF_6 pressures from 0.005 Torr to 0.5 Torr with a fixed exposure time of 5 min as shown in Table 4.2. The contact angle of cotton has reached about 148 degree and further increased in pressure have caused improvement hydrophobic properties. It has been argued that the mean free path in the gas phase is higher than the textile distance and the collision of gas molecules with the fiber surface is enhanced as compared to gas-gas collisions. This process favors a good penetration of plasma species in to the textiles at low pressure (<1 mbar) [15]. The water absorption time measurement of cotton fabric became quite hydrophobic and could resist water spreading at pressure higher than 0.3 torr in contrast to the untreated cotton where water drop spreads very quickly. However, the higher as function of

both SF_6 exposure time and pressure obtain the high contact angle and absorption time on cotton fabric. It is due to a larger concentration of fluorinating species and their shorter mean free path, increasing the rates of ionization radical formation and fluorination reactions.

Table 4.2: The contact angle and absorption time of cotton fabric as the function of pressure (power 50 W, exposure time 5 min).

Pressure (Torr)	Absorption time (min)	Contact angle (degree)
0	0	0
0.05	35	140.0 ± 5
0.1	65	143.5 ± 5
0.2	150	145.0 ± 5
0.3	> 200	146.5 ± 5
0.4	> 200	147.5 ± 5
0.5	> 200	148.0 ± 5

4.1.2 Effect of mechanical properties and weight loss of cotton.

The result of the chemical modifications is produced by the SF_6 plasma which leads to the mechanical resistance of the cotton fabrics changes. Cotton is also etched out from the surface of the fibers. Thus, it is important to correlate the percentage weight loss (%) with tensile strength.

The effects of the SF_6 exposure time

The results of SF_6 plasma exposure for varying times under a constant RF power of 50 watts on the mechanical properties of cotton are shown in Fig. 4.1(a) - (b). The tensile strength in warp direction is higher than that in the weft

direction but they follow nearly the same decreasing trend with increasing in exposure time as shown in Fig. 4.1 (a). The weight loss increased concomitantly with the reduction in tensile strength, with two clearly different loss rates. In a first stage, the combined release of moisture and etching occur leading to a pronounced outgassing which lasts ca. 1 min under our experimental conditions. The second stage, the weight loss passes through an inflection point as outgassing become dominated by a slower trend due to etching only (all the physisorbed gas and water already desorbed). The warp yarns in a fabric are stronger than the weft yarns because they are tightly stretched lengthwise.

Generally, the tensile strength in warp direction is commonly used to quantify the mechanical resistance of the fabric. However, we observed a small enhancement of tensile strength in both directions for the cotton treated for moderate exposure times. This may be the result of higher fiber to fiber friction and thus yarn to yarn friction. For exposure times shorter than 1 min, the tensile strength of treated cotton is nearly constant where the initial weight loss process is observed. Indeed, we assign this stage to outgassing of strongly bound water molecules and other gases trapped in the fabric. The weight loss is found to be more than 1% when fabrics were exposed to plasma for more than 5 min. The results of treatment times longer than 10 min are due to a clearly different process. First, the measured weight loss reached 5.2% for 30 min of plasma exposure and it continues to rise for longer treatments. The percent elongation at break, calculated from the ratio of the change in the length (4L) of the sample to its original length (L), is plotted in Fig. 4.1 (b).

These results were obtained for an SF_6 pressure of 0.5 torr. The percent elongation at break, determining the strain on a sample when it breaks, decreases from 14% for weft direction and 17% for warp direction of untreated cotton to the values between 6% and 11%. This reduction continues for longer plasma exposure times. It is noteworthy that a small increase in percent elongation in both directions occurs for the cotton treated for exposure time of ca. 20 min.

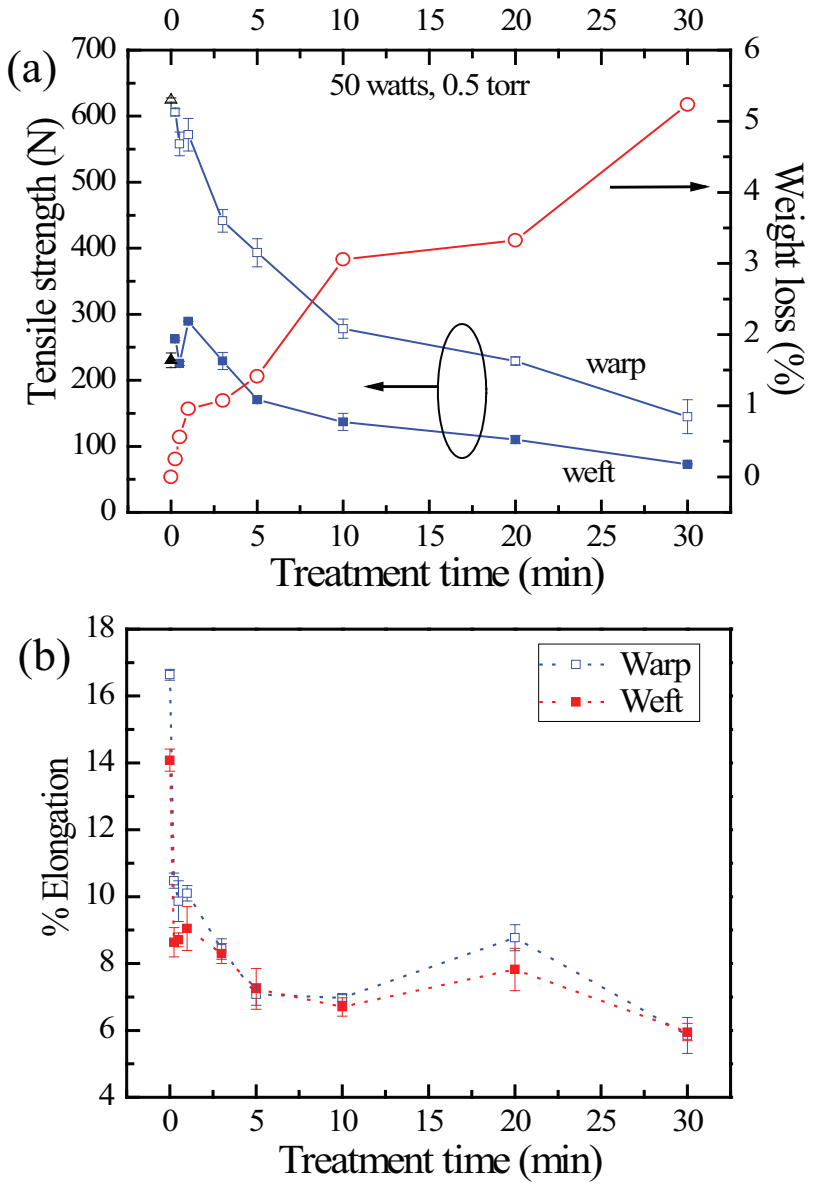

Figure 4.1: (a) The weight loss and tensile strength and (b) elongation at break of fabric versus the treatment time.

The effects of the SF_6 plasma pressure

We further investigated the effect of SF_6 pressure to the surface modification of cotton fabrics. These samples were exposed to varying SF_6 pressures in the 0.005 - 0.5 Torr range as shown in Fig. 4.2 (a). It shows that the tensile strength of samples treated in 0.005-0.3 torr range remains constant for warp and weft directions at about 550 N and 280 N, respectively. For these short treatments ($<$ 5 min) the weight loss slowly increases from 0.1% to 1.0% corresponding to the first stage described in the previous section. Figure 4.2 (b) shows the elongation at break after 5 min treatments with RF power of 50 watts. The percent elongation at break for most samples was between 7% and 9% with the lowest values obtained at the highest pressure studied.

Other works reported the effect of plasma treatments based on different types of gas on tensile strength of fabrics. Yip et al. [86] found that the tensile strength of O_2 and Ar plasma-treated nylon fabrics is not directly related to the exposure time. The tensile strength decreased slightly for a short time, increased for an intermediate time and decreased after a longer time. They suggested that a shorter exposure time favors polymerization while a longer exposure time favors etching. Hwang et al. [6] reported that the surface morphology changes of fabrics which result in increased fiber to fiber friction after exposing to He atmospheric pressure plasma play a major role in enhancing the tensile strength. McCord et al. [10] found that the tensile strength of nylon fabrics increased after processing with helium and helium/oxygen atmospheric pressure plasma without noticeable surface morphology changes. We found that the exposure time to long treatments causes more marked changes via the etching effect even if low pressure plasma is used.

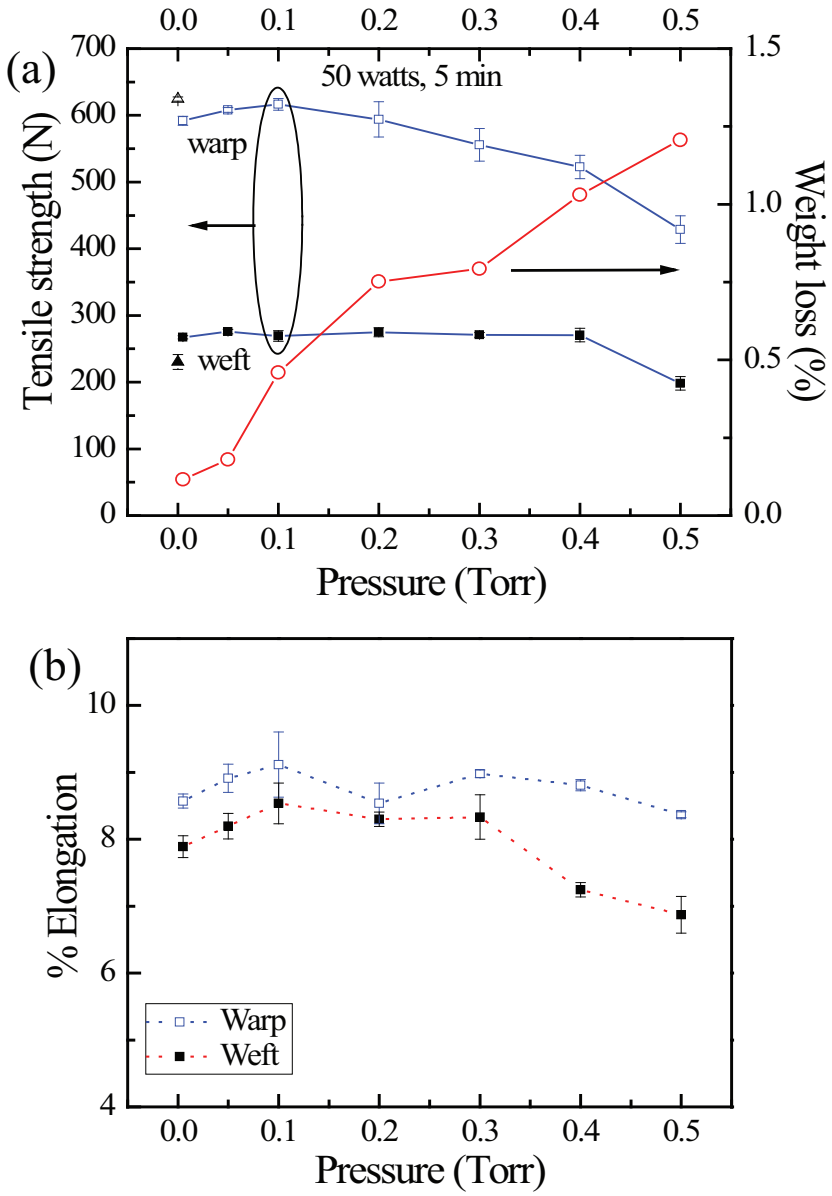

Figure 4.2: (a) The weight loss and tensile strength and (b) elongation at break of fabric versus the SF_6 pressure.

4.1.3 Weigh loss due to surface roughness of cotton

A mass spectrometry study on piranoses and disaccharides showed that plasma induced fragmentation primarily leads to loss of formaldehyde (CH_2O) and water as shown in Fig. 4.3 [87].

Formaldehyde arises from the loss of C6 consistent with our results of loss of C1 signal upon treatment. Water is produced from dehydration at position 1,2 in the glucose ring leading to the formation of (a double bond) 1,2 dehydro glucose. Both chemical changes lead to a smaller surface density of OH groups and therefore they render the surface less hydrophilic. Further fragmentation occurs leading to the lossen of CH_2O. Carbon dioxide and numerous charged fragments with 25 carbon atoms are also observed. It has been proposed that the glycosyl bond is easily broken in the plasma [87]. The loss of an entire terminal piranose ring also give rise to small charged fragments and molecules by decomposition. A crucial characteristic of the plasma induced (ionization-fragmentation) processes in pyronoses is that the large energy of the plasma species causes pronounced fragmentation as evidenced by the low abundance the molecular ion. In the case of pyrolysis of cellulose and other glucane, other fragments have been identified but in the main losses as acetic acid, formic acid, H_2O and glycolaldehyde [89]. Most likely pyrolysis will significantly alter the appearance of the fabrics and their mechanical properties. We believed that only mild modification occurs without pyrolysis setting in during our plasma treatment. Since the final appearance of the fabrics is nearly identical to that before plasma exposure.

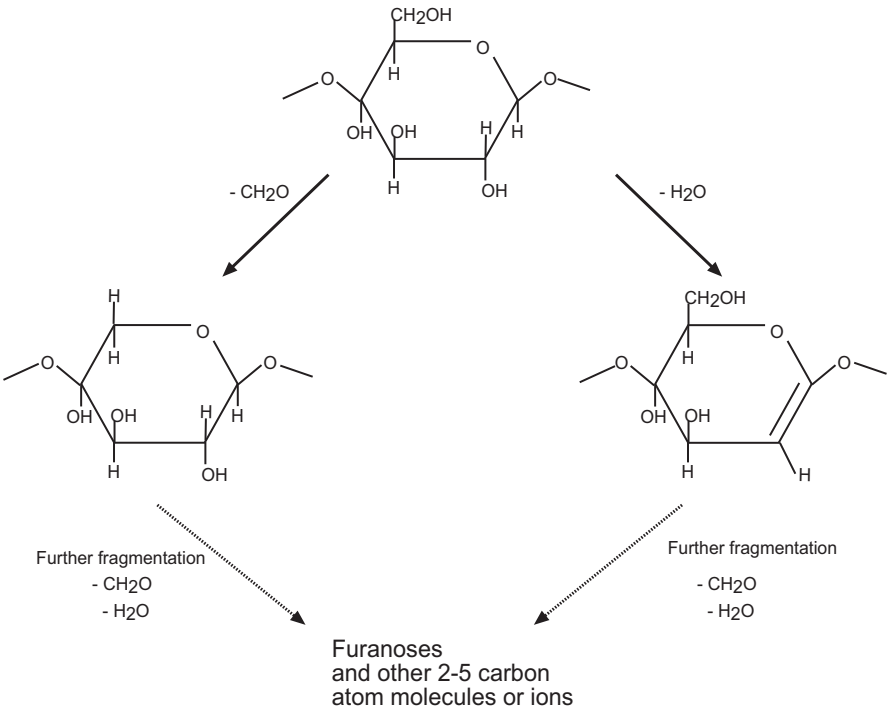

Figure 4.3: Diagram of main fragmentation losses.

4.1.4 Effect of surface morphology of cotton

The effects of the SF_6 exposure time

SEM images of cotton fabrics are shown in Fig. 4.4. It shows the surface roughness of both untreated (Fig. 4.4 (a)) and plasma-treated fabrics (Fig. 4.4(b)-(f)).

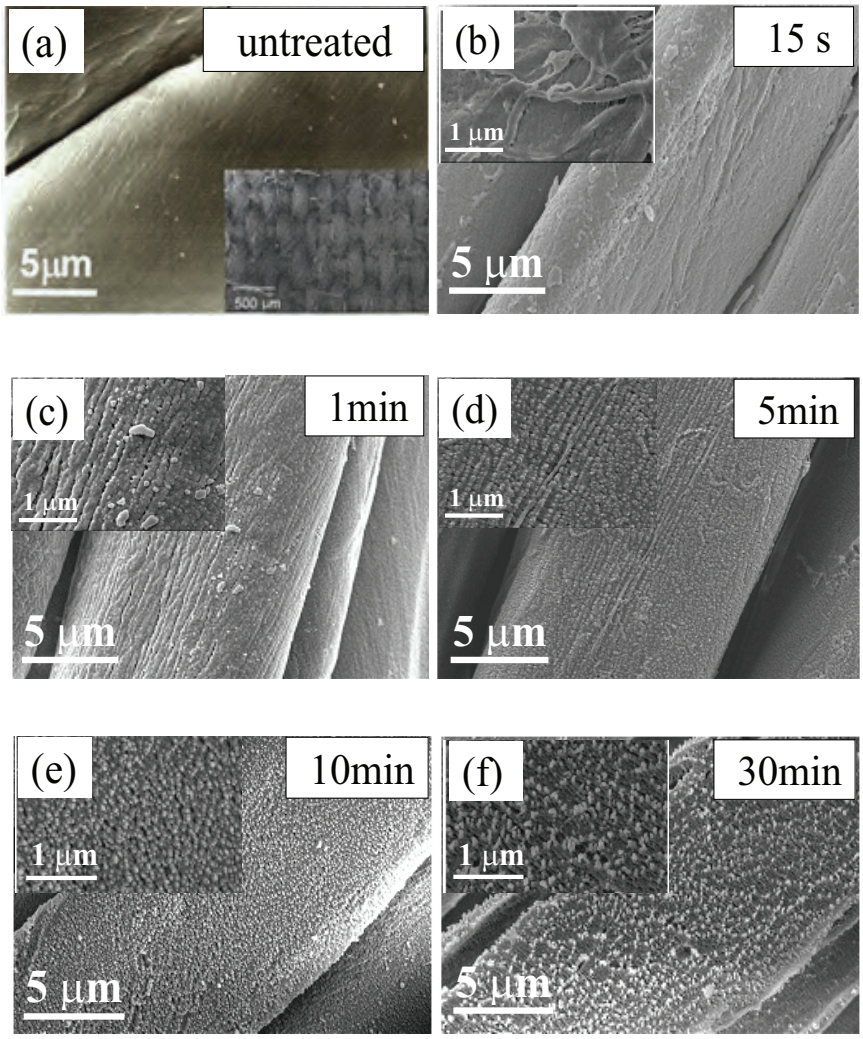

Figure 4.4: SEM micrographs of cotton fabric with magnification of 5000 and 1500 (a) untreated (b) treatment with 0.5 Torr of SF_6 and RF power of 50 watts for 15 s (c) 1 min (d) 5 min (e) 10 min (f) 30 min.

The features of cotton textiles were also shown in Fig. 4.4(a). The untreated cotton fibers were smooth, in clear contrast with the treated fibers having a granular appearance on the surface. We do not observe much difference in surface morphology of fabrics exposed to plasma for 15 s - 1 min, further supporting the hypothesis that during this stage, outgassing of adsorbed molecules is the sole source of the weight loss with the heavier loss occurring on the second stage being driven by etching the fibers which leads to the observed changes in mechanical properties and fiber morphology. Thus, for longer treatment times, the bombardment by energetic ions causes increased removal of surface materials. The roughening increases the surface area which leads to the faster etching and outgassing. The etching process from bombarding high energy species creates grooves along the fibers. When the etching process continues with longer time, the grooves become wider, started to see at the treatment time for 5 min. The granular structure was developed at treatment times longer than ca. 10 min.

The Effects of the SF_6 Plasma Pressure

The surface morphology of cotton fabrics as function of pressure is shown in Fig. 4.5(a) - (d). These samples were exposed to varying SF_6 pressures in the 0.005 - 0.5 torr range. It shows that no significant surface morphology changes were observed for 5 min treatments in this range of SF_6 pressure.

Although, our experiments reveal only minor changes of the surface morphology observed by scanning electron microscopy for different pressure used, the etching proportionally faster etching of the fibers. The bombardment by energetic ions may cause materials previously attached to the surface to be removed together with molecular fragments from degradation of glucose units causing the observed roughening the fabric surface dramatically.

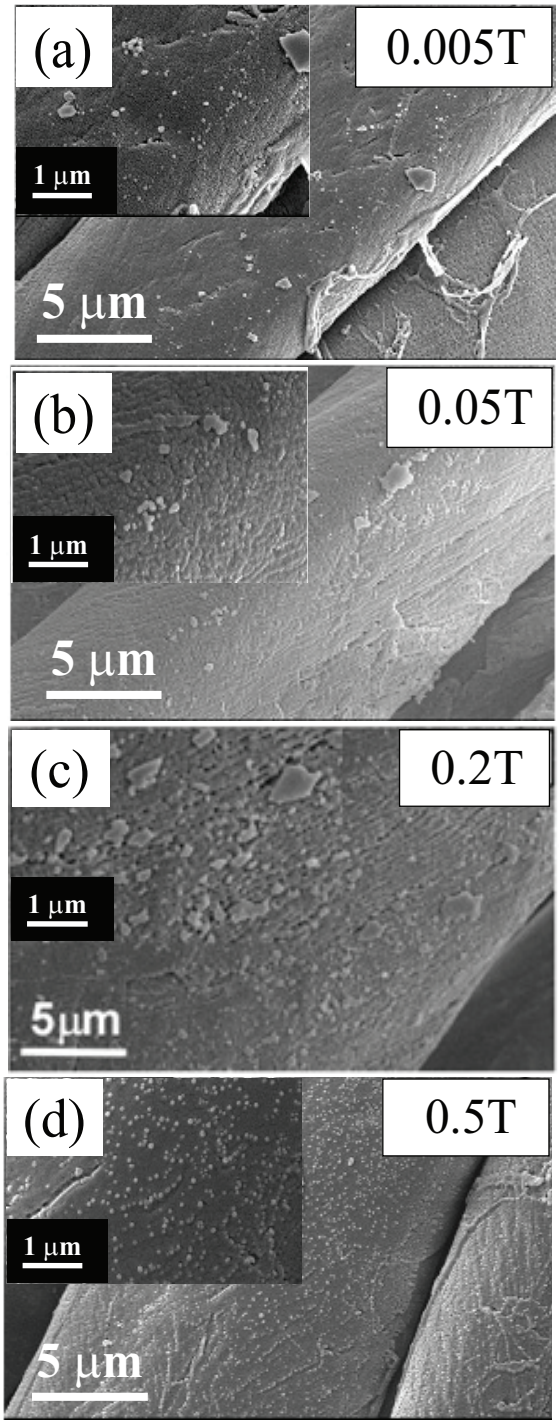

Figure 4.5: SEM micrographs of cotton fabric with magnification of 5000 and 1500 (a) treatment for 5 min with 0.005 Torr of SF_6 (b) 0.05 Torr (c) 0.2 Torr (d) 0.5 Torr.

4.1.5 Effect of roughness and etching rate on cotton surface

The changes in surface morphology of fabrics after treatment with SF_6 by SEM show the etching or ablation on fibers. However, SEM experiments are needed in connection with from atomic force microscopy (AFM) images of individual fibers to confirm the quantitatively surface roughness by the root mean square (Rms) analysis. The surface topography of untreated and SF_6 treated cotton fibers with different plasma conditions are shown in Fig. 4.6(a) - (f), respectively.

We found that the Rms roughness of cotton increased from 5 nm to 8 - 20 nm after plasma treatment. We know that the increased roughness of treated fabrics is due to plasma effect of both etching process from high energy species generated in plasma and deposition process of residue on the sample surface. However, no clear trend of the Rms surface roughness was observed in our experiments. The surface roughness is involved in the so called lotus effect of certain plant leaves in which the summits on the leaf surface support a water droplet. The surface of the hydrophobic natural plant leaves consists of an array of needles that range from 5 to 100 microns in length with separations ranging from 5 to 200 micrometers [25]. For example, the front surface of lotus leaves (Nelumbo nucifera) consists of a micron-scaled structure with about 7 micron in diameter super-imposed by nano-pillars, with half sphere peaks of average 330 nm, on top of a micro meter scale feature [26]. The micro-features are distributed randomly on the front surface with an average periodic distance and height of 20 μm and 15 μm, respectively. Comparing with our results, the extremely different of order in the surface roughness with the size of water drops is clearly seen that the lotus effect is not the reason for the improved hydrophobicity of our cotton fabrics.

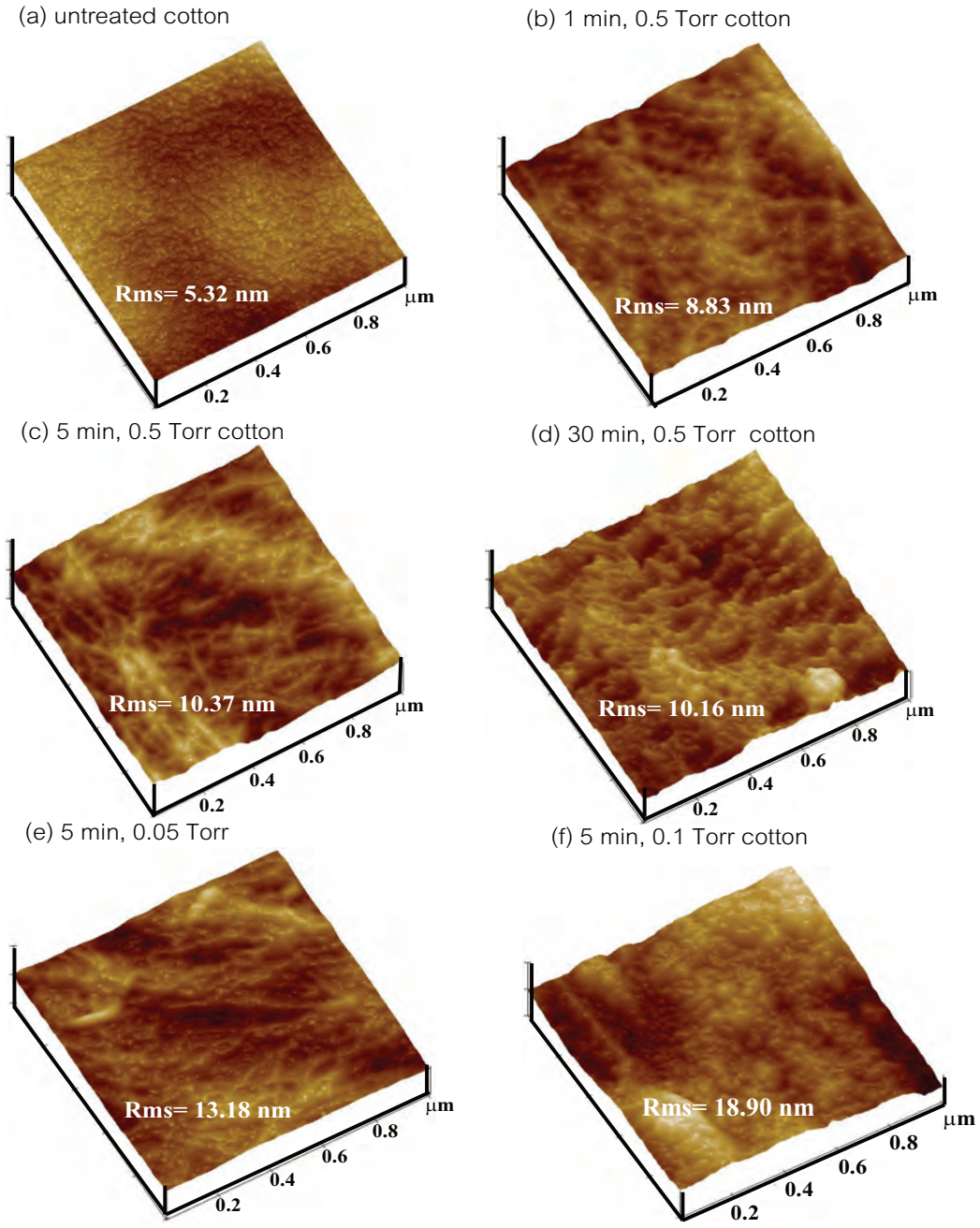

Figure 4.6: AFM images 1 μm x 1 μm of cotton fibers under SF_6 plasma conditions (a) untreated cotton (b) 1 min with 0.5 Torr (c) 5 min with 0.5 Torr (d) 30 min with 0.5 Torr (e) 5 min with 0.05 Torr (f) 5 min with 0.1 Torr.

Our results in found that the height and the distance between the nano-granuli created by plasma etching are in the range of 50-200 nm and 200-500 nm, respectively, roughly three orders of magnitude smaller than those found in water repellent plant leaves. These surface irregularities are incommensurate with the site of macroscopic water droplets. Therefore, in our case we believe that it is unlikely that the roughening makes any contribution to the improved hydrophobicity that we observe for our treated samples.

Many researchers have developed various techniques to reproduce this dual surface topology over various materials. T. serepi et al [99] reported that columnar super-hydrophobic surfaces with high-aspect-ratio nanostructures of poly (dimethyl-siloxane) (PDMS) coated on a flat silicon substrate can be achieved by plasma treatment of SF_6 gas and followed by fluorocarbon film deposition from CF. However, our attempts to carry very long (exposure time$>$ 30 min) and aggressive plasma treatments of cotton fabrics lead to notable color changes, and concluded that it is not possible to achieve superhydrophobic properties in cotton with our system. By way of comparison of the flat surface morphology and the etching rate in our process, we exposed a poly methylmethacrylate (PMMA) film to SF_6 plasma with the same conditions as cotton. We note that even PMMA does not have the same chemical composition as cellulose, we assumed that the plasma etching rate of the cotton fabric is a fraction loss of the film. The molecular weight of the PMMA used (120 kDa) was chosen for sake of comparison with the work by others [100]. In Fig. 4.7(a) - (f), show AFM images of untreated and treated PMMA films under the same SF_6 plasma conditions as cotton.

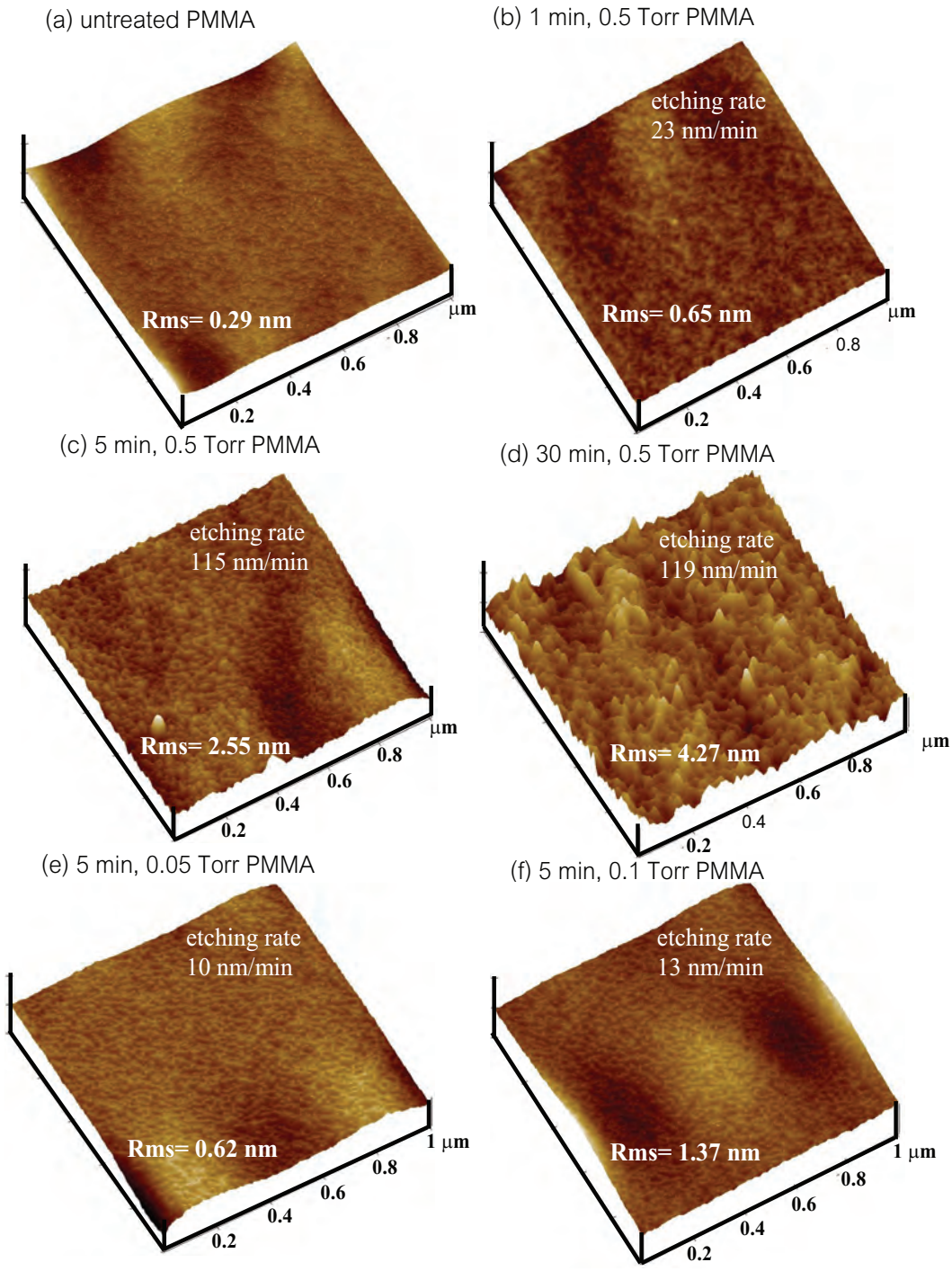

Figure 4.7: AFM images 1 μm x 1 μm of PMMA films under the same SF_6 plasma conditions (a) untreated cotton (b) 1 min with 0.5 Torr (c) 5 min with 0.5 Torr (d) 30 min with 0.5 Torr (e) 5 min with 0.05 Torr (f) 5 min with 0.1 Torr.

It is clear that there was not much change in surface morphology and RMS roughness of the PMMA films after exposing for 1 min at the pressure of 0.5 Torr and for 5 min at the lower pressure of 0.05 and 0.1 Torr. We found that process of plasma etching at higher conditions (see Fig. 4.7(c) - (d)) creates the granuli on the surface causing the increase of the RMS roughness from 0.29 nm to 2.55 nm and 4.27 nm, respectively. Some fraction of the film was scraped away to obtain the thickness of each film before and after plasma etching using the atomic force microscopy (AFM) measurements. An initial thickness of PMMA polymeric film was found to 1-4 μm depending on the number of layers deposited. After an exposure to SF_6 plasma, the thickness was reduced from which we extracted the average etching rate shown in Fig. 4.8(a) - (c).

In these experiments, we varied the exposure time and the SF_6 pressure. The etching rate of the film treated for 1 min was only 23 nm/min while the etching rate after 5 min was on the order of 100 nm/min. We conclude that < 1 min is the time (with fixed RF power of 50 watts and fixed pressure of 0.5 Torr) where no changes in surface morphology of cotton and PMMA films were seen. At high pressure (0.5 Torr), a high etching rate of $>>$ 100 nm/min was obtained. Since the sample holder is connected to ground, the sample is subjected to plasma potential only. This could be due to some capacitive coupling with the antenna resulting in high energy ion bombardment coupling with the antenna resulting in high energy ion bombardment.

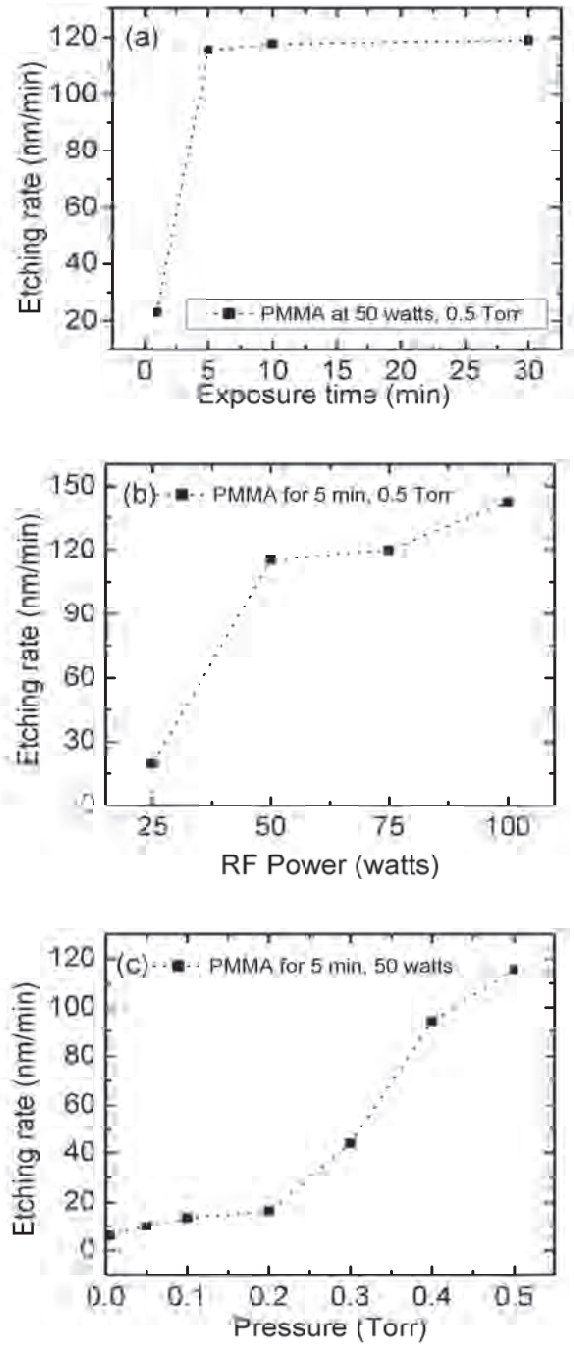

Figure 4.8: Etching rate of PMMA films versus (a) exposure time(b) RF power (c) SF_6 pressure.

In addition, we estimated the yield of fluorine species using an Ar actinometer by introducing 5% of Ar in the chamber atmosphere and monitoring the optical emission of F and Ar. To convert the emission intensities to atom density of fluorine or fluorine concentration using a known Ar concentration, we used Equation 4.1 [101];

$$[F] = 2\,[Ar]\,I_F I_{Ar} \tag{4.1}$$

where I_F is the intensity of the 704 nm F emission line, I_{Ar} is the intensity of the 750 nm Ar emission line [87], [Ar] is a known concentration of the actinometer and 2 is a proportionality constant. Figure 4.9 shows the fluorine concentration as a function of pressure. The F atom density increased with increasing SF_6 pressure, which is consistent with the increased etching rates observed at higher SF_6 pressures.

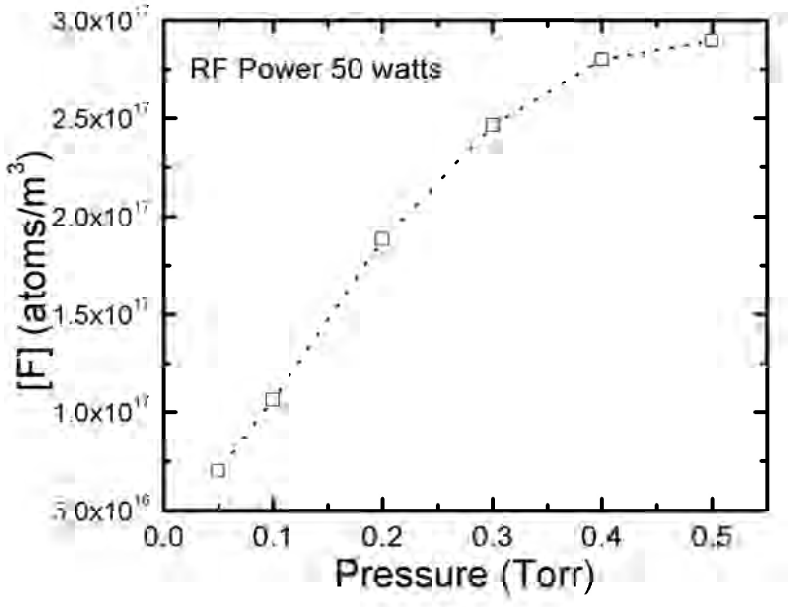

Figure 4.9: Fluorine atom density as a function of SF_6 pressure at the fixed RF power of 50 watts.

4.1.6 Chemical composition on surface cotton

Because it is difficult to observe the change in C-F bond by ATR-IR spectrum. The peak intensity change seem relatively low due to low concentration of fluorine on treated SF_6 surface [88]. So, the changes in chemical composition of the cotton surface were readily observed by X-ray photoelectron spectroscopy. Fig. 4.10 shows XPS survey spectra of untreated cotton and cotton treated at different plasma conditions. The samples exhibit the F1s signal after processing with plasma, with intensities rising as the SF_6 pressure and exposure time increased. In contrast, the peak area for C1s and O1s signals decreased with increasing pressure and exposure times. The structure of cellulose consists of glucose molecules linked together as shown in Fig. 4.11(a). In this structure, there are three different types of carbon atoms, i.e. the carbon 1s XPS spectra of untreated cotton should exhibit three distinct peaks corresponding to three different binding energies [29] as shown in Fig. 4.11(a). The signal with binding energy at 284.7 eV (C1) in our data was assigned to carbon atoms bound to a carbon atom or a hydrogen atom (-C-C/C-H), the peak at 286.2 eV (C2) corresponds to C-OH groups and the peak at 287.2 eV (C3) arises from O-C-O groups. The database of binding energy of XPS spectra was shown in appendix B.

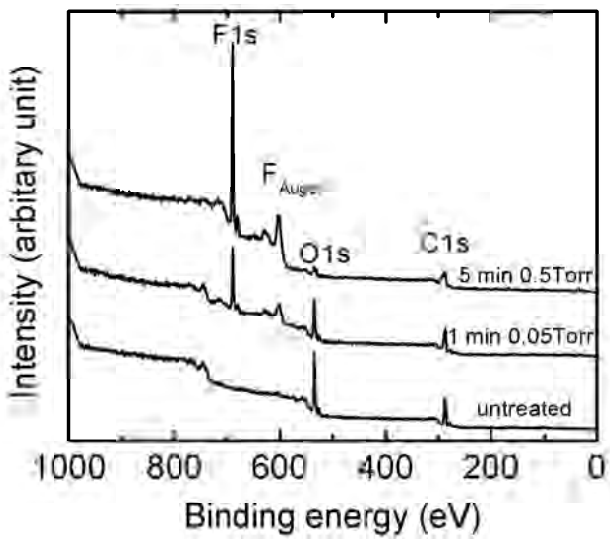

Figure 4.10: The XPS spectra for untreated and SF_6 plasma treated cotton.

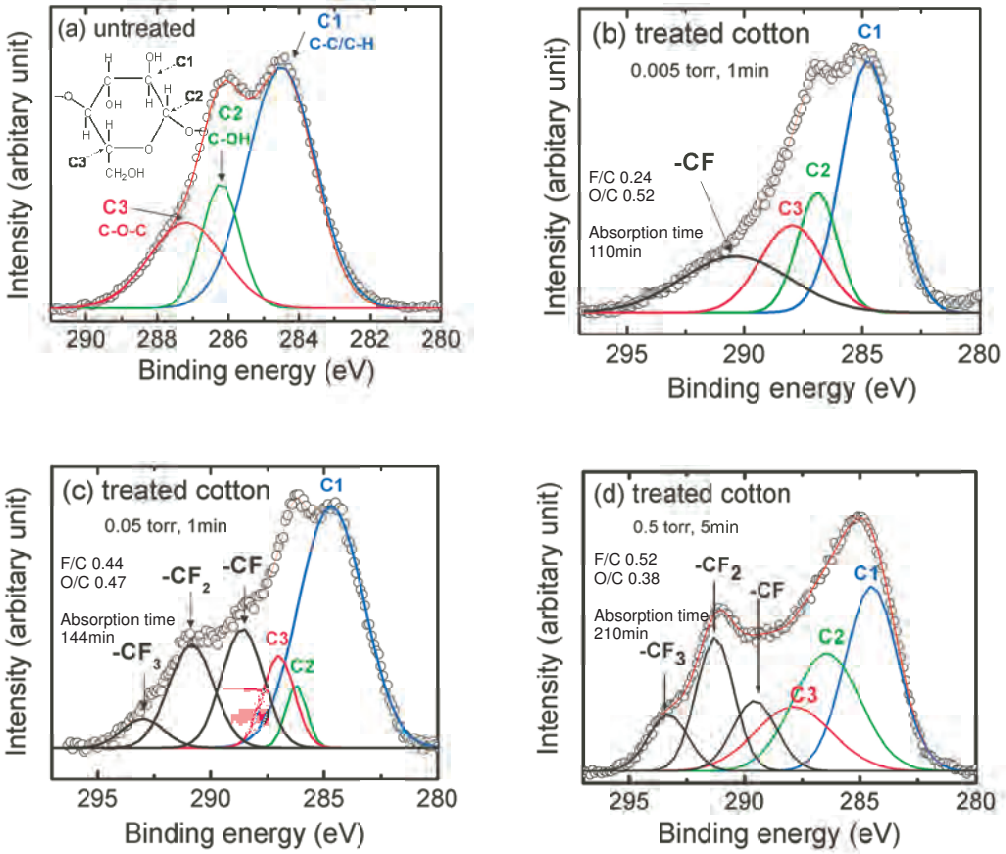

Figure 4.11: C1s XPS spectra of fabric surface (a) untreated cotton and the molecular structure of cellulose (b) cotton treated at the pressure of 0.05 Torr for 1 min (c) cotton treated at the pressure of 0.05 torr for 1 min (d) cotton treated at the pressure of 0.5 Torr for 5 min.

Figure 4.11(b) shows the XPS spectra of cotton treated for 1 min at a SF_6 pressure of 0.005 Torr and RF power of 50 watts. On the treated cotton, the XPS data shows distinct signals at 289.1 eV which is assigned to the CF moiety. The signals from pristine cotton are still evident on the spectra of the treated samples consistent with incomplete surface fluorination. In general, more pronounced changes are observed for cotton treated with high SF_6 pressure of longer exposure times as shown in Fig. 4.11(c) - (d). In particular, additional peaks become apparent at binding energies of 291 eV and 293.5 eV. These signals are attributed

to CF_2 and CF_3 groups, respectively. In summary, more intense treatments produce a grater fraction of fluorine bonds as evidenced by the increasing of total integrated areas of CF, CF_2 and CF_3 peaks.

From XPS spectra, we conclude that only F radicals are responsible for the surface chemical changes. The mechanism of fluorination relevant to our experiment is concerned with the chemistry of SF_6 discharges consisting of ionizations, dissociations, attachments, detachments, and recombination of charged and neutral species [100], [8], [102]. The XPS chemical analysis revealed that only the $F^{\bullet}$ is the active species that graft onto the fabric surface producing C-F- groups after abstraction of H and O atoms by other plasma species (ions, radicals, electrons and photons) [8]. We found that the water absorption time of the fabrics reaches the highest (210 min) when the fluorine/carbon ratio at the surface is larger than 0.4, along with a small decrease of the oxygen/carbon ratio. The calculation is based on the integrated area under the assigned C1s and F1s deconvolution peaks with sensitive factors for XPS transition. Figure 4.12 shows the F/C atomic ratios of cotton treated for different treatment time and pressures. The F/C atomic ratios slightly increase with treatment time but significantly increase with SF_6 pressure. Thus, the most important factor in enhancement of the hydrophobicity of treated cotton is the pressure. Our results agreed with the previous work on silk [8]. The number of hydrogen bonds between water molecules and surface groups of treated cotton are smaller causing the hydrophobicity. The number of hydrogen bonds between water molecules and surface groups of treated cotton are smaller causing the hydrophobicity.

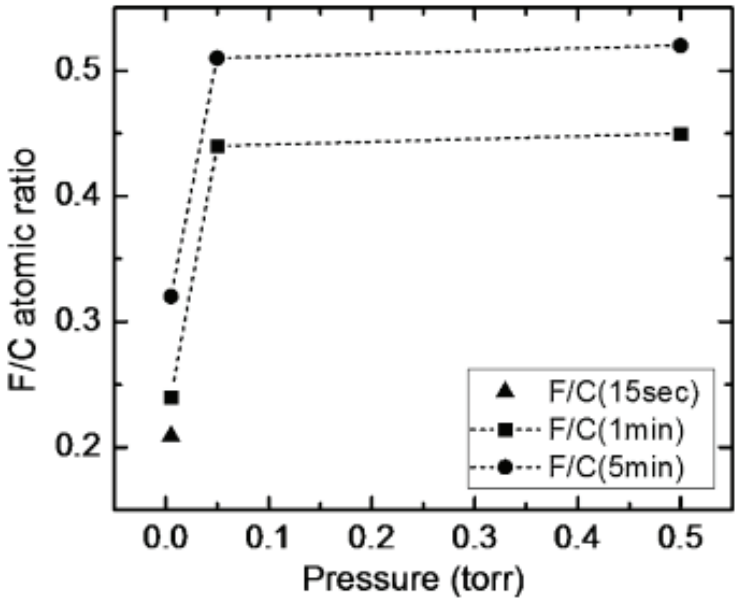

Figure 4.12: F/C atomic ratios of cotton treated at different treatment time and pressures(0.005, 0.05 and 0.5 Torr).

4.1.7 Effect of storage time and washing tests of cotton

We further checked the durability in terms of aging and washing fastness. After keeping the samples for one to four weeks, the contact angles of cotton treated for longer time than 30 s decreased by $< 30\%$ but remained higher than 100^o as shown in Table 4.3. Surprisingly, after exposure to SF_6 plasma for 30 min, the contact angle of treated cotton was still close to 100^o (see Table 4.3) and the absorption time was 30 min after washing up to five cycles (see Table 4.4). When the exposure time is less than 5 minutes, after one washing cycle the fabrics became hydrophilic. The best hydrophobic durability was obtained in the cotton fabric treated for 30 min in which the contact angle was close to 100^o after five washing cycles.

Table 4.3: Water contact angle of cotton fabrics treated by SF_6 plasma for various exposure time at a fixed pressure of 0.5 Torr.

Contact angle (±5 °) vs. Exposure time	Storage time (week)					Washing cycle (time)				
	con.	1	2	3	4	con.	1	2	3	5
untreated	0°	0°	0°	0°	0°	0°	0°	0°	0°	0°
15 s	145°	0°	0°	0°	0°	145°	0°	0°	0°	0°
30 s	145°	113°	108°	105°	102°	145°	0°	0°	0°	0°
1 min	146°	126°	123°	120°	117°	146°	0°	0°	0°	0°
3 min	147°	138°	135°	130°	126°	147°	0°	0°	0°	0°
5 min	148°	141°	139°	137°	135°	148°	20°	10°	0°	0°
10 min	149°	148°	147°	145°	142°	149°	85°	75°	50°	10°
30 min	149°	148°	147°	146°	145°	149°	120°	110°	100°	80°

Table 4.4: Water droplet absorption time of cotton fabrics treated by SF_6 plasma for various pressure at a fixed exposure time of 5 min.

Absorption time vs. (±5 °) Exposure time	Storage time (week)					Washing cycle (time)				
	con.	1	2	3	4	con.	1	2	3	5
untreated	0.5	0.5	0.5	0.5	0.5	0.5	0.5	0.5	0.5	0.5
15 s	60	0.5	0.5	0.5	0.5	60	0.5	0.5	0.5	0.5
30 s	90	5	1	0.5	0.5	90	0.5	0.5	0.5	0.5
1 min	210	15	10	5	2	210	0.5	0.5	0.5	0.5
3 min	210	210	60	50	45	210	0.5	0.5	0.5	0.5
5 min	210	210	210	180	180	210	1	1	0.5	0.5
10 min	210	210	210	180	180	210	60	30	2	0.5
30 min	210	210	210	210	210	210	120	90	60	30

Table 4.5: Water contact angle of cotton fabrics treated by SF_6 plasma for various exposure time at a fixed pressure of 0.5 Torr.

Contact angle (±5 °) vs. Pressure	Storage time (week)					Washing cycle (time)				
	con.	1	2	3	4	con.	1	2	3	5
untreated	0°	0°	0°	0°	0°	0°	0°	0°	0°	0°
0.005 s	138°	0°	0°	0°	0°	138.5°	0°	0°	0°	0°
0.05 s	140°	111°	108°	105°	95°	140°	0°	0°	0°	0°
0.1 min	144°	113°	110°	109°	105°	144°	0°	0°	0°	0°
0.2 min	145°	116°	115°	113°	111°	145°	0°	0°	0°	0°
0.3 min	147°	119°	118°	117°	115°	147°	20°	10°	0°	0°
0.4 min	148°	136°	134°	132°	131°	148°	0°	0°	0°	0°
0.5 min	148°	141°	139°	137°	135°	148°	20°	10°	0°	0°

Table 4.6: Water droplet absorption time of cotton fabrics treated by SF_6 plasma for various pressure at a fixed exposure time of 5 min.

Absorption time (±5 °) vs. Pressure	Storage time (week)					Washing cycle (time)				
	con.	1	2	3	4	con.	1	2	3	5
untreated	0.5	0.5	0.5	0.5	0.5	0.5	0.5	0.5	0.5	0.5
0.005 torr	47	0.5	0.5	0.5	0.5	47	0.5	0.5	0.5	0.5
0.05 min	61	5	3	2	0.5	61	0.5	0.5	0.5	0.5
0.1 min	210	30	20	10	5	120	0.5	0.5	0.5	0.5
0.2 min	150	35	30	20	15	150	0.5	0.5	0.5	0.5
0.3 min	210	40	35	30	22	210	0.5	0.5	0.5	0.5
0.4 min	210	60	50	45	30	210	0.5	0.5	0.5	0.5
0.5 min	210	210	60	50	45	210	1	1	0.5	0.5

As seen in Table 4.5, with the increase of SF_6 pressure, the contact angle and absorption time slowly increased. The cotton samples treated at higher pressure than 0.1 Torr still exhibited the contact angles larger than 100^o during four weeks of aging. After three washing cycles, the contact angle of cotton treated for 5 min in the highest SF_6 pressure used of 0.5 Torr was not measurable and the absorption time reduced to values (< 0.5 min) comparable to those for untreated cotton as shown in Table 4.6.

From the results of storage time and washing test seem that the hydrophobicity of cotton treated with extreme conditions appears to be durable as long as the fabric is not washed. Similar results have found by other groups [11], [89]. Li et al have found that the F/C and F/O ratios decreased after washing treated cotton [11]. Selli et al have reported that the fluorine/carbon ratio in poly (ethylene terephthalate) sample treated under RF power of 20 watts significantly decreased from 0.32 to 0.14 after 30 days storing where as the oxygen/carbon ratio did not change with aging [89]. They observed a slightly decrease in F/C for the PET samples treated at higher RF power along with unchanging hydrophobicity. Because the washing process consists of many steps such as soaking and rubbing in water and detergent. Our results showed that the SF_6 treated fabrics became less hydrophobic with the decreasing in water contact angle after washing process. The question is which step of the washing causes the removal of fluorine functional groups from the fabric surface. After I did some experiments, I found that only rubbing or washing with DI water is not the main cause of making the SF_6 treated fabrics to be hydrophilic. In contrast, if the treated sample is washed with detergent, the contact angles are gradually decreased. This is because detergent residues remain in the fabric after washing. We know that detergents which act as a surfactant have molecules with one side that prefers water (hydrophilic), and another side that prefers oils and fats (hydrophobic)as shown in Fig. 4.13 [90].

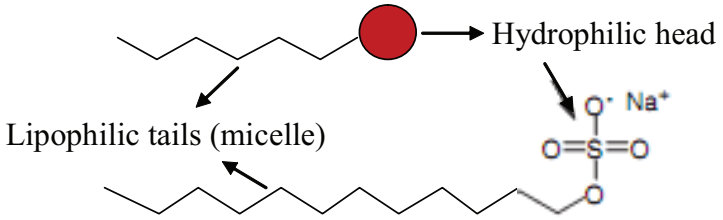

Figure 4.13: Surfactant used in laundary detergents that contain both hydrophobic (their lipophilic tails called micelle) and hydrophilic groups (their heads).

I did experiments systematically to prove that the main cause during that made the SF_6 treated fabrics to be hydrophilic after washing is the detergent. When the SF_6 treated fabrics are soaked in detergent and no rinsing, the water droplet on the fabric spreads quite quickly. Compared with after soaking and then rinsing, the water droplet spread slower. This could be that after rinsing the detergent is still remained in the fabric. Detergent acts as a connection between fabric surface and water droplet at which the hydrophilic side of detergent attaches to water molecules and another side (hydrophobic) attaches to the fabric. From this result, the water droplet spreads so quickly or less hydrophobic after the washing process.

In case of the hydrophobicity properties of the SF_6 treated fabrics, e.g. the water contact angle, decreased with the longer storage time. It means that at different storage times [91], the intensity of C-F spectra detected by XPS technique decreased. It seems like that the fluorine functional groups on the fabric surface are removed after leaving the fabric in an atmosphere for sometimes. Surprisingly, after heating that fabric at 100 ^{o}C, the fabric became hydrophobic again and the contact angle became more or less the same as before(130-135 degrees). This behavior could be explained as follows. Normally, the polar surface chains of the treated fabric after the plasma treatment re-orientate themselves in order to present a more polar surface. However, it is well known that the mobility of polymer chains increase with temperature [18]. Thus, the reorientation of the C-F bonds on surface will come back again after increasing temperature. In an-

other word, the fabric surface is completely covered by C-F groups which lower considerably the surface energy. That means the C-F bonds are not removed from the fibers but fluorine atoms introduced by the plasma treatment tend to migrate within the polymer. From this reason, we cannot observe large C-F spectra with XPS technique because of the limitation of XPS tool at which the signals from a few nanometer layers can be only detected.

4.2 Hydrophilicity of PET fabric after O_2, N_2 and Ar plasma treatment

4.2.1 Effect of contact angle and absorption time on PET fabric surface

In our study, it was clear that the plasma treatment have strong impact on the wettability of PET fabrics. The measured contact angle of the untreated fabrics quite high was about 120±5 degrees which poor wettability while those of fabrics treated O_2, N_2 and Ar plasmas for over 1 min, 25 watt and 0.1 torr can absorb water almost immediately leading to a contact angle of nearly zero degree or spreading on the surface as shown in Table 4.7 - 4.9. The zero contact angle means that the water droplet spreads on the fabric surface too quick so that we can not measure in time. From these results of contact angle show that oxygen, nitrogen and argon plasmas were effective in hydrophilicity on PET surface.

To present the hydrophilic properties of PET fabrics better than reporting the contact angle values, I chose the absorption time as functions of plasma parameters. Fig. 4.14(a) - (c) shows the results of absorption time measurement of water droplets as a function of exposure time, RF power and pressure. The dropping measurement was performed instantly after 1 min treatment of plasma. After treating PET fabrics with O_2, N_2 and Ar at plasma with exposure time even for 1 min with fixed RF power of 25 W and pressure of 0.5 Torr, the reduction

in absorption time can be seen. In the case of O_2 plasma treatment, PET surface exhibited minimum absorption time for all operating conditions. Since the plasma treatment considerably enhances the formation of polar species on fabric surface due to surface oxidation and other chemical changes, the XPS analysis will be reported in section 4.2.3 and the correlation between the hydrophilicity of fabric and O/C ratios can be also seen in the same section.

Table 4.7: The surface wettability of PET at different exposure time of Ar plasmas at 0.5 Torr pressure and 50 Watt RF power.

Exposure time (min)	Contact angle(±5 °)		
	O_2	N_2	Ar
untreated	120°	120°	120°
1 min	0°	0°	15°
5 min	0°	0°	0°
10 min	0°	0°	0°
30 min	0°	0°	0°

Table 4.8: The surface wettability of PET at different power of Ar plasmas at 0.5 Torr pressure and 50 Watt RF power.

Power (W)	Contact angle(±5 °)		
	O_2	N_2	Ar
untreated	120°	120°	120°
25	0°	10°	20°
50	0°	0°	0°
75	0°	0°	0°
100	0°	0°	0°

Table 4.9: The surface wettability of PET at different pressure of Ar plasmas at 0.5 Torr pressure and 50 Watt RF power.

Pressure (Torr)	Contact angle(±5 °)		
	O_2	N_2	Ar
untreated	120°	120°	120°
0.05	10°	20°	25°
0.1	0°	15°	20°
0.3	0°	0°	0°
0.5	0°	0°	0°

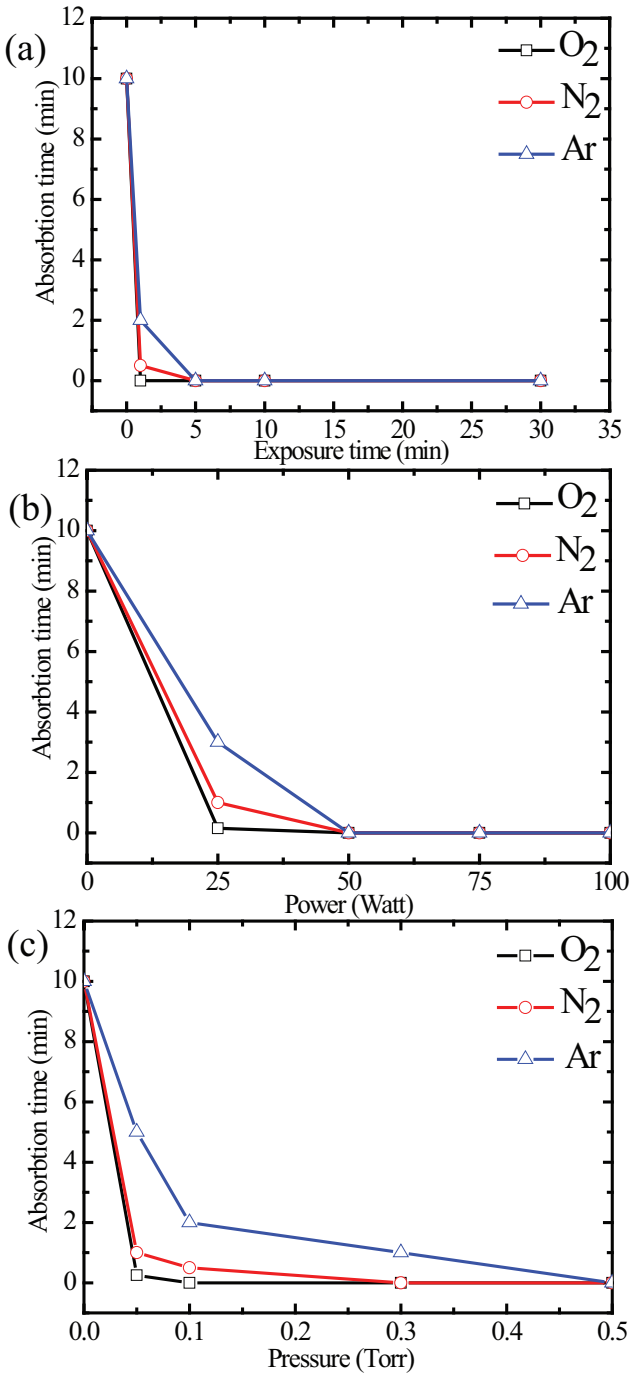

Figure 4.14: Water droplet absorption time on PET samples which treated with O_2, N_2 and Ar plasma at different (a) exposure time of 1- 30 min (b) RF power of 25-100 W (c) pressure of 0.05-0.5 Torr.

4.2.2 Effect of hydrophilic properties with plasma etching on PET fabric

In plasma treatments with non-polymer-forming gases, in general, the surface modification of plasma-treated fabrics can be achieved without changing the bulk properties of fabrics. However, the interaction of the active species in the plasma can affect the physical characteristics of fabrics. Especially, the etching process can remove something from surface leading to the change in surface morphology. In this study, the etching process on PET fabrics can be confirmed by weight loss of fabrics, the reduction of tensile strength and the morphology changes after plasma treatment observed by SEM and AFM.

The correlation of percentage of weight loss and tensile strength of PET fabrics were studied under different kinds of plasmas with exposure time of 1-30 min, RF power of 25-100 W and the pressure of 0.05-0.5 Torr. Among these three gases (O_2, N_2 and Ar), the highest weight loss and the lowest tensile strength were found in PET treated with O_2 plasma, following with N_2 and Ar plasma, respectively.

The weight loss of treated PET fabrics almost linearly increases with increasing exposure time, RF power and plasma pressure as shown in Fig. 4.15(a) - (c). It is less than 1 % when fabrics were exposed to any processing plasma for less than 5 min, 50 W and 0.5 torr and here is no observed considerable change in the surface morphology. With the treatment time of 30 min and the power of 50 W, the measured weight loss could reach 2.5 - 5.5% in PET samples treated with O_2 plasmas which also corresponded to the significant reduction in the strength of the samples.

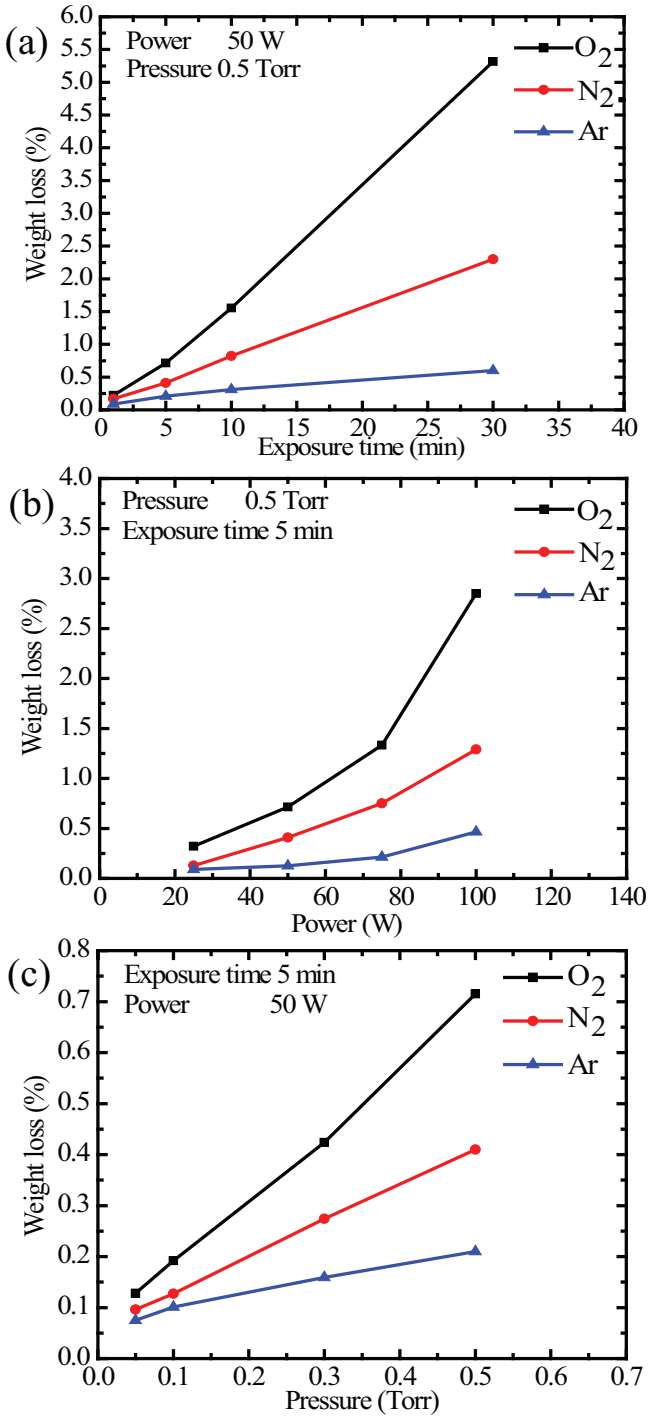

Figure 4.15: The percent weight loss of PET treated with with O_2, N_2 and Ar plasma at different (a) exposure time 1- 30 min (b) RF power 25-100 W (c) pressure 0.05-0.5 Torr.

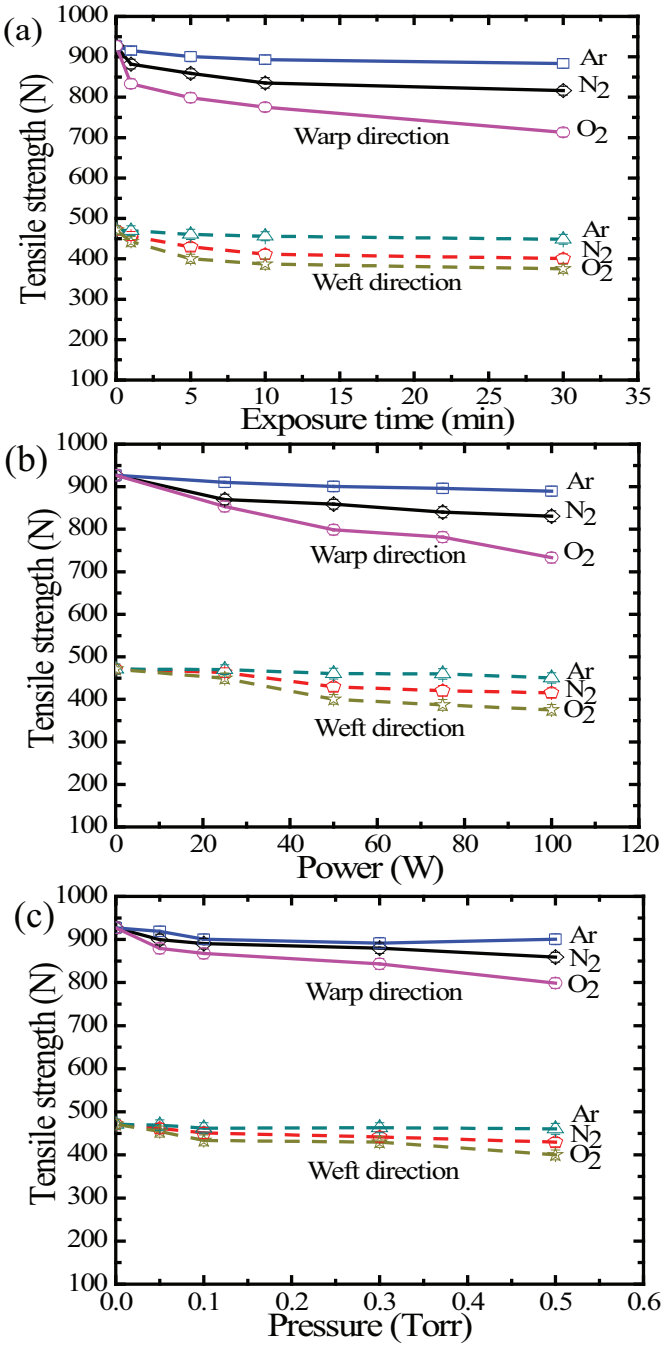

Figure 4.16: The tensile strength of PET fabrics in the warp and weft direction after treated with O_2, N_2 and Ar plasma at different (a) exposure time 1- 30 min (b) RF power 25-100 W (c) pressure 0.05-0.5 Torr.

Therefore, the weight loss of fabrics affects to the strength of fabrics which were investigated by tensile strength. As seen before in the study of cotton section 4.1.2, the tensile strength was greater in the warp direction than in the weft direction at all plasma conditions. The results of measurement tensile strength on PET fabrics both warp and weft directions were shown in Fig. 4.16(a)- (c). Overall trend, the tensile strength in warp and weft directions decreases with increasing exposure time, RF power and pressure. These results might be due to etching effect of plasma. In general, the bombardment by energetic ions causes deposited materials previously attached to the surface to be removed hence roughen the surfaces dramatically. The morphology changes can be observed in SEM and AFM images.

In Fig. 4.17(a) - (j), SEM images show the example of overall morphology of PET fiber surfaces treated with O_2, N_2 and Ar plasma at pressure 0.5 torr, exposure time 30 min and RF power 100 W and origin PET fabric. The differences in roughness when compare with untreated fabric which is very smooth, can be seen in treated samples. Notice that PET fabrics treated with O_2 plasma exhibit rougher surface than those treated with N_2 and Ar plasmas. PET fabrics, which are treated with O_2 plasma under extreme condition of exposure time 30 min, gave pore morphology on surface while the surface morphology of Ar and N_2 plasma treated PET fabrics for all condition exhibits surfaces with very slight alternations. Although, it cannot see much different roughness on surface in some conditions. It is still show good water absorption on surface under these conditions. That point confirms that the main effect of O_2, N_2 and Ar plasma to improve the hydrophilicity is superficial chemical modification, the etching effect being not relevant.

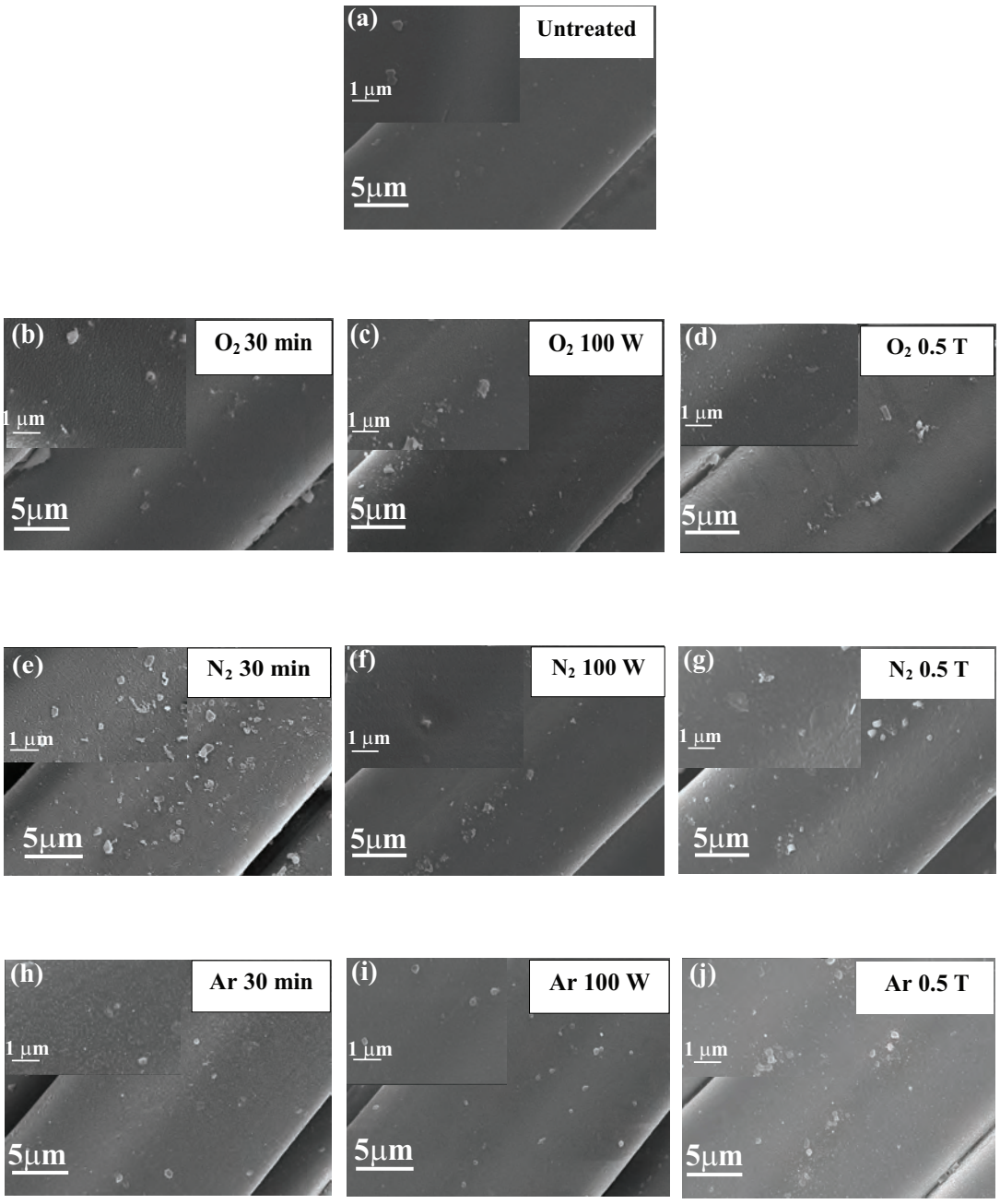

Figure 4.17: SEM photographs of untreated PET fabrics (a) and after treated with O_2, N_2 and Ar plasma at exposure time of 30 min RF power of 100 W and pressure of 0.5 Torr (b-j).

However, SEM can not give information at nanometer level. More differences of the roughness on the surface can be seen by AFM images. The surface roughness of PET was increased after O_2, N_2 and Ar plasma treatments at exposure time of 30 min, RF power of 100 W and pressure of 0.5 torr as shown in Fig. 4.18(a) - (j). The result clearly shows that the reactions from different gases cause different look on the surface morphology of PET. The O_2 plasma can produce deeper granular and wider grooves than that of N_2 and Ar plasmas, but there are more granular on PET treated by N_2 plasma. The grooves on the O_2 plasma treated fabric surface, which caused by bombardment of oxygen plasma species on the fabric, can increase the surface area inside of fiber and holes leading to more polar groups are generated. From this result, the fabric surface became more wettable fiber surface.

The root mean square roughness (Rms) and surface roughness on surface of PET treated with O_2, N_2 and Ar plasma at the same exposure time 30 min were reported in Fig. 4.19(a) - (c). We found that the root mean square roughness is in order nanometer (nm), for PET treated by O_2 plasma is about 14.84 nm, treated by N_2 plasma is about 9.73 nm and treated by Ar plasma is about 6.20 nm. In case of hydrophobicity study as described in section 4.1.5, we concluded the small decrease of O/C ratio and the increase of F/C ratio on the surface leading to the enhancement of hydrophobicity. Thus, we expected to see the same influence of specific functional groups,such as hydroxyl(OH), carbonyl (C=O) and carboxyl (COOH) in this case, on the improvement of hydrophobicity.

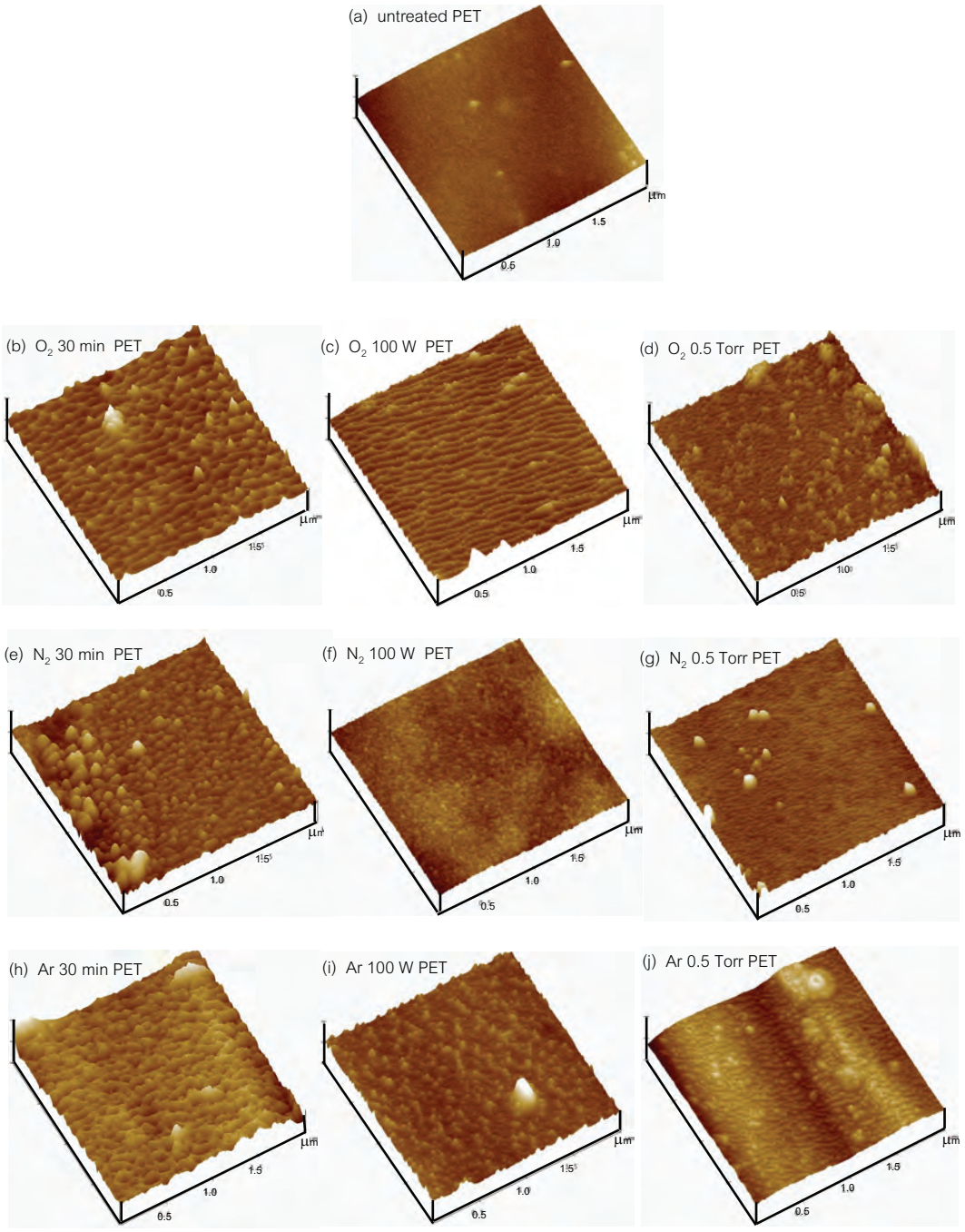

Figure 4.18: AFM photographs of untreated PET fabrics (a) and after treated with O_2, N_2 and Ar plasma at exposure time of 30 min RF power of 100 W and pressure of 0.5 Torr (b-j).

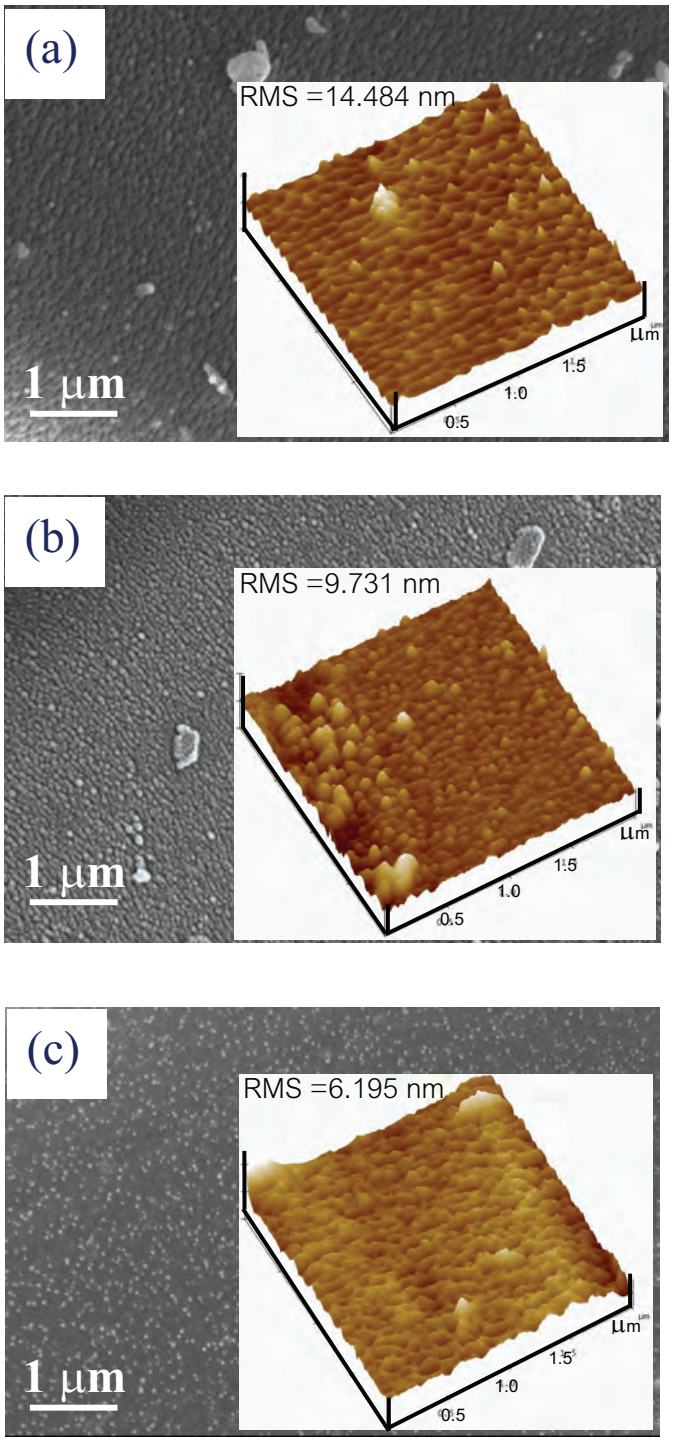

Figure 4.19: The SEM images with 1 μm inset with AFM images with 1 μm x 1 μm size of PET fibers treated for 30 min with (a)O_2 plasma (b)N_2 plasma (c) Ar plasma.

4.2.3 Effect of plasma-treated PET fabrics with surface chemical changes

Generally, the functional groups on the surface of samples can confirm by using FTIR spectrometry. In this work, we found that the FTIR-ATR spectra of treated PET fabric by Ar, O_2 and N_2 plasma at different exposure time power and pressure clearly show slightly change compare with untreated PET sample. The similar result on treated wool has found by Shahidi group [93]. They found that FTIR-ATR spectra of treated wool is slightly increase in absorbance at 1720 cm^{-1}(C=O bond) after O_2 plasma treatment and 3400 cm^{-1}, corresponding to N-H group after N_2 plasma treatment can be noticed. But after treatment with Ar plasma on PET fabric, no significant difference in the FTIR spectra compare with original samples. So, the relationship between the surface chemical structure and surface wettability of plasma of untreated and plasma-treated PET fabrics was carried out by XPS. The wettability of the fabric is tightly related to the presence of a particular functional group which resides in the outermost surface layer. To complete the investigation, PET fabrics are measured by XPS which can confirm the changing of functional group on the surface. Figure 4.20(a) - (c) show the overall XPS survey of untreated, O_2, N_2 and Ar plasma treated PET surface at exposure time of 30 min, power of 100 W and pressure of 0.5 Torr. From X-ray photoelectron spectra (XPS) analysis, the element content in the surface of PET after treatment with O_2, N_2 and Ar plasma lead to an increase in O1s intensity and a decrease in C1s intensity. Thus, it can be conclude that the new functional groups containing O and N were incorporated in to the surface components of the plasma-treated PET fabrics.

For untreated fabric, XPS signal displays the binding energy of C1s spectrum in C-C, C-H, C-O and C=O as shown in Fig. 4.21(a). After plasma treatment with all gasses at 30 min of the exposure time, 100 W RF power and 0.5 torr pressure, the intensity of -CH group in the treated PET at about 285.0 eV is decreased, but those of the -CO- and -COO- at 286.0 - 289.0 eV are increased. In

addition, the new functional group of C-OH appears on surface as compare with untreated sample as shown in Fig. 4.21(b) - (h). It can explain the significant of large amount of -CH has been oxidized into the forms of COOH or COH and these polar groups can bond with water molecules.

We know that the different gas plasmas may produce different amounts or types of new functional groups. The nature of the different functional groups on surface is ought to occur during and after plasma treatments [94]. When samples treated with oxygen and nitrogen plasma that are reactive gases, the polar groups are generated during plasma treatment by abstract hydrogen atoms from the surrounding polymeric chains. Oxygen plasma is very effective in hydrophilic modification due to formation of oxygen functional groups of carboxyl, carbonyl and hydroxyl group on surface. Nitrogen plasma is also effective in surface modification due to formation of nitrogen functionalities such as amino and amide groups. In addition, free radicals that remain on a polymer surface after a plasma treatment with both gases will also react with oxygen when the surface is exposed to the atmosphere afterward leading to the number of polar group is also increased. For the exposure of the polymer to inert gas of Ar gas plasma, the main effect of argon plasma on fabric is etching and hydrogen abstraction during chain scission leaving the free radicals at or near the surface which do not add new chemical functionalities from the gas phase during plasma treatment [95]. However, it seems that Ar plasma produces similar functional polar groups as active O_2 gas after performing with XPS experiment. Thus, it is possible that oxygen containing groups (-OH, C=O, COOH, COO-) are incorporated to the argon plasma-treated polymer surface by post-plasma reactions when they are exposed to air atmosphere cause that the plasma treated polymer surfaces become more hydrophilic [96].

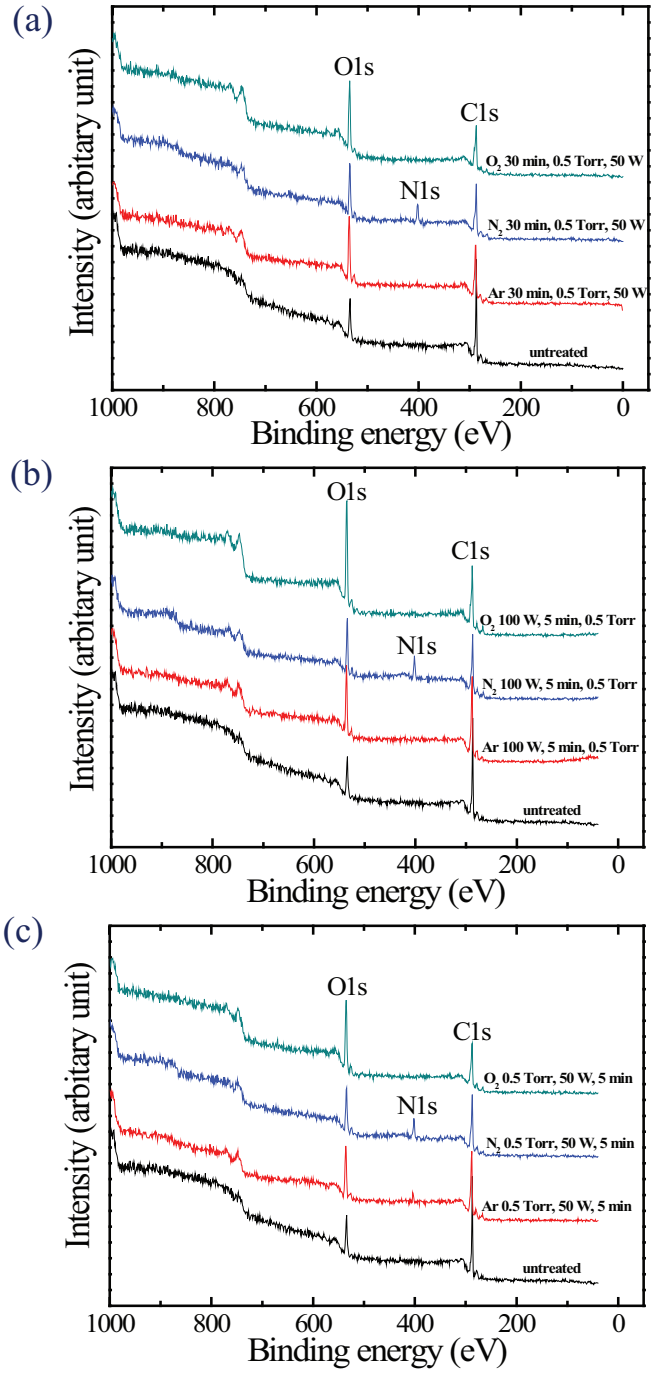

Figure 4.20: XPS survey scans of untreated PET fabrics and PET treated exposure by plasmas of O_2 , N_2 and Ar at 30 min (a), 100 W (b) and 0.5 Torr (c).

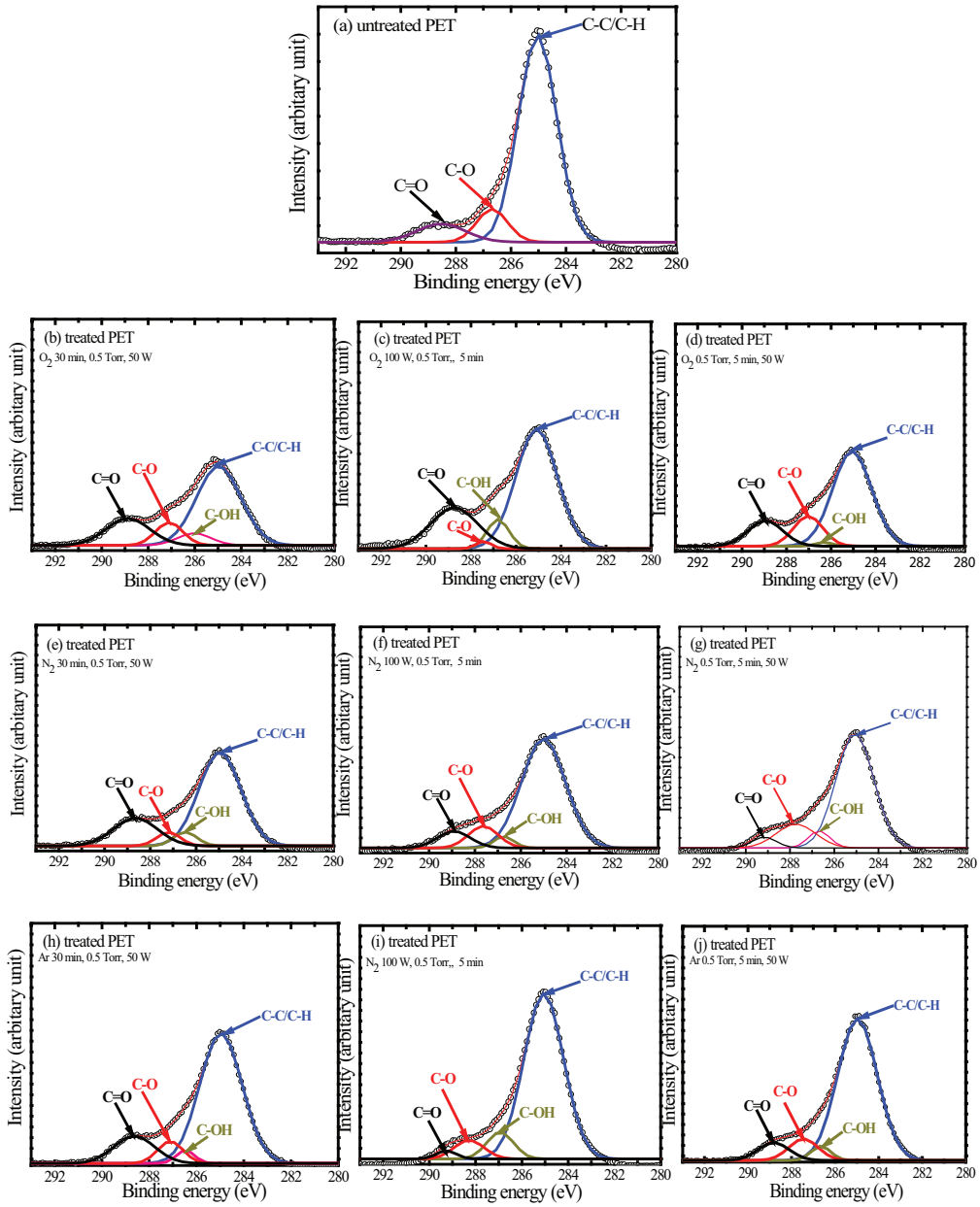

Figure 4.21: C1s XPS spectra of untreated PET fabrics (a) and (b-j) after exposure by plasmas of O_2, N_2 and Ar at 30 min, 100 W and o.5 Torr.

We further calculate the ratio of oxygen to carbon to see if there is any correlation between O/C and the plasma conditions, and also the hydrophilicity of treated PET. The ratios of O/C were plotted for all plasma conditions as shown in Fig. 4.22(a) - (c)). In the beginning of treatment, the polar groups are less generated, but with longer time treatment, more polar groups are generated. The efficiency of plasma reaction also depends on the extreme conditions used. This is due to increasing of the density of the charged species. With more plasma treatment, a larger concentration of active species occurs resulting in the increasing of the rate of ionization reactions. The results obtained from C1s and the O1s spectra can confirm the additional chemical bond formation by the O/C atomic ratio of PET surface which significantly increases from 0.24 in origin PET to 0.55 in the oxygen plasma-treated-PET. However, O_2 plasma provide the highest ratio of O/C in all conditions which means O_2 plasma is the best plasma to achieve the wettability of PET by generating functional groups (-OOH, -OH and -C=O), which are attached to the polymer surface. These functional groups form increase the surface energy of fiber and play an important role in increasing the hydrophilic properties of the fabrics.

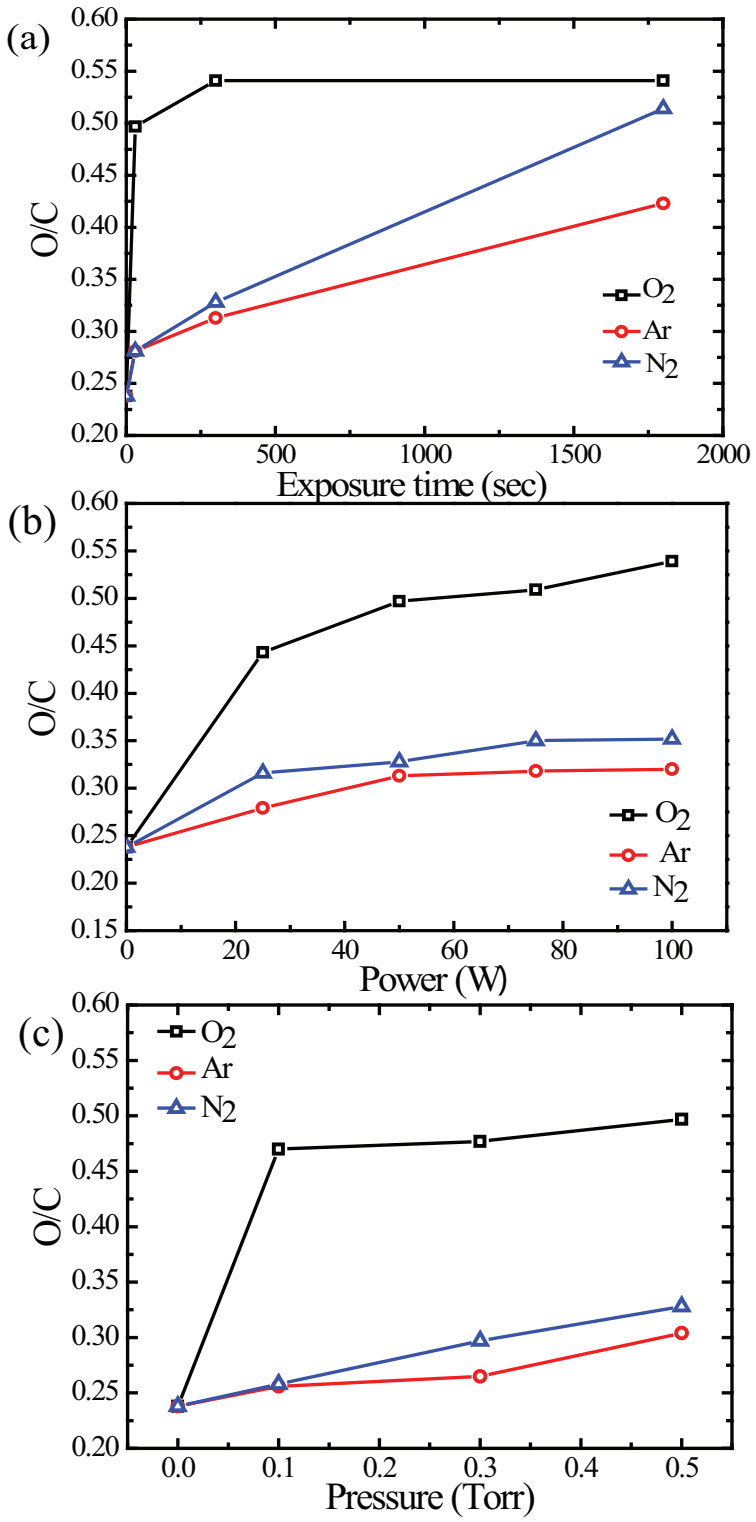

Figure 4.22: The ratios of O and C were plotted for all plasma conditions after PET treated with O_2, N_2 and Ar at different (a)exposure time (b) power and (c) pressure.

4.2.4 Effect of plasma-treated PET fabrics with average pore radius and diffusion coefficient

Due to the fast spreading of water on the surface or the low contact angle between fiber and the liquid which means high wettability, it is difficult to measure the contact angle directly. The capillary rise test was used to measure the contact angle at zero using Lucas-Washburn equation (H^2=D_Ct). This equation was already described in section 2.6.1 and section 3.3.3. We plot between H^2 and got a straight line, and the slope D_C is a capillary diffusion coefficient which is related to the size of capillary or the pore radius (R) and to the properties of the liquid. When liquid adsorbs completely which means the contact angle is zero. The three sets of experiments, data for PET treated with O_2, N_2 and Ar for different exposure time (1 min - 30 min) were shown as Fig. 4.23(a) - (c). The larger slope means the larger pore radii which is related to the average pore size of fabrics. The slope for fabrics treated with O_2 is larger than that of fabrics treated with N_2 and Ar, while the pore radiuses are increased with time for all gases. The values of R for O_2 plasma treated fabrics are ranging from 0.7 micron to 1.09 micron when the exposure time varied from 1 - 30 min which are about two times larger than that of the N_2 and Ar plasma treated fabrics when compared at the same exposure time.

For the effect of other plasma conditions, the pore radius (R) is also increased with higher pressure and power, and the diffusion coefficient is gained at intense conditions as shown in Table 4.10. We found that O_2 plasma results in the largest R values and then followed by N_2 and the last is by Ar. Figure 4.24(a) - (c) are the plots of H square versus t, time traveled by liquid at height H in the fabrics for PET treated with O_2 , N_2 and Ar for different exposure time (1 - 30 min). The slope can give the values of D_C which is a capillary diffusion coefficient. It related to the size of capillary R and to the viscosity of the liquid by equation(H^2=D_Ct). Therefore, the increasing in fabric hydrophilicity is generally related to an increase in the pore size.

Table 4.10: The values of R and D calculated by capillary rise method on PET fabrics after plasma treatment in various conditions.

Operrating parameters	R(μm			D(mm^2/s		
Condition	O_2	N_2	Ar	O_2	N_2	Ar
1min	0.70	0.25	0.15	25.36	5.49	9.14
5min	0.97	0.52	0.48	35.21	18.86	17.49
10min	1.08	0.54	0.50	39.29	19.79	18.02
30min	1.09	0.59	0.58	39.73	21.25	20.90
25W	0.74	0.30	0.25	26.70	11.06	16.87
50W	0.97	0.52	0.48	35.21	18.86	17.49
75W	0.97	0.62	0.52	35.25	22.37	18.78
100W	1.00	0.65	0.56	36.20	23.58	20.21
0.1Torr	0.69	0.47	0.43	25.15	11.06	16.87
0.3Torr	0.77	0.50	0.45	27.92	18.86	17.49
0.5Torr	0.97	0.52	0.48	35.21	18.86	17.49

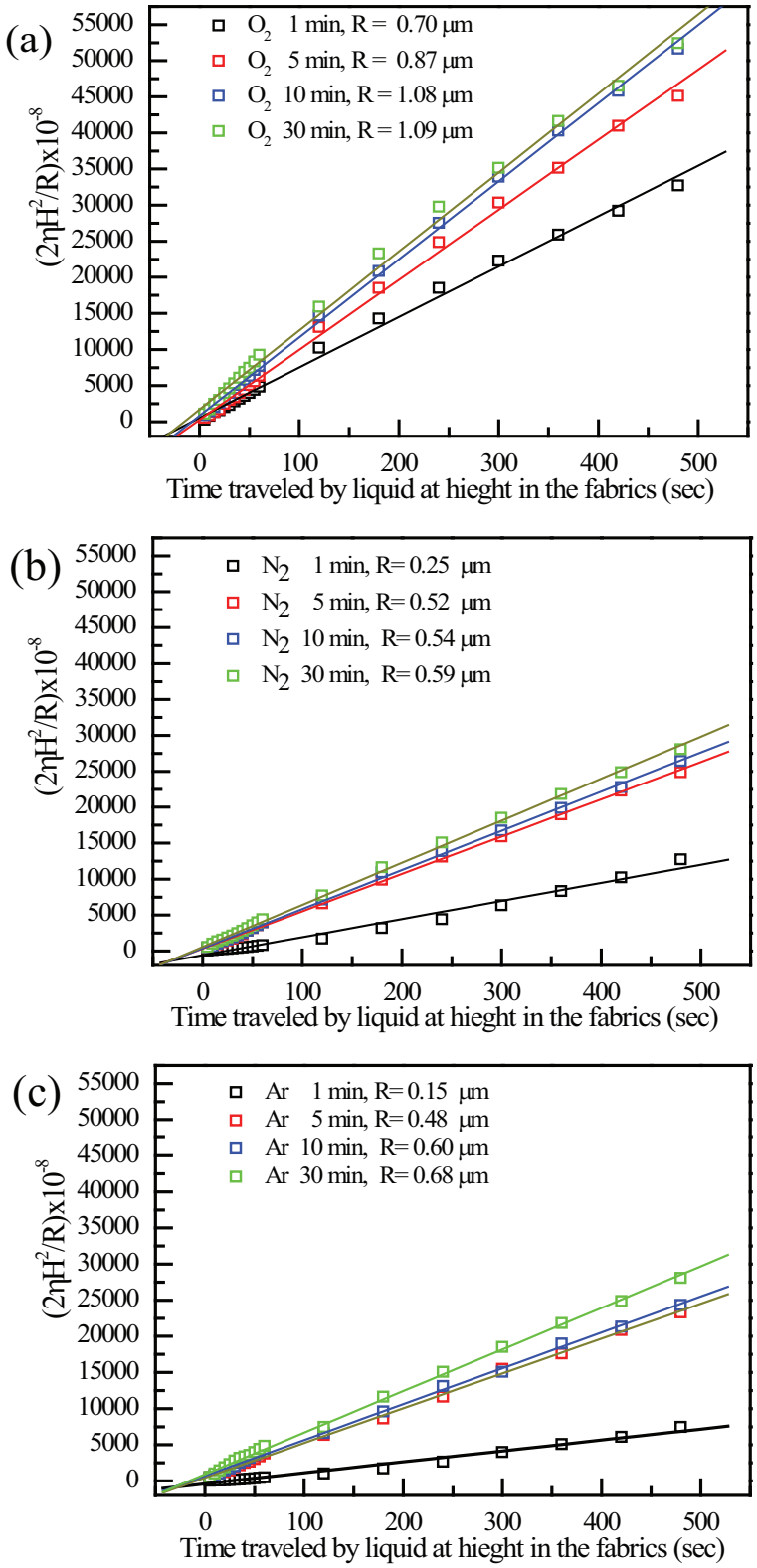

Figure 4.23: The plots of versus time traveled by liquid at height H in the fabrics for PET treated with O_2 , N_2 and Ar for different exposure time.

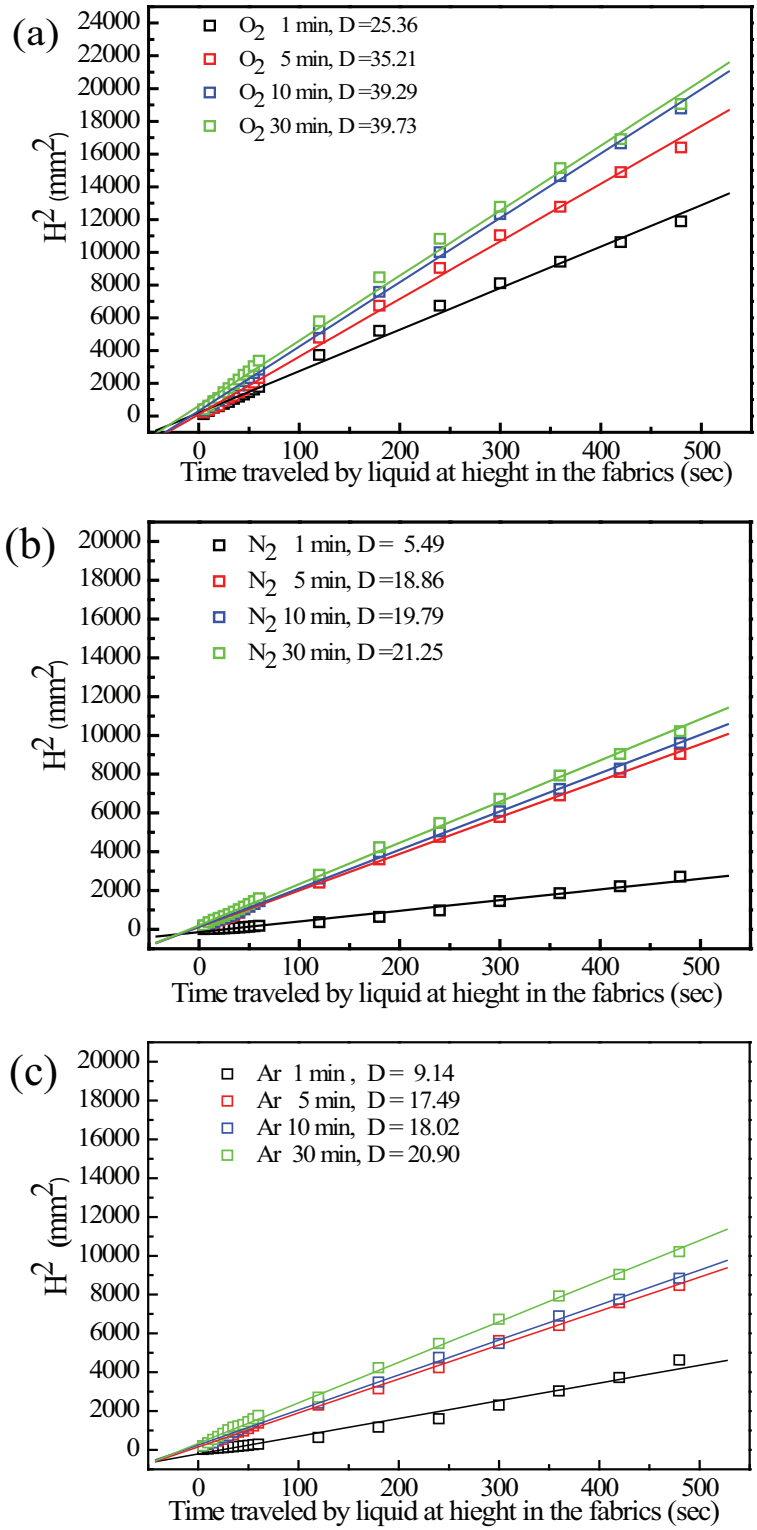

Figure 4.24: The plots of H square versus time traveled by liquid at height H in the fabrics for PET treated with O_2 , N_2 and Ar for different exposure time.

From the increase in the calculated R and D_C values, we can assume that plasma treating for longer time and at higher RF power and pressure causes generated more porosity with bigger size inside PET fabric. The resulting high porosity is due to the etching effect on the fabric surface leading to the change in the shape and size distribution of inter-fiber and inter-yarn capillary space [104]. Since the reactive gas can easily move into inter-yarn and inter-fiber space and polar groups are generated on larger surface area including the area inside the holes. Not only larger of pore radii can increase the hydrophilicity on PET fabric according to the capillary rise theory but also the more polar groups inside the capillary. It can explain by Lucas-Washburn equation(equation 2.9 and 2.11), the distance traveled by the liquid at time t (h) depends on only the inter-fiber pore structure (R) and to the surface properties of the liquid (γ). The physical parameters used to plug in the Lucas-Washburn equation is the surface tension of water (72.8 mJ/m^2), the viscosity of water, and we approximated θ to be zero. Nevertheless, we already concluded that the functional groups affect the hydrophobic and hydrophilic properties of the fabrics. Diffusion coefficient (D) can be explained by the ability of fiber to absorb water and can be determined from the slope of graph H^2 vs t. Thus, we expected that the calculated diffusion coefficient is involved with not only the physical parameters (γ, η, θ) but also the functional groups created inside the fibers. Also, we expected that the calculated pore radius is not the exact values, but only the estimated values. The calculated pore radius in our experiment could be over-estimated.

4.2.5 Dyeability of plasma-treated fabrics with different conditions

Effect of physical and dyeability

The investigation of dyeability of treated PET fabrics was obtained by different in color change both after plasma treatment and after washing which was reported as K/S values. As discussed in section 3.3.1, K/S values refer to the

reflectance of colorant layer which is related to the ratio of absorption K and scattering S coefficient. In Figure 4.25(a)-(c), the relative color strength (K/S values) before and after washing of fabric after dyeing increased gradually with the plasma treatment in all conditions. This is due to increase in dye molecule penetration into the roughening fabric surface caused by the plasma treatment and the increase in polar groups which strong were bonded with dye molecules on the surface and inside the pores. For K/S values after dyeing, O_2 plasma treatment on PET fabrics for all conditions of this study consisting exposure time (1-30 min), RF power (25-100 W) and pressure (0.1-0.5 Torr) can give the K/S values higher than those of N_2 and Ar plasma. Ar plasma provides minimum K/S values, especially at very low pressure. However, all of gases gave the good K/S values at the exposure time 30 min.

After one cycle of washing for dyed PET fabric treated with O_2 plasma for 30 min, the K/S values slightly decreased. This result can confirm the stability of dye attachment to the fabrics. This could be the effect of roughness on surface in longer treatment time, higher power and pressure that cause better attaching of dyes on fabric [103]. Another reason could be the increase in polar group on the treated PET surface is strongly bond with dye molecules.

In case of the result of color depth (I_{CD}) after the plasma treatment, dyeing on treated PET fabrics also exhibited a higher increase in color depth as compared with untreated PET, especially as a function of the exposure time shows in Fig. 4.26(a) - (c). The increasing in color depth of dyeing may be correlated to the plasma-induced increase in roughness. It is a key factor for the color deepness of dye fabric at which the holes or pores of the inter-fiber spaces and inside of fibers can hold more dyes. Also, this is the reason to make it difficult to remove dyes after washing.

Effect of surface chemical composition and dyeability

In order to confirm the relation of functional groups data with dyeability on PET fabric which considered from the ratio of O/C value and K/S value as shown in Fig. 4.27(a) - (c). It is found that PET treated with O_2, N_2 and Ar plasmas gave higher of K/S values than those of untreated fabric at which the ratio of O/C on treated fabric is increased. PET treated with O_2 plasma gives the highest K/S values in all conditions due to better plasma oxidation reactions producing oxygen-containing functional groups on the surface. Therefore, more interaction between the dye and treated PET fabrics due to the enhancement of functional groups on the surface caused the increasing of dyeability on the fabrics. However, the result of etching on the surface was related to more sensitive of dyeability which was considered in the next section.

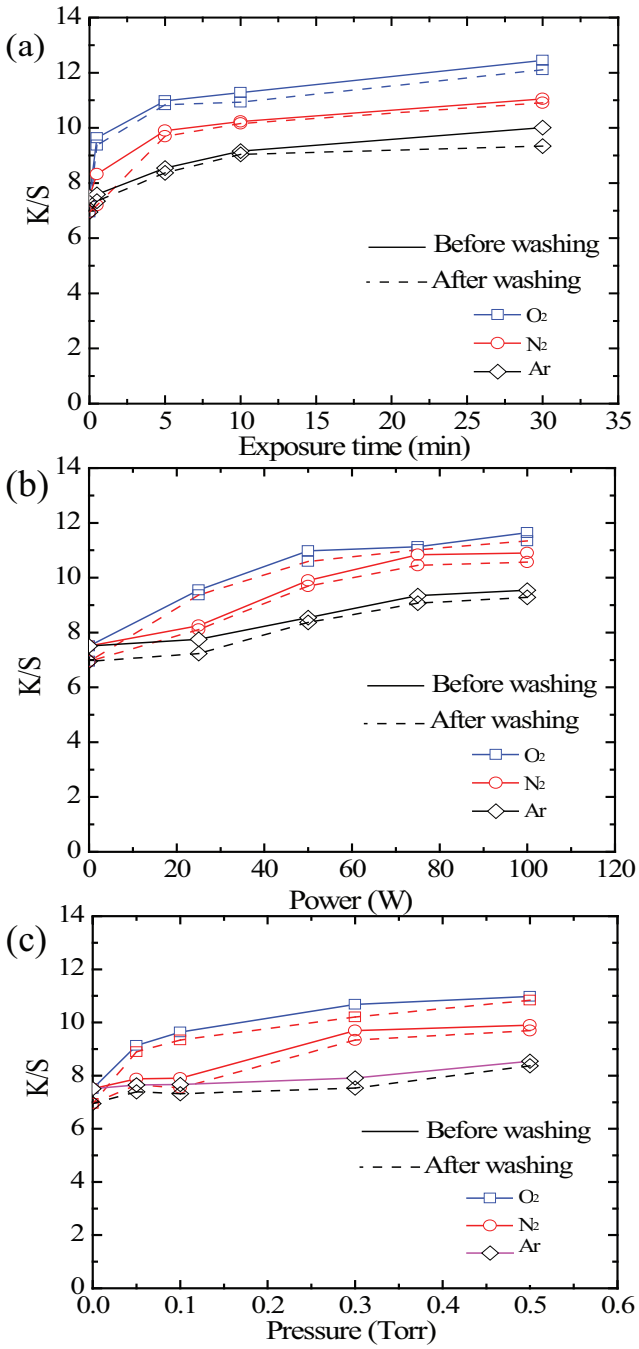

Figure 4.25: The K/S values graphs of PET fabrics treated with O_2, N_2 and Ar before and after washing.

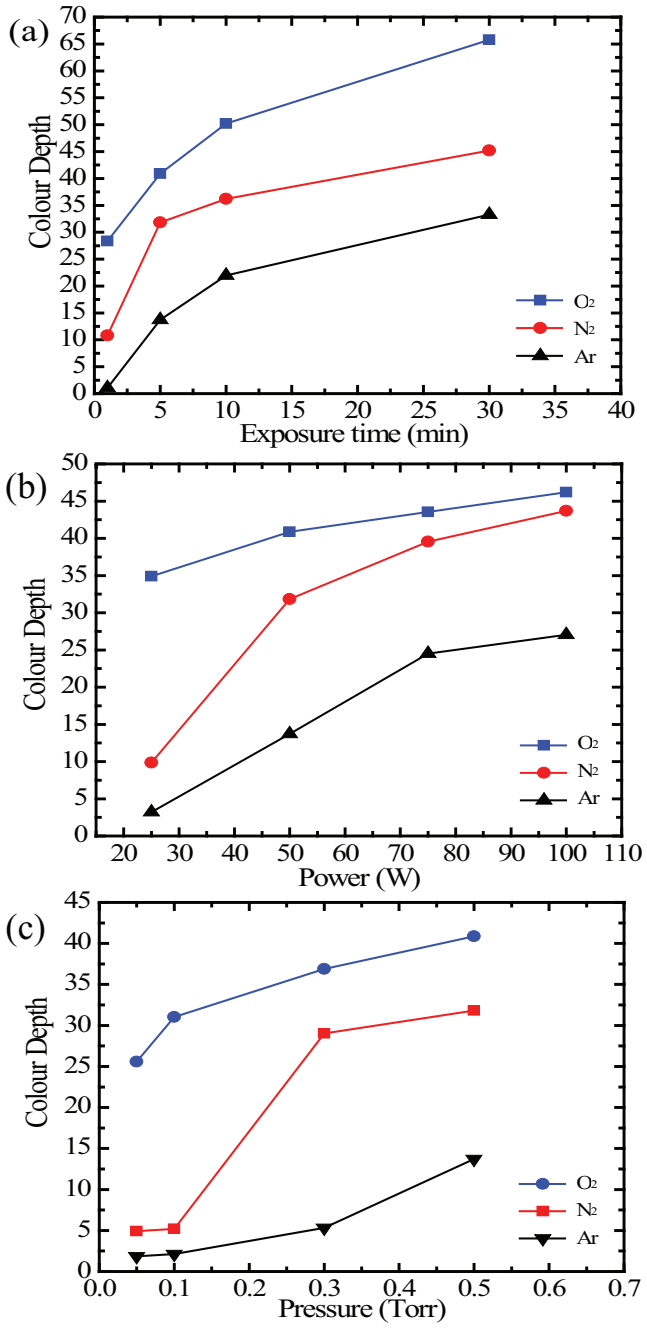

Figure 4.26: The colour depth values graphs of PET fabrics treated with O_2 N_2 and Ar.

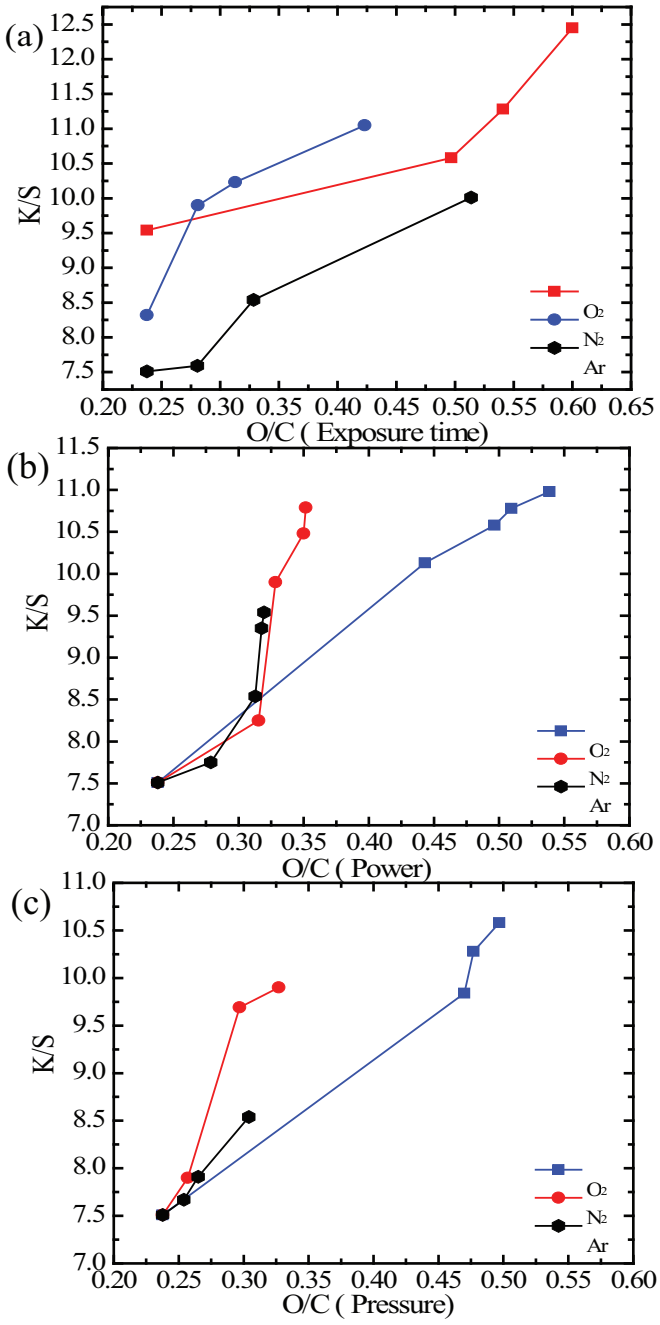

Figure 4.27: Relationship of the ratio of O/C value and K/S value after PET treated with O_2, $N_2$and Ar.

Effect of weight loss and dyeability after plasma treatment

To complete the investigation, the relationship between weight loss and dyeability as function of K/S values after plasma treatment for all gasses and various conditions were also investigated as shown in Fig. 4.28. We found that the K/S values increased with increasing weight loss. These results show that the higher weight loss or etching effect on PET fabrics surface in all conditions of plasma treatment result in the higher K/S values. Therefore, the increasing of surface roughness in nano scale can also improve the dyeability of PET fabrics. It is due to the surface roughness can increase surface area into inter-fiber spaces for enhancement of adhesion of polar groups on surface.

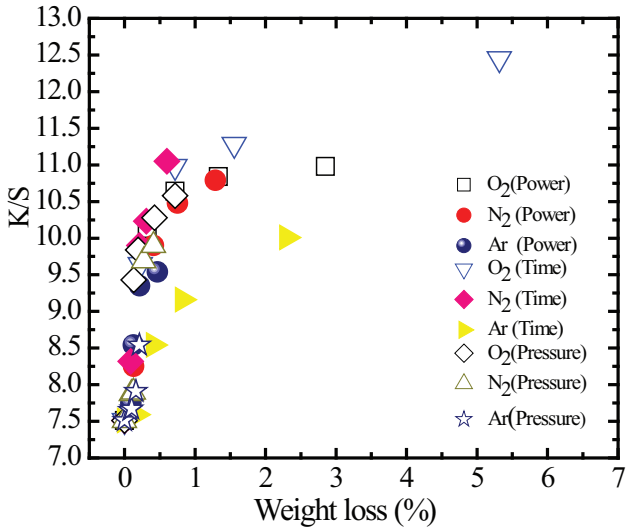

Figure 4.28: Relationship between weight loss (%) and K/S value of PET after treated with O_2, $N_2$and Ar under different conditions.

4.3 Plasma-induced graft-polymerization (PIGP) of silk fabric with organophosphorus flame retardant

4.3.1 Evidence of the grafting of polyDEAEPN and poly-DEAEP onto silk fabrics by PIGP process.

The weight gain and the phosphorus content of the DEAEPN and DEAEP treated silk fabrics, at different monomer concentrations, after washing in solvents in which the monomer and the polymer are well soluble are listed in Table 4.11.

Table 4.11: Weight gain, measured phosphorus content before and after burning, LOI and char yield of the silk fabrics treated with DEAEPN and DEAEP at different monomer concentrations.

Sample	FR monomer [%]	Weight gain [%]	%P [%]	LOI [%±0.1]	Char residue [%]	%P of char [%]
Untreated silk	-	-	-	25.0	9.38	-
DEAEPN treated silk fabric	10	6.62	0.66	29.0	18.95	4.56
	20	11.22	1.38	30.5	29.98	5.21
	30	16.68	2.10	31.0	32.50	6.69
DEAEP treated silk fabric	10	5.37	0.63	28.0	16.10	2.47
	20	10.12	1.34	29.0	25.98	3.38
	30	13.47	1.69	30.0	31.74	6.54
	40	20.10	2.18	30.5	32.70	6.23

First of all, regardless the nature of the monomer, the grafting yield is over 50% in each experiment and increases almost linearly with the initial concentration of the monomer. This result can be compared with other pad-dry-cure processes described in the literature using analogous monomers. For instance, in the experiment reported by Guan et al.[10], less than 5% of weight gain was obtained with an initial concentration of 40% (w.o.f.) of DMMEP. This result demonstrates the efficiency of the PIGP process which allows to reduce significantly the amount of chemicals. This is even more appreciable in the experiments with the phosphoramidate monomer. We explain this observation with the higher affinity of this monomer for the polar silk protein surface due to the interaction with the N-H bonds. We have already observed this behaviour with cotton fabrics where we could reduce considerably the amount of cross-linking agent [107].

The grafting of a phosphorus containing polymer by the PIGP process was evidenced by several techniques. Among them, the evaluation of the phosphorus content indicates a non-negligible amount of remaining phosphorus containing polymer, up to 2% by weight of the fabric, after washing (Table 4.11). XPS surveys exhibit the P2s and P2p components respectively at 189.0 and 130.6 eV (Figure 4.31). Finally, the FT-IR spectra of the polyDEAEPN (curve a), the control silk fabric (curve b), and the treated silk fabrics with 20% (w.o.f.) of DEAEPN (curve c) and 20% (w.o.f.) of DEAEP (curve d) are presented in Fig. 4.29. The treated fabrics, after washing, show the characteristic absorption bands at 1250, 1150, 1024-1078 and 985 cm^{-1} corresponding to the P=O, P-O-C and P-O stretching vibrations also seen in polyDEAEPN. FT-IR spectra have been recorded for treated fabrics with 10% and 30% (w.o.f.) of the monomer and they show a similar pattern of the absorption bands as in the polymers. As expected, the intensities increase with increasing concentrations. Furthermore in all spectra of the treated samples, the most intense absorption bands of the silk fabric are still visible, notably the strong N-H vibration at 1506 cm^{-1} characteristic for the peptide bond of the silk protein. This indicates that the thickness of the deposited polymer is smaller than the thickness analysable either by XPS and FT-IR.

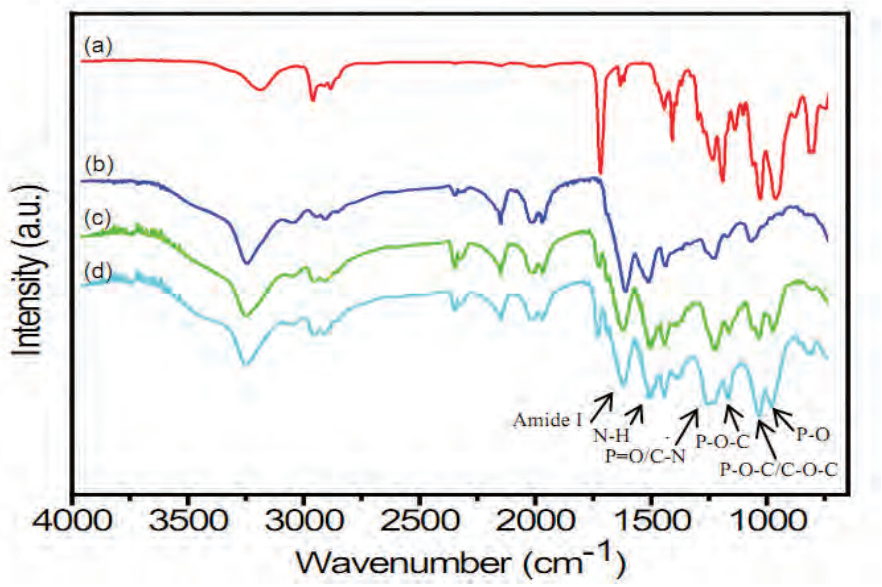

Figure 4.29: The IR-ATR spectra of (a) polyDEAEPN (b) control silk (c) DEAEPN (20% w.o.f.)treated silk and (d) DEAEP (20% w.o.f.) treated silk

In addition, the thin and homogeneous transparent coating occur on silk fabrics after flame retardant finishing can observe with surface morphology by SEM images. The surface morphology of origin silk, Ar plasma treated silk and silk grafted with 20%(w.o.f) of DEAEPN and 20%(w.o.f) of DEAEP are shown in Fig. 4.30(a)- (d). Figure 4.30(a)- (b) clearly demonstrated that untreated silk and Ar plasma treated silk fabric surface were smooth and free from roughness. In Fig. 4.30(c)- (d), the SEM micrographs of treated silk with monomer were almost the same or slightly changed on the surface when compare with origin silk. The results can prove that the flame retardant finishing on the silk surface is very thin leading to the allowing as well the breathability of the fabric.

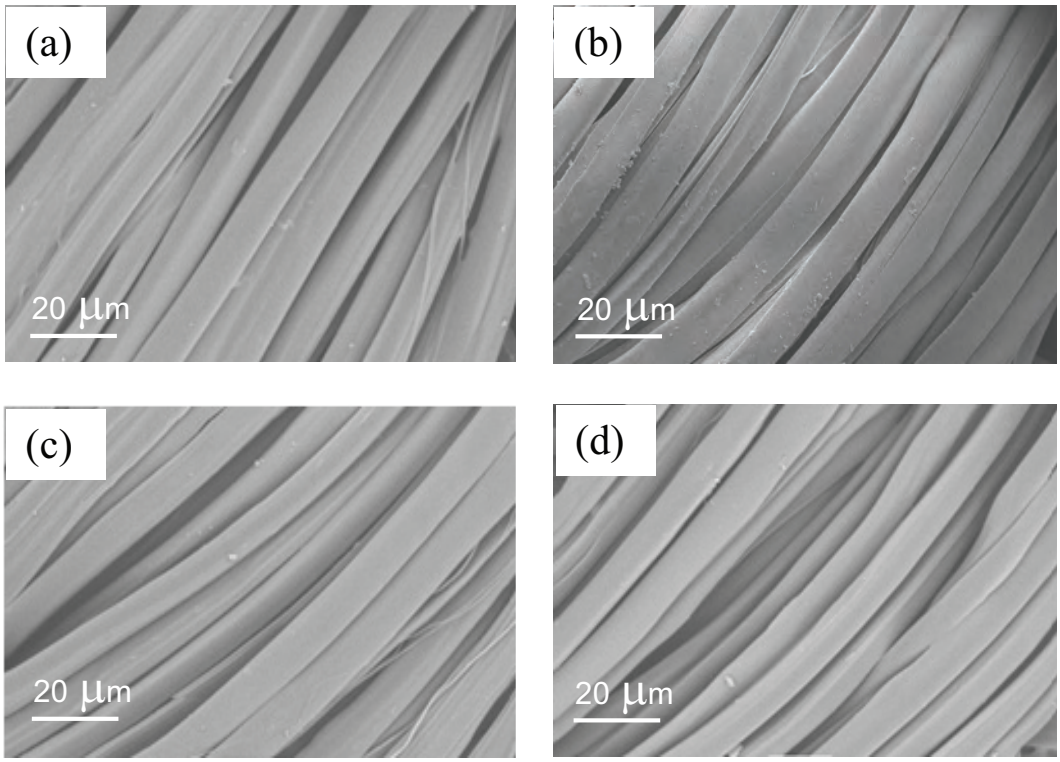

Figure 4.30: SEM micrograph of (a)origin silk (b) Ar plasma treated silk (c) DEAEPN 20% (w.o.f.) treated silk (d) DEAEP(20% (w.o.f.) treated silk

In order to investigate the chemical composition of silk-grafted with poly-DEAEPN and polyDEAEP, we performed XPS analysis on the samples prepared with concentration of 20% (w.o.f) of DEAEPN and DEAEP and treated with Ar plasma at pressure of 0.5 Torr and treatment time of 20 min. Figure 4.31 shows the survey XPS spectrum of origin silk and silk-grafted with DEAEPN and DEAEP monomers.

The main peak for C1s, N1s and O1s signals appeared in the XPS spectra of silk. In another word, The new two peaks for P2p and P2s signals also appeared in the XPS spectrum of treated silk. Line-shape analysis by peak deconvolution shows the C1s spectrum of origin silk which contains three distinct peaks as shown in Fig. 4.32 (a). These peaks correspond to binding energies of 284.7 eV (C-C/C-H), 286 eV (C-N) and 288.5 eV (C=O).

Figure 4.32 (b)- (c) show the C1s spectrum of two new peaks at 286.7 eV and 289 eV which correspond to C-O and O-C=O , respectively. Figure 4.32 (d)- (e) show the O1s spectra of silk-grafted with 20%(w.o.f) of DEAEPN and 20%(w.o.f) of DEAEPN monomers. The binding energy of 532 eV can be assigned to P=O or C=O groups, while the peak of 533 eV can be assigned to O-C-O or P-O-C groups. These absorption peaks are in agreement with the result of FTIR data. Figure 4.32 (f)- (g) show the P2p signals of silk-grafted with 20%(w.o.f) of DEAEPN and 20%(w.o.f) of DEAEPN monomers. Only one strong peak of P2p at about 134.6 eV was observed. It can be assigned to P=O group in the phosphate species. From XPS results, the appearance of double bond, carboxyl, carbonyl groups and phosphate species on silk-grafted with monomers can confirm the carbon content in the decomposed fabrics.

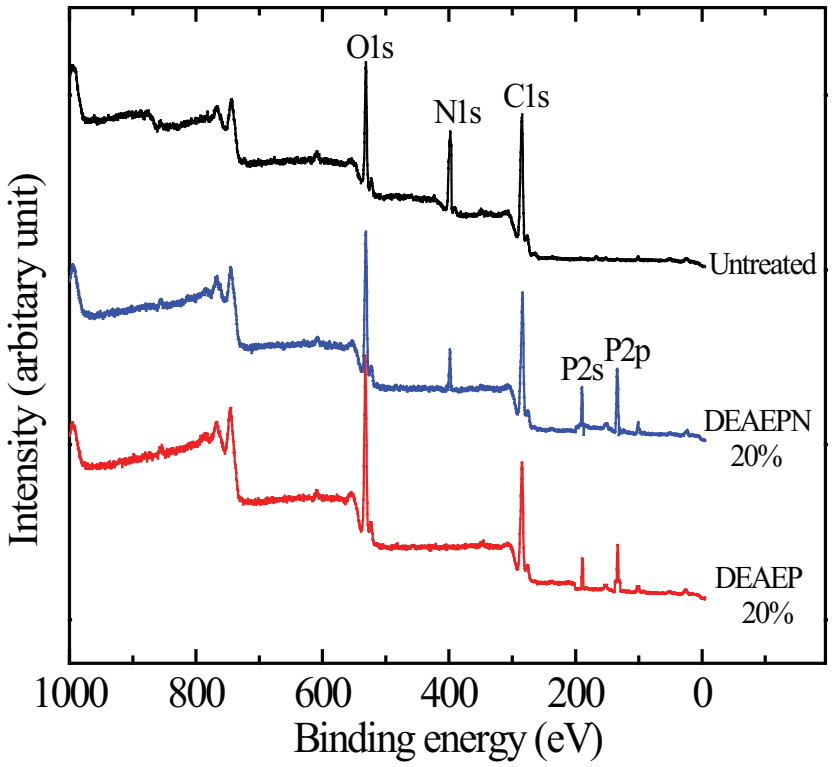

Figure 4.31: XPS survey spectrum of (a) origin silk and silk-grafted with concentration of monomers EAEPN 20% (w.o.f.) treated silk and DAEP 20% (w.o.f.) treated silk and (b) Line-shape analysis of the high-resolution C1s of origin silk

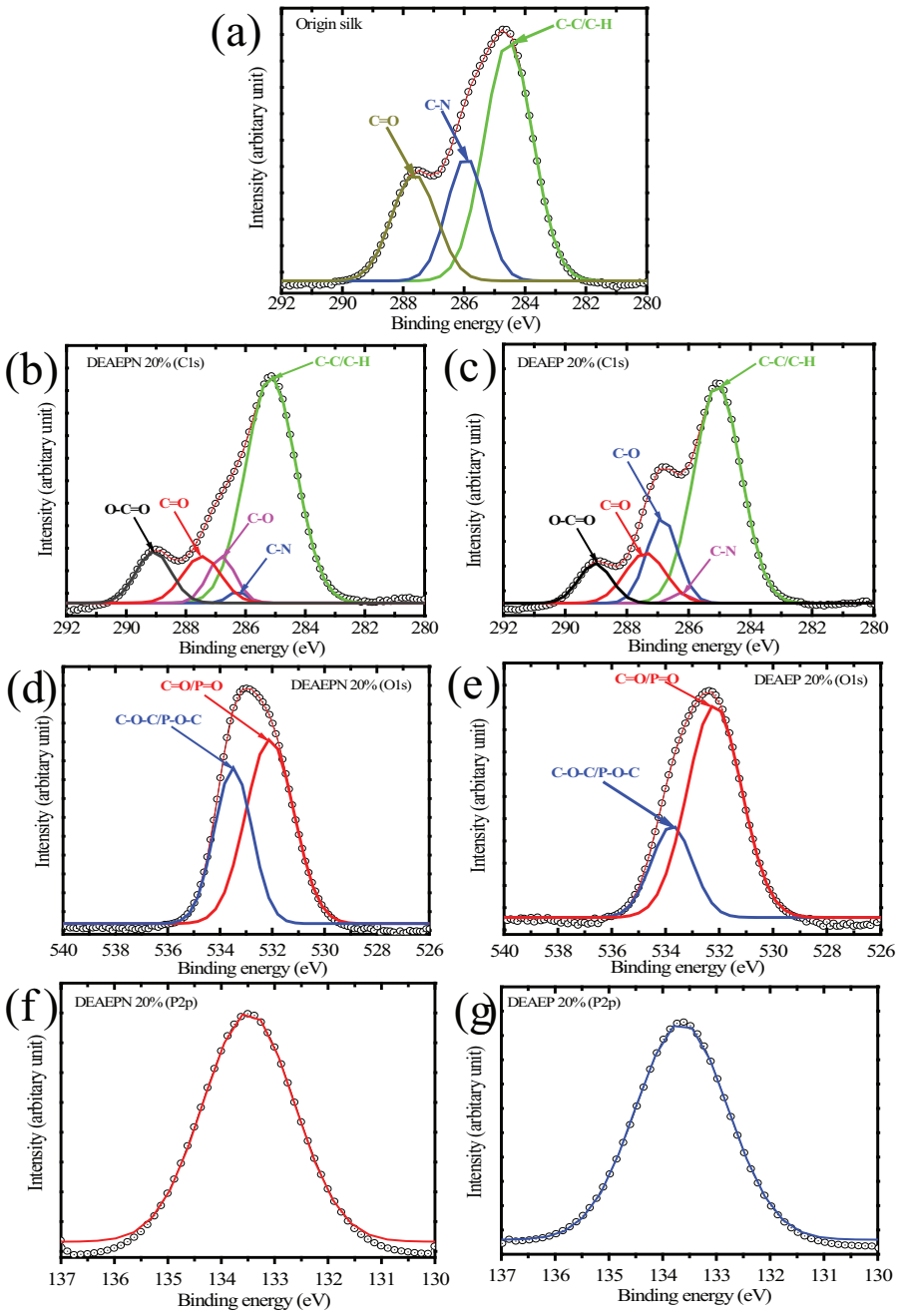

Figure 4.32: Line-shape analysis of the high-resolution C1s, O1s, and P2p of silk-grafted with concentration of monomers DEAEPN 20% (w.o.f.) treated silk and DEAEP 20% (w.o.f.) treated silk.

In order to determine whether the grafting of the polymer on the silk fabric occurred via reactions with some amino acid (AA), Amino Acid Analyses were performed on the treated silk fabrics (DEAEPN, 20% w.o.f) and compared to the untreated one. The results are shown in Table 4.12. As observed by other authors [106], the content of some amino acid decreases after the treatment which indicates their contribution in the grafting process. In our case, only the relative content of glycine which together with alanine constitutes more than 70% of the AA of this silk fabric decreases slightly (by about 2%). This observation indicates that a covalent grafting in the pIasma process may occur via a radical reaction involving the activated glycine CH_2-groups. On the contrary, Guan et al. [106] observed that DEMEP has been graft-polymerised using potassium persulfate as initiator in an acidic media,whereby mainly the AA containing polar side chains or CH_2S-SCH_2- bonds (cystine) were affected.

Table 4.12: The contents of amino acid of untreated silk and DEAEPN (20% w.o.f) treated silk fabric.

Amino acids	Untreated silk fabric [%]	DEAEPN treated silk fabric (20% w.o.f.)[%]
Histidine	0.29	0.31
Threonine	0.80	0.89
Serine	9.54	10.12
Glutamic acid	0.31	0.32
Glycine	53.35	51.68
Alanine	16.00	15.96
Valine	1.93	1.96
Methionnine	0.12	0.12
Isoleucine	0.65	0.66
Leucine	0.53	0.53
Tyrosine1	3.27	14.03
Phenylalanine	2.36	2.56
Lysine	0.02	0.03
Aspartic acid	0.37	0.38
Arginine	0.00	0.00
Proline	0.46	0.44

X-ray diffraction analysis of the control (a) and the DEAEPN (20% w.o.f.) treated silk fabric (b) have been performed in order to appreciate to which extent the grafting process affects the structure of the silk fibroin as shown in Fig. 4.33. On the diffractogram, one can see that the two curves are almost overlapping which indicates that the flame retardant finishing does not affect the crystallinity of the silk. Two hypotheses may arise from this observation, either the grafted polymer is only localized on the extreme surface of the silk fabric or it penetrates into the amorphous regions of the silk fiber. The slight content deviation observed as well with the AA analysis favors the first hypothesis.

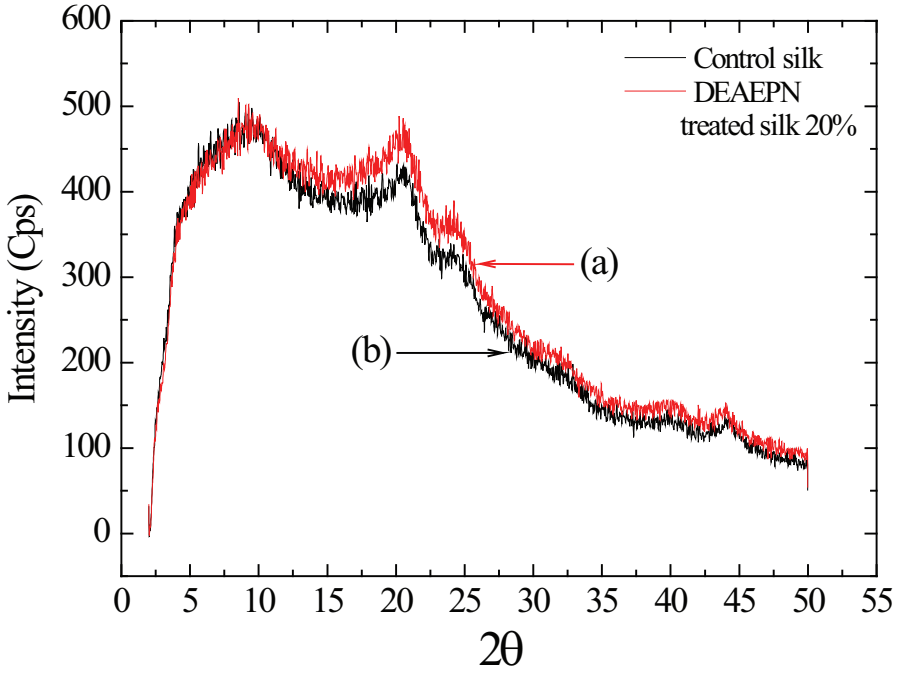

Figure 4.33: X-ray diffraction curves of (a) control and (b) DEAEPN (20% w.o.f.) treated silk.

4.3.2 Flammability of the silk fabric samples

4.3.3 LOI of silk finished fabrics at different concentrations of monomers

The flammability of the samples has been investigated by taking LOI measurements which is a straightforward and reliable analysis to compare the behaviour of different polymers. The LOI, the amount of residual char and the phosphorus content before and after burning of the DEAEPN and DEAEP treated silk fabrics at different concentrations of the monomers (w.o.f.) are listed in Table 4.11. As can be seen, the indices measured for the untreated silk fabric (25) increases up to 6 units in the fabrics which were treated either by the phosphate or the phosphoramidate monomers. The flame retardant finished silk fabrics became easily self-extinguished materials with only 5% of grafted polymer (LOI $>$ 28). Interestingly, for an equal content of grafted phosphorus atom on the fabric, the oxygen indices measured for polyDEAEPN finished fabrics are higher (1 unit) than the values obtained with polyDEAEP. We attribute this result to the presence of the nitrogen in the phosphoramidate which contributes to reduce the flammability of the fabric. Furthermore, the amount of the residual char, rich in phosphorus, increases quite rapidly with the amount of grafted polymers.

The remaining char presents interesting features that can be seen in the SEM pictures displayed in Fig. 4.34. In each case unburned and burned fabrics are presented. Figure 4.34 (b) shows that an untreated silk fabric melts while burning and the structure of filaments of the unburned fabric (2a) is completely lost. The SEM photographs of both treated silk fabrics either with 20% (w.o.f.) of DEAEPN (Fig. 4.34 (c)) or DEAEP (Fig. 4.34 (e)) exhibit no stacking of polymer between the fibres but a smooth entangling polymer film on the surfaces of the filaments. After burning, the structure of the treated fabrics can still be seen, but holes and channels are formed in place of fibroin filaments. Moreover, these pictures reveal two very different burning behaviours for the polymers. While the

first one (Fig. 4.34 (d)) coated with polyDEAEPN produces an intumescent-like layer above the molten silk, of which the thickness increases with the amount of grafted polymer (pictures not presented), the second one (Fig. 4.34 (f)) presents a thin brittle covering.

Another parameter which is indicative for the efficiency of a flame retardant finish is the burning rate. How is this rate influenced by an increase of the oxygen content? Burning rates of the control silk fabric (curve a), and silk fabrics treated with DEAEPN (curve b) and DEAEP (curve c) are given in Fig. 4.35. The burning rate of the control fabric increases slowly from 25 to 28% of oxygen and then very quickly above this concentration while remarkably the burning rate profiles of the treated fabrics remain almost flat. Clearly, the flame retardant polymer does not only retard the ignition of the fabric but also slow down the rate of burning.

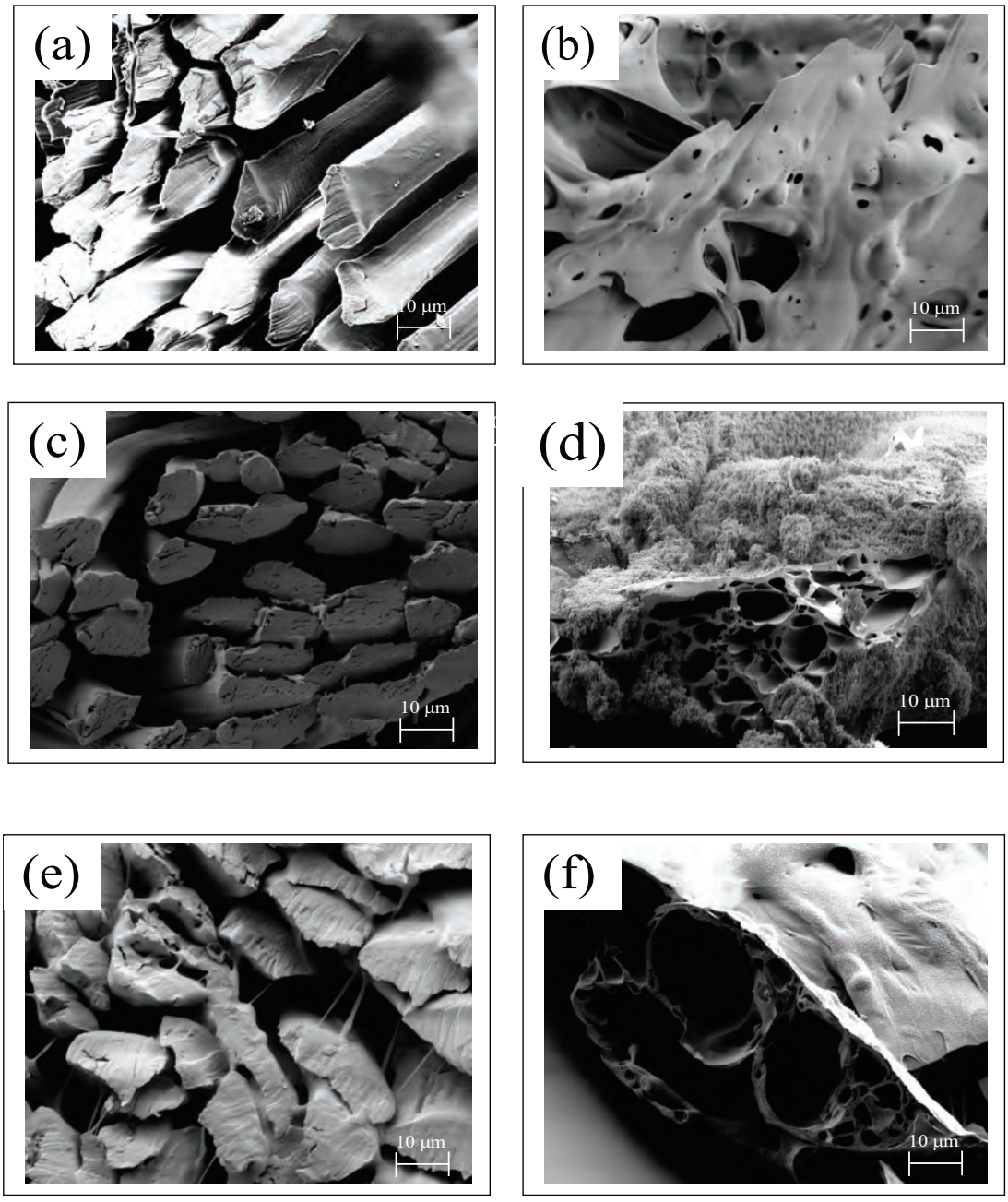

Figure 4.34: SEM micrograph of control silk unburned (a)and burned (b) DEAEPN (20%w.o.f.) treated silk (c) unburned and (d) burned, DEAEP(20% w.o.f.) treated silk (e)unburned and (f) burned.

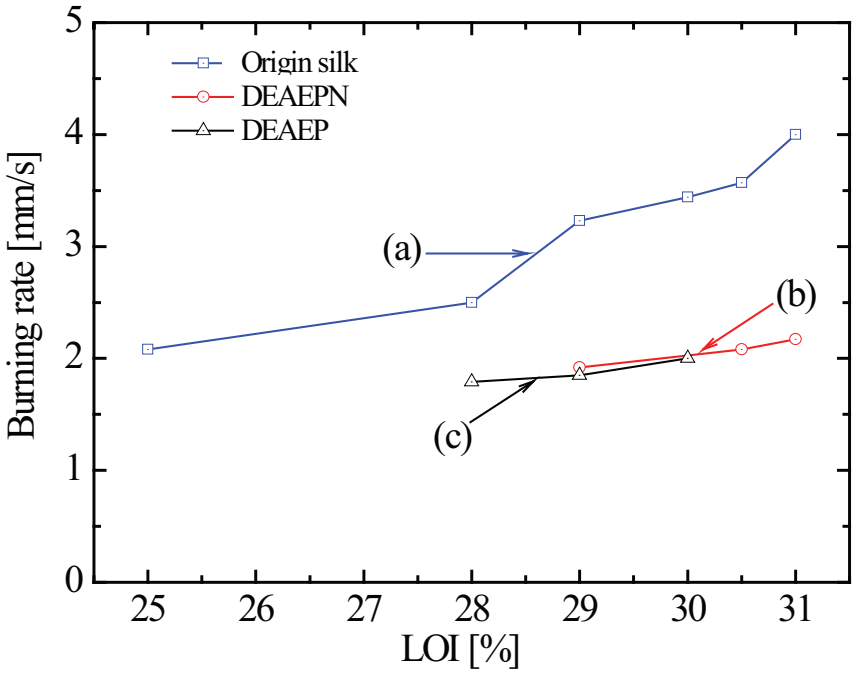

Figure 4.35: Burning rates vs LOI of (a) control silk (b) DEAEPN (20%w.o.f.) treated silk and (c) DEAEP (20%w.o.f.) treated silk

All these results suggest the formation of a protective layer which insulates the fabric from the effect of the heat as major reason for decreasing the flammability of the fabric. From the characteristics of the remaining chars, DEAEPN seems to provide a more efficient insulating coating than DEAEP. The remaining char is composed by degraded silk and flame retardant polymer, as confirmed by its high content of phosphorus (% P/g fabric) which was determined by elemental analyses (Table 4.11).

4.3.4 Pyrolysis combustion flow calorimetry(PCFC) analysis

Pyrolysis combustion flow calorimetry (PCFC) analysis is frequently applied nowadays in order to assess the flammability of polymeric materials and it is now recognized to be an effective bench scale method [109]. The heat release rate has been found very effective to evaluate fire hazards. The heat release rate versus temperature for untreated (curve a) and DEAEPN (20% w.o.f.) and DEAEP (20% w.o.f.) treated silk fabrics, respectively (curve b) and (curve c) is presented in Fig. 4.36. The total heat release (THR) and the peak heat release rate (PHRR) obtained from Fig. 4.36 are listed in Table 4.13.

Table 4.13: Thermal data calculated from Fig.4.35.

Sample	PHRR(W/g)	THR(kJ/g)	HRC (J/g.K)
Untreated silk	32 147	7.7	149
DEAEPN (20% w.o.f)	32 90	6.2	91
DEAEP(20% w.o.f)	95	6.5	97

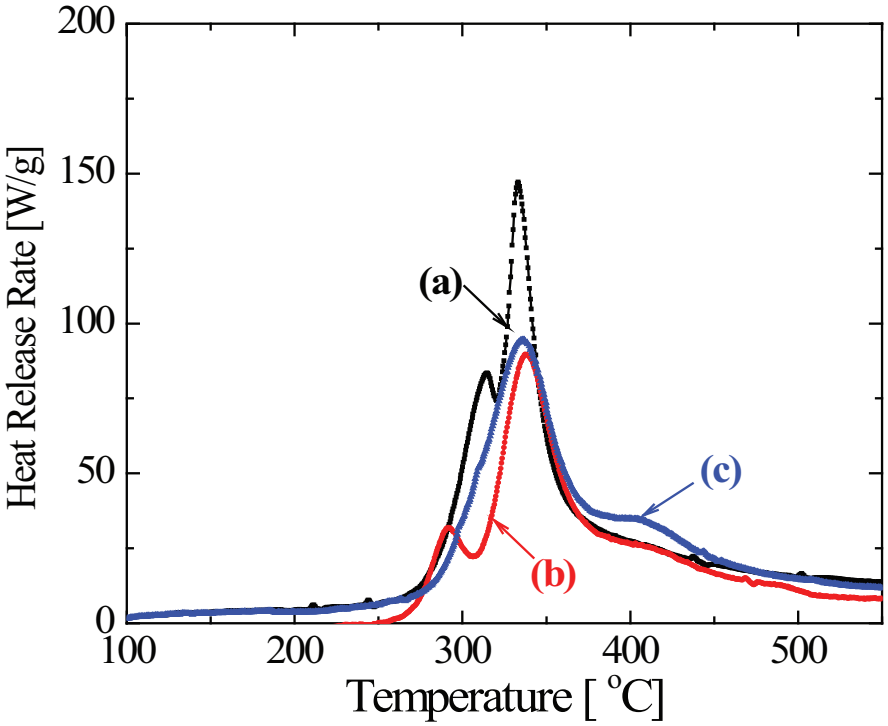

Figure 4.36: Heat release rate of (a) untreated (b) DEAEPN (20%w.o.f.) treated silk (c) DEAEP (20% w.o.f.) treated silk

Immediately, it can be seen from Fig. 4.36 and Table 4.13 that PHRRs, which are the maximum speed at which the fire of the fabric, can generate heat of the treated silk fabrics are considerably lower than for the control fabric. Indeed, they reached 90 and 95 W/g for the DEAEPN and DEAEP treated fabrics respectively compared to 147 W/g for the untreated one. The same trend is reflected in the total heat release (THR) where a decrease of about 1.2 to 1.5 kJ/g is observed. The heat release capacity follows the same pattern. The char yield increases significantly for the treated samples with a neat advantage for polyDEAPN. All these data correlate with the LOI measurements and suggest as well a condensed-phase mechanism leading to the production of char rather than flammable products.

4.3.5 Thermal analysis

In order to have more insights into the flame resistance mechanism, thermogravimetric (TG) and derivative thermal gravimetry (DTG) analysis have been performed on the untreated and the treated silk fabrics with various concentrations (w.o.f.) of DEAEPN or DEAEP. The TG and DTG curves for treated fabrics with 20% (w.o.f.) of the monomers are presented in Fig. 4.37 and Fig. 4.38.

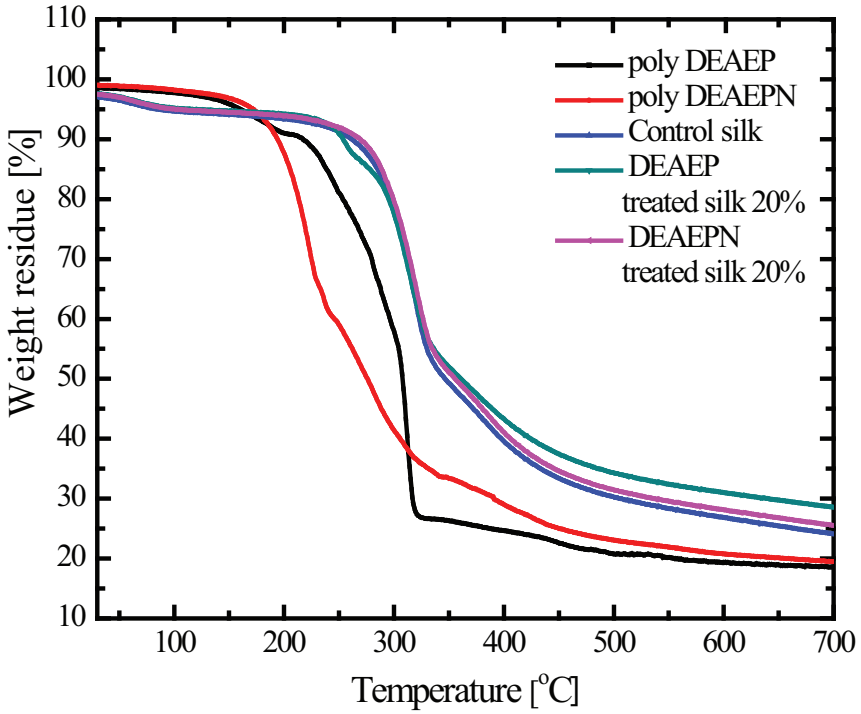

Figure 4.37: The TGA curves in nitrogen of the polyDEAEPN, polyDEAEP, untreated silk, DEAEPN (20%w.o.f.) treated silk and DEAEP (20% w.o.f.) treated silk

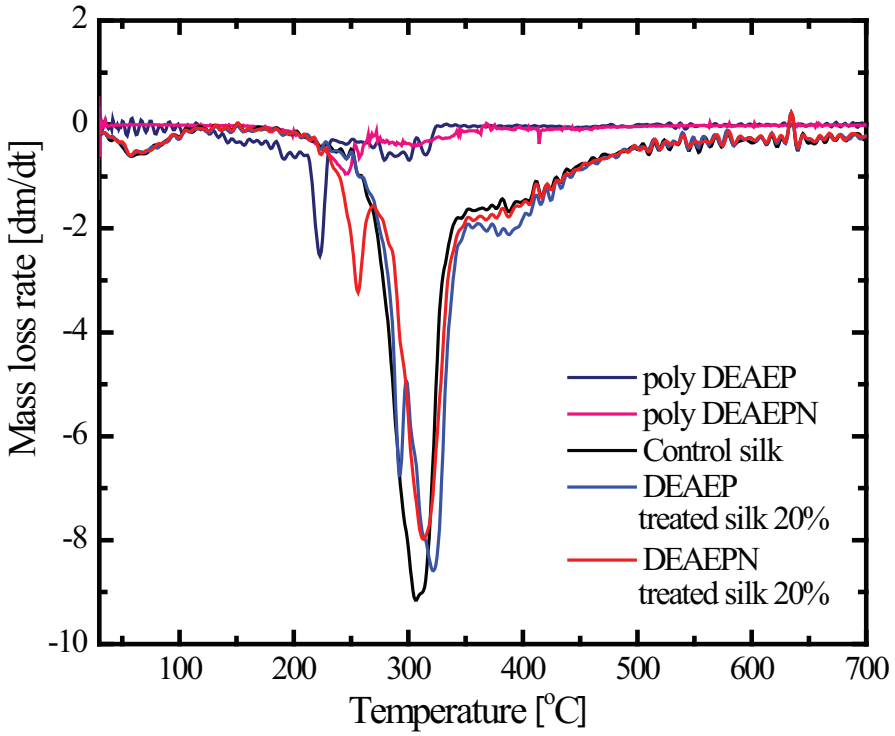

Figure 4.38: The DTG curves in nitrogen of the polyDEAEPN, polyDEAEP, control silk, DEAEPN (20%w.o.f.) treated silk and DEAEP (20% w.o.f.) treated silk;

Table 4.14: Thermal data from DTG curves in Fig.4.36.

Sample	T_i [^{o}C]	T_{max} [^{o}C]	Char at 700 [^{o}C] [%]	Temperature range of different mass loss stage [^{o}C]	Massloss [%]
Untreated silk	273	306	24.0	30-214 214-372 372-700	4.12 48.25 20.13
DEAEPN (20% w.o.f) 11.22% of grafting	238	312	29.0	30-212 212-290 290-304 340-700	4.15 10.16 28.40 27.27
DEAEP(20% w.o.f) 11.22% of grafting	264	322	25.0	30-212 212-289 289-337 337-700	4.47 11.44 27.76 25.50
Polymer DEAEPN	177	241	20.0	30-149 149-344 344-700	2.23 63.48 13.61
Polymer DEAEP	152	222	19.0	30-132 132-322 322-700	2.00 71.18 7.67

Although the pyrolysis mechanism of the silk fibre is still unknown, several authors have reported the decomposition behaviour of degummed silk fabrics of different origin. Our results are similar to those described in the literature [105].

Three main mass loss stages can be identified. The first one (4.1%, 30 - 214 ^{o}C), is attributed to desorption of the adsorbed moisture of the silk fabric. In the second stage (48.2%, 214 - 372 ^{o}C) the silk fabric decomposes into CO_2, H_2O and flammable substances. The last stage (20.1%, 372 - 700 ^{o}C) is assigned to the decomposition of the char of the silk fabric.

The decomposition of the finished silk fabrics with the flame retardant polymers follows the same pattern with almost the same onset of decomposition temperatures, with an additional mass loss stage (10.1%, 212 - 290 ^{o}C) for finished silk fabrics with DEAEPN 20% w.o.f., 11.4%, 212 - 289 ^{o}C) for finished silk fabrics with DEAEP, 20% w.o.f.), which corresponds to the degradation of the polymer. This is best visible in Fig. 4.36 (b) which exhibits for the treated fabrics two peaks in the DTG curve while only one is seen for the untreated fabric. These observations can be explained by the fact that the grafted polymer as the pure polymers decompose at lower temperatures than the silk fabric. Their decomposition into a stable phosphorus containing residue is almost complete before the silk starts to decompose. This will provide an insulating layer which will delay the decomposition of the silk, as indicated by the slightly higher decomposition temperature found in the treated samples.

4.3.6 Multifunctional properties

Fire retarded silk fabrics could be used for various purposes which require different surface energies. Finished with polyDEAEPN or polyDEAEP, the fabrics obtained in step 1 (PIGP process) are hydrophilic. In order to obtain hydrophobic ones, the flame retardant (FR) silk fabrics were submitted in step 2 (SF_6 plasma treatment) to a post-SF_6 plasma treatment (F_{SF6} = 25 sccm. P = 100 W, p = 500 mTorr, t = 5 min). The protocol is given in Fig. 4.39 and the results are

displayed in Fig 4.40.

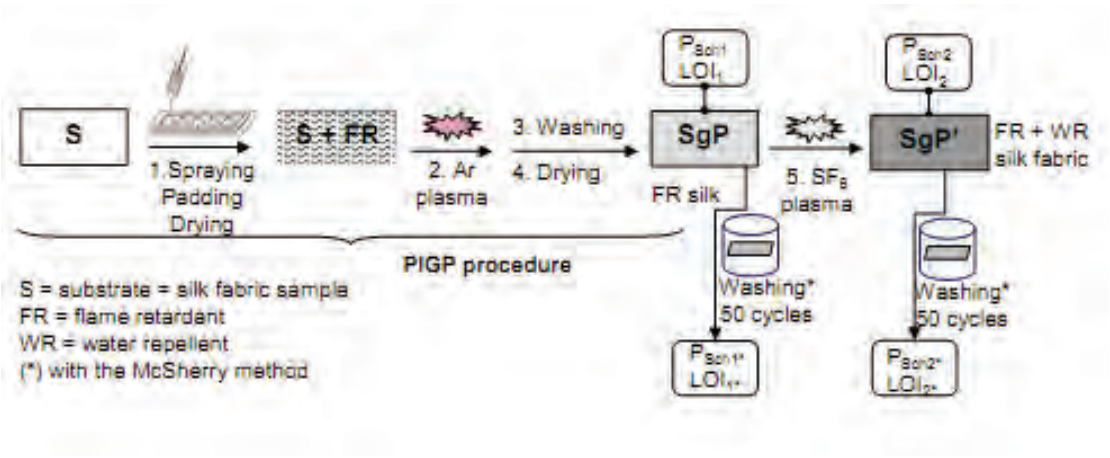

Figure 4.39: Procedure of the two-step treatment. Step 1: PIGP process of flame retardant monomers onto silk fabrics. Step 2: SF_6 plasma on the flame retardant fabrics.

Figure 4.40 shows the XPS survey spectrum of the untreated silk and the FR silk fabrics - with 20% (w.o.f.) of DEAEPN or DEAEP - exposed to a SF_6 plasma. Apart from the P2s and P2p components due to the FR finishing, one can clearly detect the F1s peak indicating a significant fluorination of the surface. Consequently, the wettability of the fabric will be affected and to evaluate the extent of this modification, the Schmerber pressures were measured according to Norm DIN 53886. Before and after the plasma treatment, the Schmerber pressures P_{sch1} and P_{sch2} were measured respectively. The results obtained are given in Table 4.15. Before the SF_6 plasma treatment, the FR silk fabrics are completely absorbent ($P_{sch1} = 0$ mbar). After the SF_6 plasma treatment, the Schmerber values, PSch2 increase significantly from 0 up to 23.5 mbar.

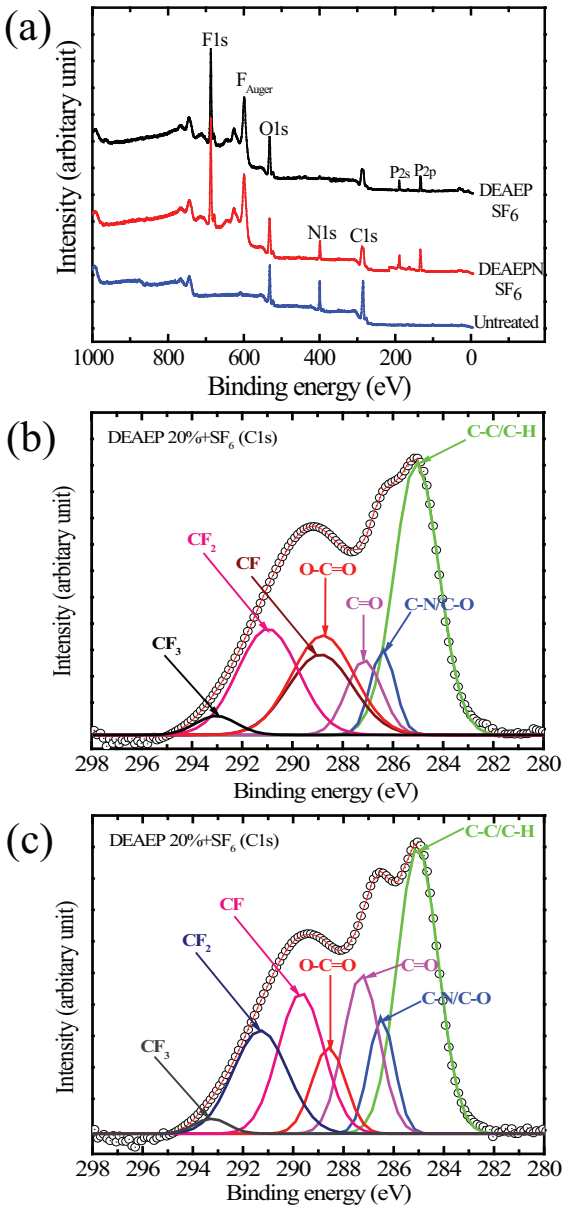

Figure 4.40: XPS survey spectra for untreated silk and SF_6 plasma treated flame retardant silk fabrics with DEAEPN and DEAEP.

Table 4.15: LOI and Schmerber pressures measured for the FR silk fabrics with DEAEPN and DEAEP before (STEP 1) and after (STEP 2)SF_6 plasma treatment.

Sample	After step 1		After step 2	
	LOI_1 [%±0.1]	P_{sch1} [mbar]	LOI_2 [%±0.1]	P_{sch2} [mbar]
Origin silk	25.0	0	25.0	23.5
DEAEPN (20% w.o.f)	30.5	0	31	23.5
DEAEP(20% w.o.f)	29	0	30.0	23.0

This high value corresponds to an apparent contact angle with water of 134 degree. The droplets of water roll on the surface which emphasizes the low surface energy achieved by this treatment. The presence of fluorine-containing groups in silk fabric structure after treatment can be obtained by fluorine ion created C-F bonding. Also, halogens are in general strongly electronegative and have large bond energies between carbons and, in particular, fluorine has the strongest bond energy of 484 kJ/mol [110]. Therefore, it can show the strong resist the polar molecule like water causing the difficult to wet and showing a high contact angle. This reason can confirm for improvement hydrophobic properties of silk fabrics. The measured contact angle of SF_6 plasma treated on flame retardant silk fabrics was about 134 degrees, while the origin silk absorb water immediately leading to the zero of contact angle as shown in Fig. 4.41.

Interestingly, the LOI is not affected by this treatment; it even slightly increases for the FR samples. Moreover, after several weeks of outdoor exposure, only a slight drop of the Schmerber pressure was noticed (by about 1 unit). The initial pressure P_{sch2} could be recovered after one hour of heating at 100 ^{o}C.

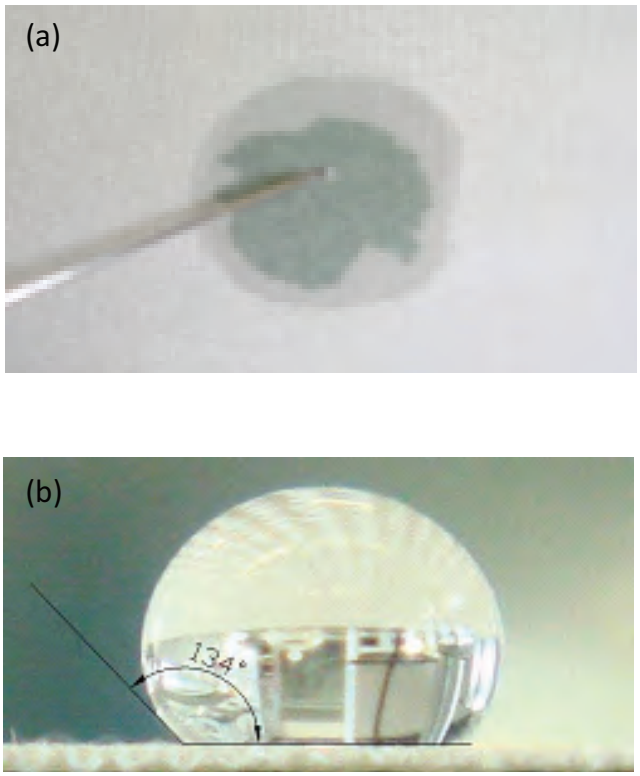

Figure 4.41: Water repellent properties of flame retardant silk fabrics with DEAEPN (a) before and (b) after SF_6 plasma treatment.

4.3.7 Fastness properties

To investigate the effect of the argon plasma induced graft polymerization of DEAEPN and DEAEP before (step 1) and after (step 2) (see Fig. 4.37) a SF_6 plasma treatment on the mechanical properties of silk fabrics, the tensile strength and the elongation at break were measured and the results are presented in Tables 4.16 and Table 4.17. The mechanical analyses revealed that an Ar plasma treatment during 20 minutes on the control fabric does not alter the tensile strength of the fabric (<1%). The value decreased slightly (<2.5%) after the application of the PIGP process with 20% (w.o.f.) of the two monomers. Note that the fabric is more affected while using the phosphate analog. On the other hand, the same textiles treated with a SF_6 plasma are subjected to almost similar

alteration of the mechanical properties after 5 minutes of treatment. However a SF_6 plasma treatment on the fabrics for more than 5 minutes has a detrimental effect and more than 20% of the tensile strength is lost after the treatment.

This behavior is reflected as well in the elongation at break measurements. The flame retardant finishing by embedding the fibers provides some elasticity to the fabric (the values increases from 19.2 to 21.2 and 20.6 for silk treated DEAEPN and DEAEP respectively) whereas a post SF_6 plasma treatment led to the opposite effect. After 5 minutes of treatment a decrease of the elongation at break value is observed for all samples, finished or not. Interestingly though this decrease of the textile strength is more remarkable for the control silk fabrics than for the flame retardant finished ones. The flame retardant coating provides a protective layer towards the abrasive action of the SF_6 plasma treatment [111]. Evidently, this effect is more intense for longer exposure time where cross-linking occur as well.

Table 4.16: Tensile strengths measured for control and for the FR silk fabrics with DEAEPN and DEAEP before (STEP 1) and after (STEP 2) SF_6 plasma treatment.

	Tensile strength (N)		
Sample	Step 1	Step 2	
		Plasma SF_6 5 min	Plasma SF_6 10 min
Origin silk: 551(±10)N	546(±9)	535(±8)	432(±8
DEAEPN (20% w.o.f)	542(±6)	533(±7)	429(±8
DEAEP(20% w.o.f)	538(±7)	531(±8)	427(±8)

With the aim to examine the effect of the PIGP process using phosphorus containing monomers followed up by a SF_6 plasma treatment on the color change of the fabrics, the degree of whiteness has been evaluated according to the gray scale color testing. The results obtained by comparing our silk fabrics samples treated with increasing amounts of FR monomers to a set of five pairs of gray/white

Table 4.17: Elongation at break measured for control and for the FR silk fabrics with DEAEPN and DEAEP before (STEP 1) and after (STEP 2) SF_6 plasma treatment.

Sample	Elongation at break (mm) and (% elongation)		
	Ar plasma	Ar and SF_6 plasma	
	20 min	5 min	10 min
Origin silk: 19.2(±11);100%	19.0±9.7;(98.9)	18.1±8.2;(94.3)	17.7±8.6;(92.2)
DEAEPN (20% w.o.f)	21.2±7.6;(110.4)	19.4±6.7;(101.0)	18.3±7.3;(95.3)
DEAEP(20% w.o.f)	20.6±7.7;(107.3)	19.2±7.9;(100.0)	18.0±7.5;(93.7)

colored plates with different degree of contrast are given in Table 4.18. A value of 4.5 on the scale ranging from 1 to 5 has been estimated for almost all silk fabrics finished with various amounts of DEAEP and DEAEPN monomers. In the case of DEAEPN, the fabric treated with an initial solution concentration of 30% (w.o.f.) corresponding to 16% of grafted polymer exhibits a lower value of 4 which indicates a slight change in colour. By comparing these results with the origin silk fabric which is at 5, one can say that the PIGP process with our monomers impacts only slightly the color properties of the fabric. It is interesting to notice that a post SF_6 plasma treatment of the flame retardant silk fabrics does not affect at all their color. Absolutely the same degrees of whiteness as before the SF_6 treatment were obtained.

The wash-fastness property of the coating has been evaluated by using the accelerated laundering protocol proposed by McSherry. In this procedure the samples are boiled for over 4 hours in a basic medium. This method is set up to mimic 50 cycles of laundering and has been applied on the treated samples with 20% (o.w.f.) of the two monomers after the first step (PIGP process) and after the second step (SF_6 plasma treatment)(see Fig. 4.37). LOI and Schmerber pressures have been taken after each step and the results obtained are listed in Table 4.19.

Table 4.18: Color-fastness properties of the treated silk fabrics by the PIGP process with various amount of DEAEPN monomer.

Sample		Grey scale	
		Step 1	Step 2
Origin	Weight gain [%]	5	5
DEAEPN	6.62	4/5	4/5
	11.22	4/5	4/5
	16.68	4	4

For each flame retardant and water repellent finished fabric the LOI is only slightly altered by the washing process. The decrease of the oxygen index is less than 1.5% even after the fabrics have been subjected twice to the washing process. In contrast the water repellent character is not resistant towards this washing. The fabrics became again absorbent. In order to understand this phenomenon which we did not observe previously when we applied a similar CF_4 plasma treatment on cotton fabrics [85], the weight of the fabrics at each step has been taken and the weight loss calculated. It appears clearly that after step 1 more than 10% of the grafted polymer is removed. This effect is repeated after step 2 where an additional 5 to 15% weight loss of matter occurs. While this affects poorly the LOI, it has dramatic consequences on the water repellent properties. Likely, while fluorination of the surface occurs during the SF_6 plasma treatment, a concomitant surface degradation (etching) takes place leading to a weakening of the polymer which loses readily its thin external fluorinated layer.

Table 4.19: Wash-fastness properties of the flame retardant silk fabrics with DEAEPN and DEAEP before (Step 1) and after (Step 2) (SF_6 plasma treatment).

Monomer(w.o.f)	Before washing		After washing-Step 1			After washing-Step 2		
	%G1	LOI1	%G1	LOI1	P_{Sch1}	%G2	LOI2	P_{Sch2}
Untreated silk	0	25	0	25.0	0	0	25.0	0
DEAEPN (20%)	22	30.5	9.45	29.2	0	0	29.0	0
DEAEP (20%)	16	29	8.99	28.0	0	0	27.5	0

CHAPTER V

CONCLUSIONS

Modification of surface characteristics of hydrophobicity, hydrophilicity and flame retardancy on cotton, PET and silk fabrics, respectively by plasma process was studied. We investigated and characterized the influence of plasma treatment with different types of gases and plasma-induced graft polymerization (PIGP) procedure by mean of changes in physical, chemical and thermal properties. In addition, our goal was to find the optimum operating conditions for improvement hydrophobicity, hydrophilicity and flame retardancy without altering the surface physical of treated fabrics.

In the first study, we have chosen cotton fabric to study the effect of SF_6 plasma on hydrophobic properties. Clearly, the plasma treatment greatly enhanced hydrophobicity on the cotton fabric. We found that the contact angle of the treated fabric is in the range of 145-149 degree and the absorption time increased from 0 to beyond our limiting (200 min) with optimal plasma treatment conditions. Moreover, the SF_6 plasma fired at higher exposure time and pressure were more effective in increasing contact angle and absorption time on cotton fabric. Although the surface roughness can increase the hydrophobicity of certain surfaces by the so called Lotus effect. Our samples became hydrophobic mainly due to the replacement of hydrophilic species by fluorine containing moieties. After fluorination of the fibres, a smaller number of hydrogen bonds between water molecules and surface groups can be formed, thus reducing the hydrophilicity. Therefore, the main reaction for the enhancement of hydrophobicity is surface fluorination on the fabric which is confirmed by X-ray photoelectron

analysis. The water absorption time and contact angle of cotton fabric is the highest when the fluorine/carbon ratio at the surface increases. A small decrease of the oxygen/carbon ratio was also observed on the fabrics that showed the longest absorption times. We expected that the change of hydrophobicity of cotton fabric is resulted from surface deposition of C-F residue on cotton fabric. In addition, we confirmed the etching effect, which is strongly related to changes in physical property change, by the weight loss and tensile strength. The tensile strength of fabrics decreases as the treatment time and SF_6 pressure increases resulting from etching process. The exposure time plays an important role in the change of mechanical properties of fabric with the SF_6 pressure having secondary effects. In conclusions, we did not observe dramatically surface morphology changes from SEM images for the cotton owning the weight loss less than 1%. A two-stage weight loss was observed which was attributed to desorption and fragmentation of surface molecule respectively. Overall good and durable hydrophobic properties on cotton can be achieved only for the longer treatments used but the mechanical strength of the fabrics are compromised to a significant extent. We found that the optimal plasma conditions to enhance hydrophobicity without losing tensile strength and weight of fabric is in the pressure range of 0.005-0.3 Torr or the treatment time less than 1 min, but with less hydrophobic durability in terms of aging and washing cycles.

The second finishing application studied in this thesis is the improvement hydrophilicity and dyeability of polyethylene terephthalate (PET) fabric by radio frequency O_2, N_2 and Ar plasmas. Using modified Lucas-Washburn's equation through the capillary rise method, effective mean pore radius (R) and diffusion coefficient (D_C) of the fabric were determined and the hydrophilicity of PET could be characterized. The etching process from O_2, N_2 and Ar plasmas led to the changes in surface morphology of PET surface. The mean pore radius of the fabrics was proportional to the D_C values increased with increasing exposure time, pressure and RF power O_2, N_2 and Ar plasmas. Comparison with the same plasma conditions, O_2 plasma results in the largest R values (0.7-1.1 μm) which is two

times higher than that of N_2 and Ar plasmas. Therefore, the hydrophilicity was achieved not only the results of polar groups but also the results of increase in calculated R and D_C values. The increase in R and D_C values could be related to the higher etching effect in which we confirm by the decreasing of weight. In this study, the etching process on PET surface can be observed by weight loss, SEM and AFM. The surface hydrophilicity was found to be increased due to the created functional polar groups during the plasma treatment. Polar groups were generated more for O_2 plasma on the fabric surface which was confirmed from XPS analysis. The SEM image showed the formation of grooves, pikes and granular which increase the roughness of the fabric surface. O_2 plasma can produce deeper and wider grooves than that of N_2 and Ar plasmas due to more etching effect causing more roughness along with the increase in polar groups on PET surface. In addition, the result in generated holes or pores on PET surface can increase in color depth of dye because the dyes can be ingrained into holes or pores and also exhibited the washing durability compared with the untreated PET.

In last study, the flame retardation and multifunctional of hydrophobicity on flame retardant on silk fabrics by grafting and polymerization of monomers containing phosphorus and SF_6 plasma using the novel PIGP procedure has been investigated. By the mean of a two steps process, i. e. argon induced graft polymerization of phosphorus containing monomers followed by a SF_6 plasma treatment, a thin colorless flame retardant and water repellent polymer has been grafted on the surface of silk fabrics. Diethyl 2-(acryloyloxyethyl)phosphate (DEAEP) and diethyl 2-(acryloyloxyethyl)phosphoramidate (DEAEPN) have been used for this purpose. The LOI of the treated fabrics reaches 29 and 30.5 for DEAEP and DEAEPN, respectively. It can be noted that the first step occurred with a grafting yield above 50%. It is clearly shown that the phosphoramidate monomer decreases more the flammability of the silk fabrics than the phosphate analog, which is consistent with a P-N synergistic effect. Furthermore, SEM analyses of the residual char reveal two different morphologies. While textiles finished with polyDEAEPN exhibit an intumescent like protective layer, those with DEAEP

present a thin one. This suggests two different behaviors during the burning process although they both operate in the solid phase as confirmed by the decrease of the heat of combustion and the increase of the residual char of the treated fabrics compared to the non-treated one. In the second step, the flame retarded fabrics have been exposed to SF_6 plasma. After 5 minutes of treatment, the fabrics which were originally absorbent became water repellent and exhibited an apparent contact angle of 134^o. This property remains even after several weeks of air exposure. This multifunctional silk fabric retains the original characteristics of the untreated fabric. Indeed, only a slight variation of the tensile strength and the color fastness has been noticed. However, although a good flame retardant behavior remains after 50 cycles of laundering (McSherry method), the water repellent properties disappeared under these conditions. Our future research efforts will concentrate on the improvement of this second step in order to provide wash-resistant multifunctional silk fabrics.

References

[1] Sharnina, L. Low-temperature plasma as the basis for creation of modern textile chemical technologies. *Fibre Chem.* 36 (2004): 431–436.

[2] Yu, M., Gu, G., Meng, W. D., and Qing, F. L. Superhydrophobic cotton fabric coating based on a complex layer of silica nanoparticles and perfluorooctylated quaternary ammonium silane coupling agent. *Appl. Surf. Sci.* 253 (2007): 3669–3673.

[3] Yang, H. Y., Zhu, S., and Pan, N. Studying the mechanisms of titanium dioxide as ultraviolet-blocking additive for film and fabrics by an improved scheme (Journal of Applied Polymer Science. *J. Appl. Polm. Sci.* 92 (2003): 3201–3210.

[4] Saito, M. Antibacterial, Deodorizing and UV Absorbing Materials Obtained with Zinc Oxide (ZnO) Coated Fabrics. *J. Ind. Text.* 23 (1993): 150–164.

[5] Song, X., Liu, A., Ji, C., and Li, H. The effect of nano-particle concentration and heating time in the anti-wrinkle treatment of silk.. *Journal of Jilin Institute of Technology* 22 (2001): 24–27.

[6] Hwang, Y.. Characterization of Atmospheric pressure plasma interactions with textile/polymer substrates. Master's thesis North Carolina State University 2003.

[7] Rosace, G. and Canton, R. Influence of low-temperature plasma conditions on wicking properties of PA/PU knitted fabric. *J. Appl. Polym. Sci.* 107 (2008): 3702–3706.

[8] Hodak, S., Supasai, T., Paosawatyanyong, B., Kamlangkla, K., and Pavarajarn, V. Enhancement of the hydrophobicity of silk fabrics by SF6 plasma. Applied Surface Science. *Appl. Surf. Sci.* 254 (2008): 4744–4749.

[9] Chen, J. R. Study on free radicals of cotton and wool fibers treated with low-temperature plasma. *J. Appl. Polym. Sci.* 62 (1996): 1325–1329.

[10] McCord, M. G., Hwang, Y. J., Qiu, Y., Hughes, L. K., and Bourham, M. A. Surface analysis of cotton fabrics fluorinated in radio-frequency plasma. *J. Appl. Polm. Sci.* 88 (2003): 18892137.

[11] Li, S. and Jinjin, D. Improvement of hydrophobic properties of silk and cotton by hexafluoropropene plasma treatment. *Appl. Surf. Sci.* 253 (2007): 5051–5055.

[12] Iriyama, Y., Yasuda, T., Cho, D. L., and Yasuda, H. Plasma surface treatment on nylon fabrics by fluorocarbon compounds. *J. Appl. Polym. Sci.* 39 (1990): 249–264.

[13] Laia, J. et al. Study on hydrophilicity of polymer surfaces improved by plasma treatment. *Appl. Surf. Sci.* 252 (2006): 3375–3379.

[14] Wong, K., Tao, X., Yuen, C., and Yeung, K. Low Temperature Plasma Treatment of Linen. *Text. Res. J.* 69 (1999): 846–855.

[15] Pandiyaraj, K. N. and Selvarajan, V. Non-thermal plasma treatment for hydrophilicity improvement of grey cotton fabrics. *J. Mater. Process. Tech.* 199 (2008): 130–139.

[16] Akovali, G. and Gundogan, G. Studies on flame retardancy of polyacrylonitrile fiber treated by flame-retardant monomers in cold plasma. *J. Appl. Polym. Sci.* 41 (1990): 2011–2019.

[17] Jinping, G. and Guoqiang, C. Graft copolymerization modification of silk fabric with an organophosphorus flame retardant. *Fire Mater.* 34 (2010): 261–270.

[18] Tsafacka, M. and Levalois-Grtzmacher, J. Towards multifunctional surfaces using the plasma-induced graft-polymerization (PIGP) process: Flame and waterproof cotton textiles. *Surf. Coat. Tech.* 201 (2007): 5789–5795.

[19] Molina, R., Jovani, P., Comelles, F., Bertran, E., and Erra, P. Shrink-resistance and wetting properties of keratin fibres treated by glow discharge. *Journal of Adhesion Science and Technology* 16 (2002): 1469–1485.

[20] Raffaele-Addamo, A. et al. Cold plasma-induced modi?cation of the dyeing properties of poly(ethylene terephthalate) ?bers. *Appl. Surf. Sci.* 252 (2006): 2265–2275.

[21] Mokbul, M. and Herrmann, A. Plasma Hydrophilization Effect on Different Textile Structures. *Plasma Process. Polym.* 3 (2006): 299–307.

[22] Morgan, A. B. and Charles, A.. *Flame retardant polymer nanocomposite.* John wiley & Sons 2007.

[23] Reddy, P. R. S., Agathian, G., and Kumar, A. Ionizing radiation graft polymerized and modified flame retardant cotton fabric. *Radiat. Phys. Chem.* 72 (2005): 511–516.

[24] Shishoo, R.. *Plasma technologies for textiles.* Woodhead 2007.

[25] Bittencourt, J.. *Fundamentals of Plasma Physics.* Pergamon Press 1986.

[26] Boulos, M., Fauchais, P., and Pfender, E. P. E.. *Thermal Plasmas: Fundamental and Applications.* Springer 1994.

[27] Schutze, A. et al. The Atmospheric-Pressure Plasma Jet: A Review and Comparison to Other Plasma Sources. *IEEE T. Plasma Sci.* 26 (1998): 1685–1694.

[28] Chapman, B.. *Glow Discharge Processes: Sputtering and Plasma Etching.* Wiley-Blackwell 1980.

[29] Bell, A., Raymond, F., and Robert, S.. *The application of plasma to chemical processing eds..* MIT Press. 1967.

[30] Wai, K. C. and Wah, M. C. Plasma technology in wool. *Textile Progress* 39 (2007): 121–187.

[31] Fridman, A.. *Plasma Chemistry*. Cambridge university press 2008.

[32] Francis, G.. *The glow discharge at low pressure*. Springer 1956.

[33] Roth., J.. *Industrial Plasma Engineering, Volume II, Applications to Non-thermal Plasma Processing*. Bristol: Institute of Physics Publishing 2001.

[34] Loffhagen, D. and Sigeneger, F. Advances in Boltzmann equation based modelling of discharge plasmas. *Plasma Sources Sci.* 32 (2008): 323–331.

[35] Conrads, H. and Schmidt, M. Plasma generation and plasma sources. *Plasma Sources Sci. T.* 9 (2000): 441–454.

[36] Laroussi, M., Hippler, R., Kersten, H., Schmidt, M., and Schoenbach, K.. *Low Temperature Plasmas. Fundamentals, Technologies and Techniques vol. 2*. Wiley-VCH 2008.

[37] Rossnagel, S. and andW.D. Westwood, J. C.. *Handbook of plasma processing technology: fundamentals, etching, deposition and surface interactions*. Noyes 1990.

[38] Salem, M., Loiseau, J., and Held., B. Impedance matching for optimization of power transfer in a capacitively excited rf plasma reactor. *Eur. Phys. J. Appl. Phys* 3 (1998): 91–95.

[39] Kherman, V.. *Plasma Science and Technology*. Cornell University Press 1982.

[40] Raizer, Y., Shneider, M., and Yatsenko, N.. *Radio-frequency capacitive discharges*. CRC Press 1995.

[41] Lay, B., Moss, R. S., Rauf, S., and Kushner, M. J. Breakdown processes in metal halide lamps. *Plasma Sources Sci. Tech.* 12 (2003): 8–21.

[42] Kushner, M. J. Modelling of microdischarge devices: plasma and gas dynamics. *J. Phys. D: Appl. Phys.* 38 (2005): 1633–1643.

[43] Raizer, Y.. *Gas Discharge Physics.* Springer 1991.

[44] Hopwood, J. Review of inductively coupled plasmas for plasma processing. *Plasma Sources Sci. T.* 1 (1992): 109–116.

[45] Shul, R. and Stephen, J.. *Handbook of advanced plasma processing technology: High Density plasma Sources.* Springer 2000.

[46] Franck, C. et al. Measurements of spatial structures of different discharge modes in a helicon source. *Plasma Sources Sci. Tech.* 14 (2005): 226–235.

[47] Bosisio, R., Wertheimer, M., and Weissfoch, C. Generation of large volume microwave plasmas. *J. Phys. ESci.Instrum.* 6 (1973): 628–630.

[48] Werner, F., Korzec, D., and Engemann., J. Slot antenna 2.45 GHz microwave plasma source. *Plasma Sources Sci. T.* 3 (1994): 473–481.

[49] Pfuch, A. and Cihar, R. Deposition of SiO thin films by microwave induced plasma CVD at atmospheric pressure. *Surf. Coat. Tech.* 183 (2004): 134–140.

[50] Luklema, J.. *Fundamentals of Interface and Colloid Science.* Academic Press 1995.

[51] Christian, O. Plasma surface modification of polymers for biomedical use. *Nuclear Instruments and Methods in Physics Research Section B: Beam Interactions with Materials and Atoms* 208 (2003): 40–47.

[52] Beake, B., Ling, J., and Leggett., G. Scanning Force Microscopy Investigation of Poly(ethylene terephthalate) Modified by Argon Plasma Treatment. *J. Mater. Chem.* 8 (1998): 1735–1742.

[53] Sparavigna, A.. *Plasma treatment advantages for textiles.* Department in applied Physics 2003.

[54] Yasuda, H. and Marsh, H. ESCA Study of Polymer Surfaces Treated by Plasma. *J. Appl. Polm. Sci.* 15 (1997): 991–1019.

[55] Friedricha, J. et al. Ageing and degradation of poly(ethylene terephthalate) in an oxygen plasma. *Polym. Degrad. Stab.* 31 (1991): 97–114.

[56] Gomathi, N., Sureshkumar, A., and Neogi, S. RF plasma-treated polymers for biomedical applications. *Curr. Sci.* 11 (2008): 1478–1486.

[57] Tsafack, M. J.. Plasma-Induced Graft Polymerization of Organophosphorus Monomers:A Novel Approach to Flame Retard Polyacrylonitrile and Cotton Textiles. Master's thesis Swiss Federal Institute of Technology Zurich 2005.

[58] Moody, V. and Needles, H.. *Tufted Carpet-Textile Fibers, Dyes, Finishes, and Processes.* William Andrew Publishing 2004.

[59] Needles, H.. *Textile Fibers, Dyes, Finishes And Processes.* William Andrew Publishing 1987.

[60] Brown, D. and Pailthorpe, M. Antistatic Fibres and Finishes. *Review of Progress in Coloration and Related Topics* 16 (1986): 8–15.

[61] Chwastiak, S. A wicking method for measuring wetting properties of carbon yarns. *J. Coll. Interf. Sci.* 42 (1973): 298–309.

[62] Geneq inc. Sciencticfic instruments. Available from: http:www.geneq.com_ catalog_ encontact_ angle_ meter.html 2007, January 25.

[63] Hamdaoui, M., Fayala, F., and Nasrallah, S. B. Dynamics of Capillary Rise in Yarns: In?uence of Fiber and Liquid Characteristics. *J. Appl. Polym Sci.* 104 (2007): 3050–3056.

[64] Washburn, E. The dynamics of capillary flow. *Phys. Rev.* 17 (1921): 273 283.

[65] Ghali, K., Jones, B., and Tracy, J. Experimental technique for measuring parameters describing wetting and wicking in fabrics. *Textile Res. J.* 64 (1994): 106–111.

[66] Zhmud, B., Tiberg, F., and Hallstensson, K. Dynamics of capillary rise. *J. Colloid. Interf. Sci.* 228 (2000): 263–269.

[67] Hsieh, Y. Liquid Transport in Fabric Structures. *Text. Res. J.* 65 (1995): 299–307.

[68] Laughlin, R. and Davies, J. Some aspects of capillary absorption in fibrous textile wicking. *Textile Res. J.* 31 (1961): 904–910.

[69] Kornev, K. and Neimark, A. Spontaneous penetra-tion of liquids into capillaries and porous mem-branes revisited. *J. Colloid. Interf. Sci.* 235 (2001): 101–113.

[70] Perwuelz, A., Casetta, M., and Caze, C. Liquid organization during capillary rise in yarns-influence of yarn torsion. *Polym. Test.* 20 (2001): 553–561.

[71] Perwuelz, A., Mondon, P., and Caze, C. Experimental study of capillary flow in yarns. *Textile Res. J.* 70 (2000): 333–339.

[72] Pociute, M., Lehmann, B., and Vitkauskas, A. Wetting Behaviour of Surgical Polyester Woven Fabrics. *Mater. Sci.* 9 (2003): 410–411.

[73] Sarmadi, A., Ying, T., and Denes, F. Surface modification of polypropylene fabrics by acrylonitrile cold plasma. *Text. Res. J.* 63 (1993): 697–705.

[74] Poll, H. and Scheiter, S. Industrienahe Plasmabehandlung textiler Bahnware. *Melliand Textilber.* 79 (1998): 466–468.

[75] Hossain, M. M., Hegemann, D., Herrmann, A. S., and Chabrecek, P. Contact angle determination on plasma-treated poly(ethylene terephthalate) fabrics and foils. *J. Appl. Polym. Sci.* 102 (2006): 1452–1458.

[76] Eli, M. and Liepins, R. Flame retardants. *Environ. Health Perspect.* 11 (1975): 59–69.

[77] Geschftsfeld, T. and Bereich, L Environmental Aspects of Flame Retardants in Textiles. Report for Austrian Standards Institute Consumer Council. OEFZS L-0057, Appril 1999.

[78] Nort Central Regional Facts about fabric flammability. Extention publication 174, revised, July 2003.

[79] REM, Purdue University, West Lafayette. Available from: http://www.purdue.edu/rem/rs/sem.html 2010.

[80] Lee, S. Chemical Functionalization of AFM Cantelevers. Master's thesis Massachusetts Institute of Technology USA 2002.

[81] Chemsultants International, Inc. Available from: http://www.chemsultants.com/testing equipment products/testing devices/contact angle meter.aspx.

[82] Wikipedia's X-ray photoelectron spectroscopy as translated by GramTrans. Available from: http://epo.wikitrans.net/Perlumigu fotelektronospektroskopy/X-ray photo electron spectroscopy.

[83] Recording Microbalances for Special Applications. Available from: http://www.cielec.com/lab/microbalance/weight force recording microbalance.html.

[84] Richard, E., A., Water, R.N. and Stoliarov S.I.Screening Flame Retardants for Plastics Using Microscale Combustion Calorimetry. *Polymer. Eng. Sci.* 10 (2007): 1501–1510.

[85] Tsafack, M. and Levalois-Grtzmacher, J. Towards multifunctional surfaces using the plasma-induced graft polymerization (PIGP) process: Flame and waterproof cotton textiles. *Surface & Coatings Technology* 201 (2007): 5789–5795.

[86] Yip, J., Chan, K., Sin, M., and Lau, K. Low temperature plasma-treated nylon fabrics. *J. Mater. Process. Tech.* 123 (2002): 5–12.

[87] Taylor, V., March, R., Longerich, H., and Stadey, C. A mass spectroetric study of glucose, sucrose, and fructose using an inductively coupled plasma and electrospray ionization. *Int. J. Mass Spectrom.* 243 (2003): 71–84.

[88] Suanpoot, P., Kueseng, K., Ortmann, S., Kaufmann, R., Umongno, C., Nimmanpipug, P., Boonyawan, D. and Vilaithong, T. Surface analysis of hydrophobicity of Thai silk treated by SF_6 plasma. *Surf. Coat. Tech.* 202 (2008): 5543–5549.

[89] Evans, R., Wang, D., Agblevor, F., Chum, H., and Baldwin, S. Mass spectroetric studies of the thermal decomposition of carbohydrates using C-labeled cellulose and glucose. *Carbohydr. Res.* 281 (1996): 219–235.

[90] Vishnu K.T. and Hardesh K.M. Water-promoted unprecedented chemoselective nucleophilic substitution reactions of 1,4-quinones with oxygen nucleophiles in aqueous micelles. *Tetrahedron Lett.* 51 (2010): 3843–3847.

[91] Elena, S., Claudia, R., Maria, R.M., Bruno, M.Surface Modifications of silk by cold SF6 Plasma Treatment. *Macromol. Chem. Phys.* 202 (2001): 1672–1678.

[92] Leroux, F., Campagne, C., Perwuelz, A. and Gengembre, L.Fluorocarbon nano-coating of polyester fabrics by atmospheric air plasma with aerosol. *Appl. Surf. Sci.* 254 (2008): 3902–3908.

[93] Shahidi, S., Ghoranneviss, M., Moazzenchi, B., Rashidi, A. and Dorranian, D. Study of surface modification of wool fabrics using low temperature plasma. 2004.

[94] Ataeefarda, M., Moradiana, S., Mirabedini, M., Ebrahimi, M. and Asiabanc, S. Investigating the effect of power/time in the wettability of Ar and O_2

gas plasma-treated low-density polyethylene. *Prog. Org. Coat.* 64 (2009): 482–488.

[95] Liston, E.M., Martinu, L. and Wertheimer, M.R. Plasma surface modification of polymers. VSP Publishers 1994.

[96] Gomathi, N. and Sudarsan, N.Surface modi?cation of polypropylene using argon plasma: Statistical optimization of the process variables. *Appl. Surf. Sci.* 255 (2009): 7590–7600.

[97] Oiseth, S.K., Krozer, A., Kasemo, B. and Lausmaa, J. Surface modification of spin coated high-density polyethylene films by argon and oxygen glow discharge plasma treatments. *Appl. Surf. Sci.* 202 (2002): 92–103.

[98] France, R.M. and Short, R.D. Plasma treatment of polymers: the effects of energy transfer from an argon plasma on the surface chemistry of polystyrene, and polypropylene. A high-energy resolution X-ray photoelectron spectroscopy study. *Langmuir.* 14 (1998): 4827–4835.

[99] Tserepi, A., Vlachopoulou, M., and Gogolides, E. Nanotexturing of poly(dimethylsiloxane in plasmas for creating robust super-hydrophobic surfaces). *Nanotechnology.* 17 (2006): 3977–3983.

[100] Kokkoris, G., Vourdas, N., and Gogolides, E. Plasma etching and roughening of thin polymeric films: A fast, accurate, in situ method of surface roughness measurement. *Plasma Process. Polym.* 5 (2008): 825–833.

[101] Gogolides, E. et al. Si etching in high-density SF6 plasma for microfabrication: surface roughness formation. *Micro. Electron. Eng.* 73-74 (2004): 312–318.

[102] National Institute of Standard and Technology, NIST Atomic Spectra Database, Available from: http://www.physics.nist.gov/cgi-bin/ASD/line1.pl. 2003.

[103] Chunyang, W. and Chaoxia, W. Surface pretreatment of polyester fabric for inkjet printing with radio frequency Oxygen plasma. *Fibers and Polymers* 11 (2010): 223–228.

[104] Malek, R. and Holme, I. The effect of plasma treatment on some properties of cotton. *Iran. Polym. J.* 12 (2003): 271–280.

[105] Guan, J. and Chen, G. Flame Resistant Modification of Silk Fabric with Vinyl Phosphate . *Fibe. Polym.* 9 (2008): 438–443.

[106] Guan, J., Q., C., b., Y., and Chen, G. Formaldehyde-free flame retardant finishing of silk using a hydroxyl-functional organophosphorus oligomer. *Polym. Degrad. Stab.* 94 (2009): 450–455.

[107] Tsafack, M. and Levallois-Grutzmacher, J. Flame retardancy of cotton textiles by plasma-induced graft-polymerization (PIGP). *Surf. Coat. Tech.* 201 (2006): 2599–2610.

[108] Liu, W., Chen, D., Wang, Y., Wang, D., and Qu, M. Char-forming mechanism of a novel polymeric flame retardant with char agent . *Polym. Degrad. Stab.* 92 (2007): 1046–1052.

[109] Lyon, R. and Walters, R. Pyrolysis combustion flow calorimetry. *J. Anal. Appl. Pyrol.* 71 (2002): 27–46.

[110] Mario, P. and Rosaria, C. New fluorinated functional materials. *J. Mater. Chem.* 15 (2005): 4981-4991.

[111] Kamlangkla, K., Paosawatyanyongb, B., Pavarajarnc, V., Hodakd, J. H., and Hodak, S. K. Mechanical strength and hydrophobicity of cotton fabric after SF6 plasma treatment. *Appl. Surf. Sci.* 256 (2010): 5888–5897.

APPENDICES

Appendix A

Preparation and characterization of the monomers

Diethyl (acryloyloxyethyl) phosphoramidate (DEAEPN) monomer

MF : $C_9H_{18}N0_5P$ and MW: 251.21 g/mol

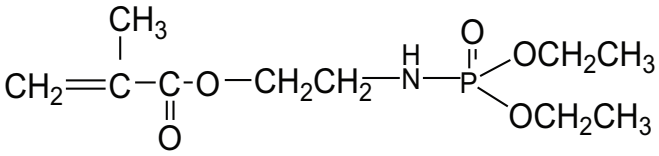

Synthesis procedure and characterization of Diethyl (acryloyloxyethyl) phosphoramidate (DEAEPN) monomer

17.2 g (0.10 mol) of diethyl chlorophosphate was added dropwise to a mixture of 6.1 g (0.10 mol) of ethanolamine and 10.1 g (0.10 mol) of triethyamine in 100 ml dichloromethane at 0 ^oC, under argon. After completion of the addition, the mixture was warmed to room temperature and stirred for 2 h. The precipitated triethylamine hydrochloride was removed by filtration. The filtrate was then cooled to 0 ^oC, and to this stirred solution was added 12.1 g (0.12 mol) of dry triethylamine under an atmosphere of argon. A solution of acryloyl chloride (9.05 g, 0.10 mol) in 100 ml of dry dichloromethane was then introduced dropwise. The reaction mixture was then allowed to attain room temperature and stirred overnight. The precipitates were filtered off and washed with dichloromethane. The combined filtrates were washed with an aqueous solution of Na_2CO_3, the solvent was evaporated and the residue was distilled under vacuum after adding a small amount of hydroquinone. In Fig. 3.4 shows the 1H-NMR spectra ($CDCl_3$) of DEAEPN monomer.

^{1}H-NMR (300.1 MHz, $CDCl_3$)δ= 1.10 (t, ^{3}JHH = 7.0 Hz, 6H,-CH_3), 2.88-3.00 (m, 2H, -OCH_2)N, 3.73-3.97 (m, 7H, -OCH_2 and NH) 5.60 (dd, ^{2}JHH =1-7 Hz, ^{3}JHH= 10.5 Hz, 1H, =CH cis), 5.87 (dd, ^{3}JHn= 17.3Hz, ^{3}JHH 10.3 Hz, 1H, HC=C), 6.18 (dd, ^{2}Jn,i =1.7 Hz, 3Jim = 17.3 Hz, 1H, =CH trans).

^{13}C-NMR (75.5 MHz, CDCl3)δ= 16.0 (-CH_3),40.0 (CH_2N), 61.9 ($POCH_2$), 64.4 (-OCH_2), 127.9 (=CH-), 130.9 (=CH_2), 165.7 (-C=0).

^{31}P-NMR (121.5 MHz, $CDCl_3$) δ=9.0(s)

Diethyl (acryloyloxyethyl) phosphate (DEAEP) monomer.

MF : $C_9H_{17}0_6P$ and MW: 252.20 g/mol

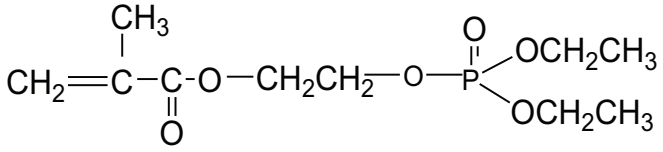

Synthesis procedure and characterization of Diethyl (acryloyloxyethyl) phosphate(DEAEP) monomer

To a cooled (0 - 5^{o}C) mixture of 11.6 g (0.10 mol) of 2-hydroxy ethyl acrylate, 12.1 g (0.12 mol) of dry triethylamine and 0.1 g of CuCl in 100 ml of dry diethyl ether, 17.2 g (0.10 mol) of diethylchlorophosphate was added dropwise while magnetically stirring under argon. The system was then allowed to attain room temperature and stirred overnight. The precipitated was filtered and washed with ether. The filtrate was washed with ice cold aqueous solution of NaOH (2%), followed with distilled water then dried over anhydrous MgO_4 The ether was evaporated off and the residue was distilled under vacuum after adding a small amount of hydroquinone. A colorless liquid was obtained; yield: 15 g, 59.2%. Bp: 105C/0.1 mmHg. In Fig. 3.6 shows the 1H-NMR spectra ($CDCl_3$) of DEAEP monomer.

^{1}H-NMR (300.1 MHz, $CDCl_3$)δ= 1.34 (t, ^{3}JHH = 7.0 Hz, 6H,-CH_3), 3.83-4.40 (m, 8H, -OCH2$_2$)), 5.88 (dd, ^{2}JHH =1-7 Hz, ^{3}JHH= 10.2 Hz, 1H, =CH cis), 6.11 (dd, 3JHn= 17.3Hz, ^{3}JHH 10.2 Hz, 1H, HC=C), 6.48 (dd, ^{2}Jn,i =1.7 Hz, 3Jim = 17.3 Hz, 1H, =CH trans).

^{13}C-NMR (75.5 MHz, CDCl3)δ= 16.2 (-CH_3),63.2-66.3 (-OCH_2),128.1 (=CH-),131.5(=CH_2),165.7(-C=0).

^{31}P-NMR (121.5 MHz, $CDCl_3$) 5 = 0.08 (s)

Appendix B

Band assignments for ATR-FTIR spectrum

Table 1: Band assignments for ATR-FTIR spectrum

Wavenumber (cm^{-1})	Assignment
3440	O-H stretching vibration
3076	C-H stretching vibration
1737	C=O stretching vibration
1613	C=C stretching vibration
1250	P=O stretching vibration
1150	P-O-C stretching vibration
1024-1078	P-O-C and C-O-C overlapped stretching vibration
985	P-O stretching vibration

Appendix C

Database of XPS spectra

Table 2: C1s, O1s and P2p binding energy and functional groups

	Binding energy (eV)	Functional groups
C 1s	284.7	C-C/C-H
	286.0	C-N
	286.2	C-OH
	286.6	C-O
	287.2	C-O-C
	288.5	C=O
	289.1	C-CF
	291.0	$C-CF_2$
	293.0	$C-CF_3$
O 1s	533.0	C-C-C/C-O-P/P-O-P
	532.0	C=O/O-C=O
P 2p	135.0	P-O-C/P=O

Appendix D

Conference presentations and Publications

International Presentations:

2009. K. Kamlangkla, S. K. Hodak, and B. Paosawatyanyong. The Wettability of PET Treated by O_2, N_2, and Ar Plasma by Capillary Rise Method. Oral presentation at CAPPSA 2009 International Congress on Cold Atmospheric Pressure Plasmas: Sources and Applications at Ghent University's Research Unit Plasma Technology (Department of Applied Physics), Belgium, (21-24 June; 2009).

Local Presentations:

2010. K. Kamlangkla, Jolle Levalois-Grtzmacher and S. K. Hodak. Compatibility of Flame Retardantcy and Hydrophobicity on Silk Fabric by Plasma. Oral presentation at The 3^{rd} progress report of Commission on Higher Education (MUA) scholarship, Pattaya, Chonburi, Thailand, (9-11 September; 2010).

2009. K. Kamlangkla, S. K. Hodak, and B. Paosawatyanyong. The Hydrophilicity of PET Treated by O_2, $N2_2$, and Ar Plasma by Capillary Rise Method. Oral presentation at The Science Forum 2009, Faculty of Science, Chulalongkorn University, Bangkok, Thailand,(12-13 March; 2009).

2009. K. Kamlangkla, S. K. Hodak, and B. Paosawatyanyong. The Wettability of PET Treated by O_2, $N2_2$, and Ar Plasma by Capillary Rise Method. Oral presentation at The 4^{th} Siam Physics Congress 2009, Cha Am, Petchaburi, Thailand, (18-21 March; 2009).

2008. K. Kamlangkla, S. K. Hodak, and B. Paosawatyanyong. Mechanical Stength and Hydrophobicity of Cotton Fabric After SF_6. Oral presentation at The 3^{rd} Siam Physics Congress 2008, Khao Yai, Nakhorn Ratchasima, Thailand, (20-22 March; 2008).

2007. K. Kamlangkla, S. K. Hodak, and B. Paosawatyanyong. and Satreerat K.Hodak. Studty on Wettability of Spandex Fabric Surfaces Improved by Oxygen Plasma Treatment. Oral presentation at The 2^{rd} Siam Physics Congress 2007, Nakhorn Pathom, Thailand, (22-24 March; 2007).

PUBLICATIONS:

2011. K. Kamlangkla, S. K. Hodak, Jolle Levalois-Grtzmacher. Multifunctional Silk Fabrics by Meaans of the PIGP Process. Surface and coatings Technology, Volume 256, pages 5888-5897. (2011), (impact factor: 1.793).

2010. K. Kamlangkla, B. Paosawatyanyong, V. Pavarajarn, Jose H.Hodak, Satreerat K. Hodak. Mechanical Strength and Hydrophobicity of Cotton Fabric after SF_6 Plasma Treatment. Applied Surface Science, Volume 256, pages 5888-5897. (2010), (impact factor: 1.576).

2010. K. Kamlangkla, S. K. Hodak, and B. Paosawatyanyong. The Hydrophilicity of PET Treated by O_2, $N2_2$, and Ar Plasma by Capillary Rise Method. Applied Surface Science, manuscript in preparation.

2010. B. Paosawatyanyong, K. Kamlangkla, S. K. Hodak. Hydrophobic and Hydrophillic Surface Nano-modification of PET fabric by plasma Process. Journal of Nanoscience and Nanotechnology, Volume 10, pages 7050-7054. (2010), (impact factor: 1.987).

2008. S.K. Hodak, T. Supasai, B. Paosawatyanyong, K. Kamlangkla, V. Pavarajarn. Enhancement of Hydrophobicity of Hydrophobicity of silk by SF_6 Plasma. Applied Surface Science, Volume 254, Issue 15, pages 4744-4749. (2008), (impact factor: 1.436).

Vitae

Mr. Kanchit Kamlangkla was born on January 14^{th} 1975 in Phangnga, Thailand. I graduated bachelors degree from Thaksin University in Science-Physics, Thailand in March, 1998. I completed my master degree in Education Physics from Srinakharinwirot University in March, 2002.

After recieving master degree, I became a lecturer at Rajamangala University of Technology Krungthep (RMUTK) for 3 years before persuring PhD. degree in June, 2006 in Nanoscience and Technology program at Chulalongkorn University. My thesis focused on modification of the surface characteristics of fabrics by plasma process.

During my study as a PhD. student, I have received the scholarship from the Commision on Higher Education to do research aboard. I joined Grützmacher Research Group at Eidgenössische Technische Hochschule Zürich - ETH (Swiss Federal Institute of Technology) in Switzerland for one year. I have benefited personally and professionally from these experiences.